MARS

Model for Applications at Regional Scale

Scientific model description

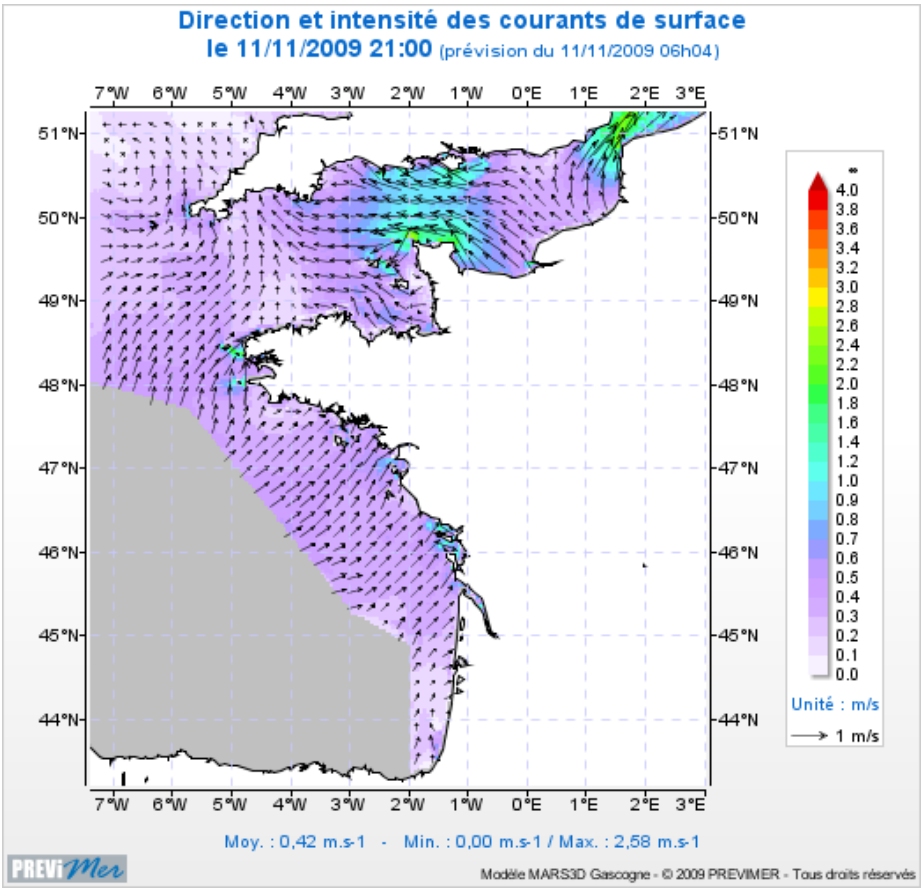

DUMAS Franck† LANGLOIS Gilbert‡

November 2009

‡IFREMER-DYNECO/PHYSED. *e-mail*: franck.dumas@ifremer.fr
‡Ema2. *e-mail*: gilbert.langlois@orange.fr

Contents

Introduction **1**

1 Formalism and hypothesis **2**
1.1 Governing equations . . . 3
1.1.1 Conservation of mass . . . 3
1.1.2 Conservation of momentum . . . 3
1.1.3 Energy equation . . . 4
1.2 Hypotheses and approximations . . . 6
1.2.1 Turbulence: An introduction . . . 6
1.2.2 Hypotheses and approximations . . . 6
1.2.3 First order equations . . . 8
1.2.4 Reynolds stress . . . 9
1.3 Geophysical equations . . . 11
1.3.1 Momentum equations . . . 11
1.3.2 Continuity equation . . . 11
1.3.3 Advection-diffusion equation . . . 11
1.3.4 State equation . . . 11
1.4 Sigma coordinate . . . 13
1.4.1 Transformations . . . 13
1.4.2 Horizontal pressure gradient . . . 15
1.4.3 Equations . . . 16
1.4.4 Advection-diffusion equation . . . 17

2 Parameterizations and closures **18**
2.1 Turbulence models . . . 19
2.1.1 Algebraic formulations . . . 19
2.1.2 Single equation models . . . 20
2.1.3 Two equations models . . . 22
2.1.4 Horizontal diffusion . . . 27
2.2 Air-sea interactions . . . 28
2.2.1 Radiative fluxes . . . 28
2.2.2 Turbulent fluxes . . . 32
2.3 Vertical boundary conditions . . . 41
2.3.1 Bottom . . . 41
2.3.2 Surface . . . 41
2.4 Open boundary conditions . . . 42
2.4.1 The method of characteristics . . . 42
2.4.2 Barotropic characteristics . . . 42
2.5 Moving boundaries . . . 44

3 Numerical techniques **45**
3.1 Barotropic-baroclinic splitting . . . 46
3.1.1 Vertical discretization . . . 46
3.1.2 Vertical summing . . . 46
3.1.3 2Dh model . . . 47
3.1.4 2D-3D model . . . 48
3.2 Numerical schemes . . . 49
3.2.1 2D time scheme . . . 49
3.2.2 2D-3D time scheme . . . 50
3.2.3 Automatic time step control . . . 51
3.2.4 Advection schemes . . . 53
3.3 Vertical and horizontal discretization . . . 60
3.3.1 Horizontal grid . . . 60
3.3.2 Vertical grid . . . 61
3.4 Turbulence schemes . . . 62
3.4.1 1Dv model . . . 62
3.4.2 Turbulence equations discretization . . . 63
3.4.3 Generic length scale values . . . 67
3.5 Wetting and drying scheme . . . 69
3.5.1 An FCT approach . . . 69
3.5.2 Upholding a positive depth . . . 72

4 Numerical formulations **74**
4.1 2Dh formulations . . . 75
4.2 2D-3D formulations . . . 78
4.3 Transport formulations . . . 81
4.4 Boundary formulations . . . 82
4.5 WAD algorithm . . . 83

Bibliography **85**

A Second order equations **90**
A.1 Turbulent fluctuation equations . . . 90
A.1.1 Continuity equation . . . 90
A.1.2 Momentum equations . . . 90
A.1.3 Salt equation . . . 90
A.1.4 Thermal conservation . . . 90
A.2 Second order equations . . . 90
A.2.1 Reynolds tensor . . . 91
A.2.2 Turbulent kinetic energy . . . 91

B Spherical coordinate **92**
B.1 Momentum equations . . . 92
B.2 Continuity equation . . . 92
B.3 Advection-diffusion equation . . . 92

C 2Dh linearized scheme **93**
C.1 Equations 93
C.2 Von Neumann analysis 93
C.3 Numerical formulations 94
C.4 Numerical analysis 95
C.4.1 Case $Fr = 0$: 96
C.4.2 Case $Fr \neq 0$: 96

D Tridiagonal matrix **100**

Table of symbols **102**

Introduction

The coastal ocean receives a great attention due to the increasing utilization of its resources. A comprehensive approach that addresses the sustainable use of the coastal ocean should incorporate ecosystem-based science. The ocean circulation provides the basis for the physical-biological interactions that take place while the physical oceanography of coastal and shelf seas involves many complex processes. Nowadays, numerical models are operational tools that are used to investigate the basic mechanisms which govern circulation over the continental shelf.

This report provides a detailed description of the fundamentals involved in the MARS numerical modelling system developed over the past few years by IFREMER.

The MARS[1] model is a three dimensional model based on a set of mathematical methods and numerical procedures. It is used to provide realistic descriptions of coastal phenomena.

The first part of this report describes the model equations, turbulent closure models, numerical schemes, parameterizations and algorithms used to develop the MARS model code.

Model performance has been tested in a variety of applications. The realism of the model is illustrated in the second part of this report.

The MARS model is used as part of the French coastal ocean forecasting program known as "Previmer" (www.previmer.org).

[1]MARS : Model for Applications at Regional Scale

Chapter 1

Formalism and hypothesis

Most flows encountered in the coastal oceans are turbulent. Furthermore, these flows are three-dimensional. Fluid mechanics deal with the flow of fluids. In this chapter our aim is to understand the elementary concepts of fluid mechanics involved in the MARS modelling system.

1.1 Governing equations

Geophysical fluid flows obey conservation laws for mass, momentum and energy in a rotating frame (The Earth rotates towards the east). These laws can be stated in the *differential* form, applicable at a fluid element.

1.1.1 Conservation of mass

The mass $\mathcal{M}$ of a moving fluid element does not change in time (t):

$$\frac{d\mathcal{M}}{dt} = 0 \tag{1.1}$$

When we introduce fluid density ρ we get :

$$\frac{\partial \rho}{\partial t} + \nabla.(\rho \mathbf{u}) = 0 \tag{1.2}$$

$\mathbf{u}$ is the particle velocity, ∇ is the hamiltonian operator.

Developing $\nabla.(\rho \mathbf{u})$, we can write the form:

$$\frac{d\rho}{dt} + \rho \nabla.\mathbf{u} = 0 \tag{1.3}$$

A fluid obeying $d\rho/dt = 0$ is usually called *incompressible*. In such a case, the equation of continuity becomes:

$$\nabla.\mathbf{u} = 0 \tag{1.4}$$

1.1.2 Conservation of momentum

The law of conservation of momentum is obtained by applying Newton's law of motion to an infinitesimal fluid element. The law states that the mass times the acceleration equals the sum of forces $\mathbf{F}$ applied per unit volume. Thus, we write:

$$\underbrace{\frac{\partial \mathbf{u}}{\partial t}}_{(1)} + \underbrace{L(\mathbf{u})}_{(2)} = \underbrace{\mathbf{F}}_{(3)} - \underbrace{\frac{1}{\rho}\nabla \mathbf{p}}_{(4)} + \underbrace{\nabla.\Phi^{\mu}}_{(5)} \tag{1.5}$$

The underlined term (1) is the acceleration of the fluid element in a Eulerian frame [1]. The second term (2) is the result of the spatial variations of the fluid velocity and will be acting even in a stationary velocity field. The symbolic form L represents the scalar product $(\mathbf{u}.\nabla)\mathbf{u}$. On the right hand side of the equation, the underlined term (3) symbolizes the sum of the forces $\mathbf{F}$ applied to the fluid element. $\nabla \mathbf{p}$ denotes the pressure forces acting on the fluid element. This term is present even if the fluid is at rest. The fifth terms $\nabla.\Phi^{\mu}$ describes the divergence of the viscous stresses, as internal fluid effects.

As all fluids have viscosity, this equation remains valid for coastal waters.

[1] The Eulerian specification of the flow field is a way of looking at fluid motion that focuses on specific locations in the space through which the fluid flows

For a motionless fluid ($\mathbf{u} = 0$), eq. (1.5) becomes :

$$\rho \mathbf{F} = \nabla \mathbf{p} \tag{1.6}$$

which defines the *hydrostatic* principle.

Let us consider a *perfect* and *incompressible* fluid. The constitutive equation of such a fluid flow is simplified: eq. (1.5) gives the *Euler* equation:

$$\frac{\partial \mathbf{u}}{\partial t} + L(\mathbf{u}) = \mathbf{F} - \frac{1}{\rho}\nabla \mathbf{p} \tag{1.7}$$

For a *newtonian* fluid, the viscosity effects can be expressed as a linear function of the velocity gradients. This means that for such fluid flow, when compressibility effects can be neglected, we get the *Navier-Stokes* equation:

$$\frac{\partial \mathbf{u}}{\partial t} + L(\mathbf{u}) = \mathbf{F} - \frac{1}{\rho}\nabla \mathbf{p} + \mathbf{F} + \mu \nabla^2 \mathbf{u} \tag{1.8}$$

μ is the molecular viscosity, ∇^2 is the Laplacian.

The governing equations for a geophysical viscous and incompressible fluid cannot be solved analytically and therefore require numerical solutions.

Introducing the gravity effect and the Coriolis force in eq. (1.8) gives the final form:

$$\frac{\partial \mathbf{u}}{\partial t} + 2\mathbf{\Omega} \wedge \mathbf{u} + L(\mathbf{u}) = -\frac{1}{\rho}\nabla \mathbf{p} + \mathbf{F}_g + \mu \nabla^2 \mathbf{u} \tag{1.9}$$

with: $\mathbf{\Omega}$: vector rotation; $2\mathbf{\Omega} \wedge \mathbf{u}$: Coriolis acceleration; $\mathbf{F}_g$: gravity.

A detailed exposition of the Coriolis acceleration can be found in the books of Kundu [18], pp 94-99 and Cushman-Roisin [9], pp 16-29.

1.1.3 Energy equation

The first law of thermodynamics states that the internal energy I_e gained by a parcel of matter is equal to the heat $\mathcal{Q}$ it receives minus the mechanical work it performs:

$$\frac{dI_e}{dt} = \mathcal{Q} - p\frac{d\vartheta}{dt} \tag{1.10}$$

$I_e = C_p T$ is the internal energy per mass unit, T is temperature, $\vartheta = 1/\rho$ is the specific volume and C_p is the heat capacity at constant volume. Geophysical fluids do not contain heat sources, thus the heat gained by a unit volume of sea water is the result of diffusion. According to the

standard diffusion formulation, we write: $\rho\mathcal{Q} = \mathcal{K}\nabla^2 T$ where $\mathcal{K}$ is the thermal conductivity of the fluid. Then eq. (1.10) becomes:

$$\rho C_p \frac{dT}{dt} - \frac{p}{\rho}\frac{d\rho}{dt} = \mathcal{K}\nabla^2 T$$

By elimination of $d\rho/dt$ from the continuity equation (1.3), we get:

$$\rho C_p \frac{dT}{dt} + p\nabla.\mathbf{u} = \mathcal{K}\nabla^2 T$$

Introducing eq. (1.4), for an incompressible fluid, the energy conservation law can be witten as:

$$\rho_0 C_p \frac{dT}{dt} = \mathcal{K}\nabla^2 T \tag{1.11}$$

1.2 Hypotheses and approximations

The set of equations given in the previous section are instantaneous forms of fluid dynamics. Yet, as they stand, these forms are still too complicated for the purpose of geophysical fluid hydrodynamics. Further simplifications can be used to investigate the basic mechanisms which govern the circulation in the coastal ocean.

1.2.1 Turbulence: An introduction

First, it appears justifiable to introduce a RANS decomposition (*RANS : Reynolds Averaged Navier-Stokes*). All the state variables ($\mathbf{q}$) are split into two terms :

$$\mathbf{q} = \overline{\mathbf{q}} + \mathbf{q}' \tag{1.12}$$

where $\mathbf{q}'$ is the *eddy* part of the fluid state (a fluctuation) and $\overline{\mathbf{q}}$ is the *coherent* part of the time variant variable (the mean) over a period δ (a few minutes). This second part satisfies :

$$\overline{\mathbf{q}} = \frac{1}{\delta}\int_{\delta} \mathbf{q}\ dt \tag{1.13}$$

The operator $\bar{\cdot}$ meets the following properties (λ is a parameter):

$$\begin{aligned}
\overline{q+\lambda r} &= \bar{q} + \lambda\bar{r} \\
\overline{q.\bar{r}} &= \bar{q}.\bar{r} \\
\bar{\bar{q}} &= \bar{q} \\
\bar{q'} &= 0 \\
\overline{\frac{\partial q}{\partial t}} &= \frac{\partial \bar{q}}{\partial t} \\
\overline{\frac{\partial q}{\partial x}} &= \frac{\partial \bar{q}}{\partial x}
\end{aligned}$$

t is time, x space coordinate.

1.2.2 Hypotheses and approximations

The set of hypotheses and approximations can be summarized as follows:

1 - The horizontal scale L_D of the model is supposed lower than R_T the Earth radius ($L_D \ll R_T$). The spatial coordinates can be expressed in a cartesian frame (x, y, z) with (z) along the gravity vector $\vec{g}$ (Figure 1.1).

2 - The previous equations are written on a rotating frame (with a constant rotation rate $\mathbf{\Omega}$) and the centrifugal force $\Omega^2\mathbf{R}$ can be added to the Newtonian gravity $\vec{g}$ (Figure 1.2).

3 - *Boussinesq* approximation. In the ocean, the fluid density ρ does not change greatly from a reference value ρ_0 (*cf.* [9] p 37). Thus, we write:

$$\rho = \rho_0 + \tilde{\rho}(x, y, z, t) \tag{1.14}$$

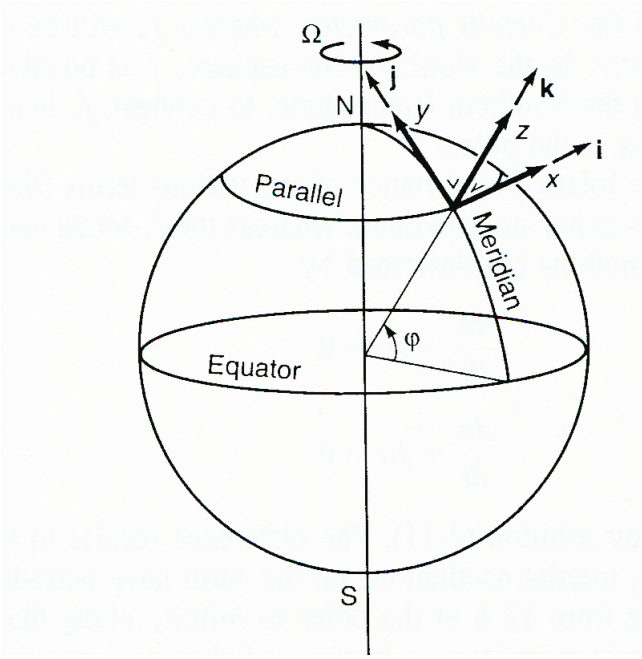

Figure 1.1: Definition of the local Cartesian framework of reference on a spherical earth.

Introducing this decomposition in the conservation of mass (1.3), we get :

$$\underbrace{\rho_0 \nabla.\mathbf{u}}_{I} + \underbrace{\tilde{\rho} \nabla.\mathbf{u}}_{II} + \underbrace{\frac{d\tilde{\rho}}{dt}}_{III} = 0$$

Underlined terms II and III are associated with relative variations of density. They are both together of the same order. However these terms are lower than the first term I because : $\tilde{\rho} \ll \rho_0$. Therefore, we can write :

$$\nabla.\mathbf{u} = 0$$

In practice, this approximation leads us to adopt the incompressible form (1.4) of the continuity equation and write $\rho \approx \rho_0$ in the momentum equations, except in the *buoyancy* [2] component of the horizontal pressure gradient $-\frac{1}{\rho}\nabla\mathbf{p}$ (*cf.* §1.4.2).

4 - The vertical velocity component is lower than the horizontal ones. Thus we can neglected the vertical acceleration in front of $\vec{g}$.

5 - The contribution of the vertical component of the Coriolis "force" can be neglected, except near the equator (*cf.* [9] p 42) where $f = 0$.

In summary, the vertical component of the momentum balance reduces to the simple hydrostatic form (1.6) which we can write:

$$\frac{\partial p}{\partial z} = -\rho g \tag{1.15}$$

[2] Buoyancy is defined by eq. 1.44)

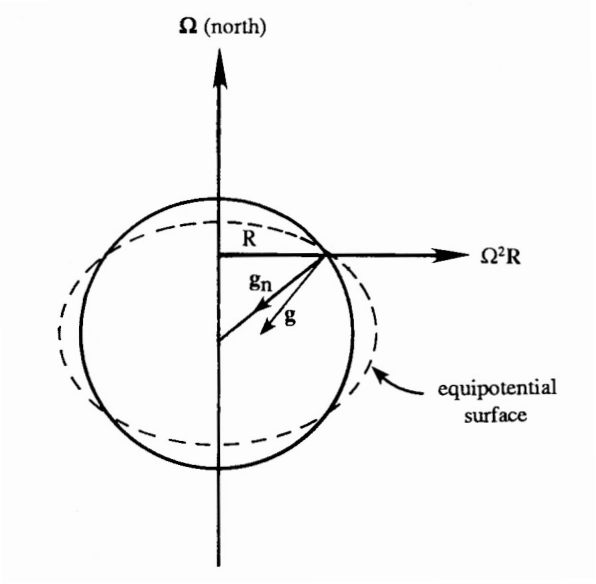

Figure 1.2: Effective gravity $\vec{g}$ and equipotential surface (*cf.* [18] p 98).

1.2.3 First order equations

First order equations are obtained by subsituting the Reynolds decomposition (1.12) into the instantaneous equations derived under the assumptions detailed above. Next the time operator defined in (1.13) is applied to these equations. Thereafter, we adopt a cartesian tensor notation.

Continuity

Integrating continuity equation (1.4) gives:

$$\frac{\partial \overline{u_i}}{\partial x_i} = 0 \tag{1.16}$$

Momentum

$$\rho_0 \frac{D\overline{u_i}}{Dt} = -\frac{\partial \overline{p}}{\partial x_i} - 2\epsilon_{ijk}\rho_0 \Omega_j \overline{u}_k - \overline{\rho} g \delta_{i3} - \rho_0 \frac{\partial}{\partial x_j}\overline{u_i' u_j'} + \mu \frac{\partial}{\partial x_j}\left(\frac{\partial \overline{u_i}}{\partial x_j} + \frac{\partial \overline{u_j}}{\partial x_i}\right) \tag{1.17}$$

g is gravity. δ_{ij} the Kronecker symbol: $\delta_{i3} = 1$ if $i = 3$; 0 otherwise.

and ϵ_{ijk} the *alternating* tensor:

$$\epsilon_{ijk} = \begin{cases} 1 & \text{if } ijk = 123, 231 \text{ ou } 312 \\ 0 & \text{if two suffixes are the same} \\ -1 & \text{if } ijk = 321, 213, \text{ or } 132 \end{cases}$$

D/Dt is frequently used in place of d/dt in fluid mechanics. For a variable a, we have:

$$\frac{Da}{Dt} = \frac{\partial a}{\partial t} + \overline{u_j}\frac{\partial a}{\partial x_j}$$

Thus, concerning the velocity components we get:

$$\frac{Du_i}{Dt} = \frac{\partial \overline{u_i}}{\partial t} + \overline{u_j}\frac{\partial \overline{u_i}}{\partial x_j}$$

The vertical component of (1.17) gives the simple relation:

$$g = -\frac{1}{\overline{\rho}}\frac{\partial \overline{p}}{\partial x_k} \tag{1.18}$$

Salt conservation

$\mathcal{D}$ is the molecular diffusion coefficient of salt. We can write:

$$\frac{D\overline{S}}{Dt} = \frac{\partial}{\partial x_j}\left(\mathcal{D}\frac{\partial \overline{S}}{\partial x_j} - \overline{S'u'_j}\right) \tag{1.19}$$

Thermal energy

Eq. (1.11) reads :

$$\rho_0 C_p \frac{D\overline{T}}{Dt} = \frac{\partial}{\partial x_j}\left(\mathcal{K}\frac{\partial \overline{T}}{\partial x_j} - \rho_0 C_p \overline{T'u'_j} - \overline{R_j}\right) \tag{1.20}$$

R_j is the heat budget.

1.2.4 Reynolds stress

The final system composed of eqs. (1.16)-(1.17) and (1.19)-(1.20) is not "closed" as five additional terms $\overline{u_i}$ $(i = 1, 3)$, $\overline{T}$, $\overline{S}$ and twelve crossed terms $\overline{u'_i u'_j}$, $\overline{S'u'_j}$, $\overline{T'u'_j}$ arise in the forms. These terms are called *turbulent fluxes* of momentum, salt and heat.

In the momentum equations, we write:

$$\overline{u\prime_i u\prime_j} = \frac{\tau_{ij}}{\rho_0} \tag{1.21}$$

τ_{ij} is called the *Reynolds stress*. The turbulent fluctuations of momentum may be grouped together in a Reynolds stress tensor of nine components (*cf.* [18] p 30).

In the same way, for a constituent c (temperature, salt, or dissolved element) we get :

$$\overline{c'u'_j} = F_j^c \tag{1.22}$$

Molecular diffusion is neglected for high Reynolds number (Re) flows. This assumption remains valid in the coastal ocean.

Note: For every variable q, from now on the $\bar{\cdot}$ notation is omitted.

The second-order equations for momentum can be found in appendix A along with the Turbulent Kinetic Energy (TKE) equation (in this document TKE is noted e).

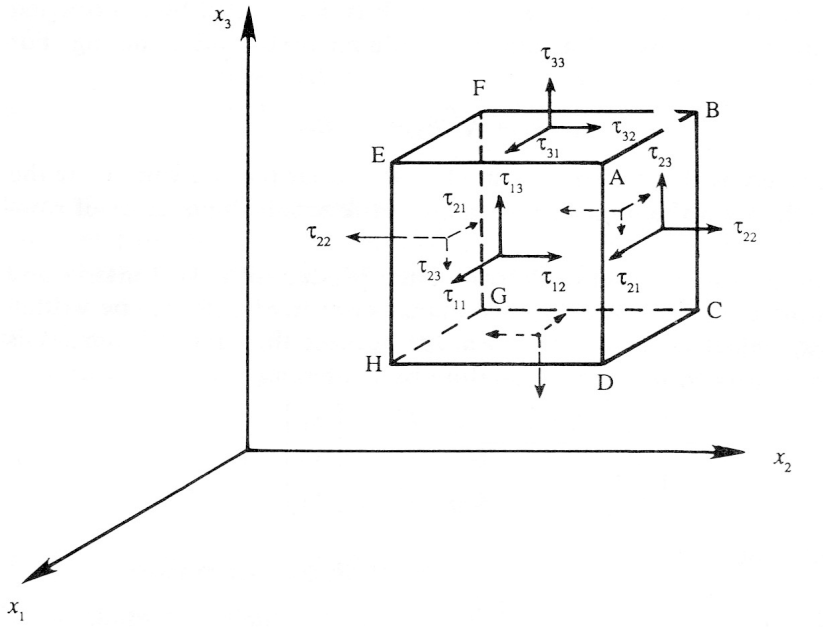

Figure 1.3: Stress field at a point.

1.3 Geophysical equations

The previous hypotheses and approximations have simplified the governing equations drastically. Hereafter, the final equations are given in a Cartesian frame. The forms in a spherical frame can be found in appendix B

1.3.1 Momentum equations

$$\frac{\partial u}{\partial t} + u\frac{\partial u}{\partial x} + v\frac{\partial u}{\partial y} + w\frac{\partial u}{\partial z} - fv = -\frac{1}{\rho_0}\frac{\partial p}{\partial x} + \frac{1}{\rho_0}\left(\frac{\partial \tau_{xx}}{\partial x} + \frac{\partial \tau_{xy}}{\partial y} + \frac{\partial \tau_{xz}}{\partial z}\right) \quad (1.23)$$

$$\frac{\partial v}{\partial t} + u\frac{\partial v}{\partial x} + v\frac{\partial v}{\partial y} + w\frac{\partial v}{\partial z} + fu = -\frac{1}{\rho_0}\frac{\partial p}{\partial y} + \frac{1}{\rho_0}\left(\frac{\partial \tau_{yx}}{\partial x} + \frac{\partial \tau_{yy}}{\partial y} + \frac{\partial \tau_{yz}}{\partial z}\right) \quad (1.24)$$

$$\frac{\partial p}{\partial z} = -\rho g \quad (1.25)$$

with the velocity vector $\mathbf{u}(u, v, w)$.

$f = 2\Omega \sin\varphi$ (Coriolis parameter) ; φ is latitude at location (x, y).

1.3.2 Continuity equation

$$\frac{\partial u}{\partial x} + \frac{\partial v}{\partial y} + \frac{\partial w}{\partial z} = 0 \quad (1.26)$$

1.3.3 Advection-diffusion equation

For a constituent c we have :

$$\frac{\partial c}{\partial t} + \frac{\partial}{\partial x}\left(uc - F_x^c\right) + \frac{\partial}{\partial y}\left(vc - F_y^c\right) + \frac{\partial}{\partial z}\left(wc - F_z^c\right) = h(s^c - p^c) \quad (1.27)$$

where we added a term s^c to take into account a local flux of material c and a "sinking" term p^c to represent the decreasing law of biological constituent. h is the instantaneous depth at location (x, y).

1.3.4 State equation

The density of sea water is a function of temperature, pressure and salt. The international equation of state for seawater, IES80 (UNESCO 1981), gives the most widely accepted representation of this relation. However, this equation is computationally expensive to use in numerical models where the density must be calculated for each time step.

An alternative is that of Mellor [26] (S ($^o/_{oo}$), T (^oC) and p (Pa) the hydrostatic pressure):

$$\rho = \rho_{TS} + \frac{p}{cr^2\left(1 - 2p/cr^2\right)} \quad (1.28)$$

where $cr = 1449.1 + 0.0821\ p + 4.55\ T - 0.045\ T^2 + 1.34(S - 35.)$

and:

$$\rho_{TS} = \rho_T + S(0.824493 - 4.0899\ 10^{-3}\ T_+ 7.6438\ 10^{-5}\ T^2 - 8.2467\ 10^{-7}\ T^3 + 5.3875\ 10^{-9} * T^4) \\ +|S|^{1.5}(-5.72466\ 10^{-3} + 1.0227\ 10^{-4}\ T - 1.654610^{-6}\ T^2) + 4.831410^{-4}\ S^2$$

$$\rho_T = -0.157406 + 6.793952\ 10^{-2}\ T - 9.095290\ 10^{-3}\ T^2 + 1.001685\ 10^{-4}\ T^3 \\ -1.120083\ 10^{-6}\ T^4 + 6.536332\ 10^{-9}\ T^5$$

Using the hypothesis (**3**) stated in § 1.2.2, we can introduce a linearized form:

$$\rho = \rho_0(1 - \alpha_T(T - T_0) + \beta_S(S - S_0))$$

with the following constants (ρ_0 (kg/m^3), T (^oC), S en $^o/_{oo}$)

ρ_0	1027
α_T	$0.16\,10^{-3}$
T_0	10.0
β_S	$0.8\,10^{-3}$
S_0	35.5

1.4 Sigma coordinate

The oceans have complicated geometry and large changes in bottom depth. It is therefore difficult to resolve the water column equally and efficiently in both shallow and deep regions of an oceanic region simultaneously. Furthermore, since turbulent mixing plays an important role in the circulation in the coastal ocean, a better simulation of both the upper and bottom mixed layers is necessary. This is possible with a topographically conformal vertical coordinate system, the so-called *sigma* (σ) coordinate system.

Following the SCRUM model (HEDSTRÖM, 2000 [14]) the vertical coordinate chosen is :

$$z = \zeta(1+\sigma) + H_c\sigma + (H - H_c)C(\sigma) \tag{1.29}$$

where H is the bottom depth. H_c is either the minimum depth or a shallow water depth above which we wish to have more resolution. $C(\sigma)$ is defined as:

$$C(\sigma) = (1-\beta)\frac{\sinh(\theta\sigma)}{\sinh\theta} + \beta\frac{\tanh[\theta(\sigma+1/2)] - \tanh(\theta/2)}{2\tanh(\theta/2)} \tag{1.30}$$

θ and β are surface and bottom control parameters.

The instantaneous depth h is given by :

$$h(x,y,t) = H(x,y) + \zeta(x,y,t) \tag{1.31}$$

where ζ is the surface elevation.

In the stretched system σ, everywhere (x,y,z) and any time (t), we get:

$$-1 \leq \sigma \leq 0$$

Eq. 1.29 leads to $z = \zeta$ for $\sigma = 0$ and $z = H$ for $\sigma = -1$. It is convenient to define H_z :

$$H_z = \frac{\partial z}{\partial \sigma} = (\zeta + H_c) + (H - H_c)\frac{\partial C(\sigma)}{\partial \sigma} \tag{1.32}$$

1.4.1 Transformations

The rules for this "s" transformation are :

$$\left(\frac{\partial}{\partial x}\right)_z = \left(\frac{\partial}{\partial x}\right)_\sigma - \frac{1}{H_z}\left(\frac{\partial z}{\partial x}\right)_\sigma \frac{\partial}{\partial \sigma} \tag{1.33}$$

$$\left(\frac{\partial}{\partial y}\right)_z = \left(\frac{\partial}{\partial y}\right)_\sigma - \frac{1}{H_z}\left(\frac{\partial z}{\partial y}\right)_\sigma \frac{\partial}{\partial \sigma} \tag{1.34}$$

$$\frac{\partial}{\partial z} = \left(\frac{\partial \sigma}{\partial z}\right)\frac{\partial}{\partial \sigma} = \frac{1}{H_z}\frac{\partial}{\partial \sigma} \tag{1.35}$$

$$\left(\frac{\partial}{\partial t}\right)_z = \left(\frac{\partial}{\partial t}\right)_\sigma + \left(\frac{\partial \sigma}{\partial t}\right)\frac{\partial}{\partial \sigma} \tag{1.36}$$

where :

$$\frac{1}{H_z} = \frac{\partial \sigma}{\partial z} \tag{1.37}$$

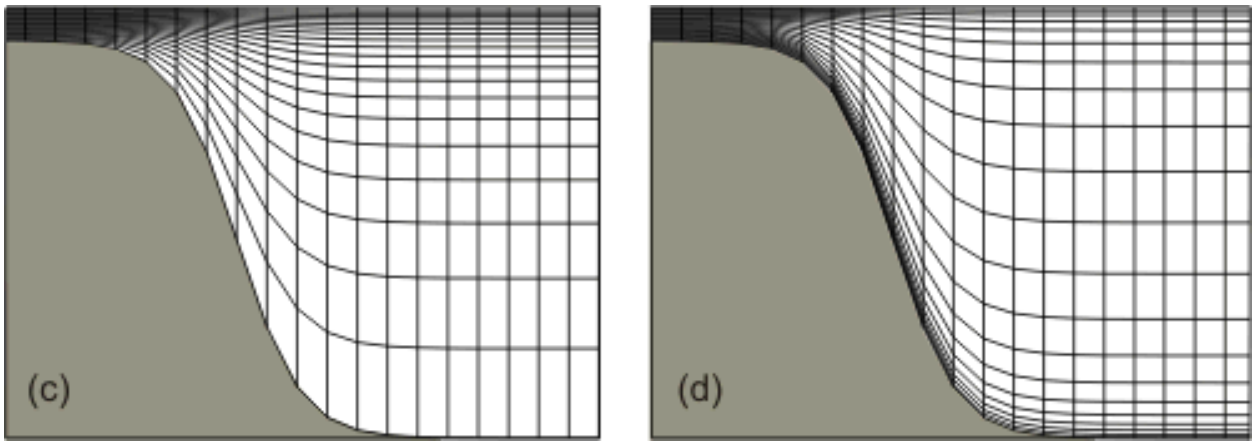

Figure 1.4: Vertical discretization for terrain-following (σ) coordinate model with 20 levels. (c): stretched coordinate ($\theta = 5$) for higher resolution near the surface, (d): stretching ($\theta = 5, \beta = 1$) for boundary layer resolution. (http://www.ocean-modeling.org)

Vertical velocity component

Because acceleration is not measured by the rate of change in velocity at a fixed location but by the change in velocity of a fluid particle as it moves with the flow, the time derivatives consist of both the local time rate of change and the so-called advective terms. This leads us to write:

$$\frac{\mathrm{D}}{\mathrm{D}t} = \frac{\partial}{\partial t} + u\frac{\partial}{\partial x} + v\frac{\partial}{\partial y} + w\frac{\partial}{\partial z} \tag{1.38}$$

Introducing eqs. (1.33) to (1.36) in this form gives:

$$\left(\frac{\mathrm{D}}{\mathrm{D}t}\right)_z = \left(\frac{\partial}{\partial t}\right)_\sigma + u\left(\frac{\partial}{\partial x}\right)_\sigma + v\left(\frac{\partial}{\partial y}\right)_\sigma + \underbrace{\frac{1}{H_z}\left[w - \left(\frac{\partial z}{\partial t}\right)_\sigma - u\left(\frac{\partial z}{\partial x}\right)_\sigma - v\left(\frac{\partial z}{\partial y}\right)_\sigma\right]}_{\tilde{w}}\frac{\partial}{\partial \sigma} \tag{1.39}$$

In this expression, the new variable noted $\tilde{w}$ is the vertical velocity in the σ coordinates.

From (1.29), we get:

$$\frac{\partial z}{\partial t} = (1+\sigma)\frac{\partial \zeta}{\partial t}$$

Therefore, in the σ coordinates, we can write:

$$\tilde{w} = \frac{1}{H_z}\left(w - (1+\sigma)\frac{\partial \zeta}{\partial t} - u\frac{\partial z}{\partial x} - v\frac{\partial z}{\partial y}\right) \tag{1.40}$$

and also :

$$w = H_z\tilde{w} + \frac{\partial z}{\partial t} + u\frac{\partial z}{\partial x} + v\frac{\partial z}{\partial y} \tag{1.41}$$

Continuity equation

The continuity equation (1.26) becomes :

$$\frac{\partial u}{\partial x} - \frac{1}{H_z}\left(\frac{\partial z}{\partial x}\right)_\sigma \frac{\partial u}{\partial \sigma} + \frac{\partial v}{\partial y} - \frac{1}{H_z}\left(\frac{\partial z}{\partial y}\right)_\sigma \frac{\partial v}{\partial \sigma} + \frac{1}{H_z}\frac{\partial w}{\partial \sigma} = 0$$

The derivate eq. (1.41) gives $\partial w/\partial\sigma$. Substitution in the preceding expression gives the following form:

$$\frac{\partial H_z}{\partial t} + \frac{\partial (H_z u)}{\partial x} + \frac{\partial (H_z v)}{\partial y} + \frac{\partial (H_z \tilde{w})}{\partial \sigma} = 0 \tag{1.42}$$

where $\tilde{w}$ is defined by (1.40).

1.4.2 Horizontal pressure gradient

In the σ coordinates, applying the transformation (1.35) in the hydrostatic relation (1.25) gives:

$$\frac{\partial p}{\partial \sigma} = -H_z \rho g \tag{1.43}$$

After integration of this form from a σ level to the surface level ($\sigma = 0$), we get:

$$p(\sigma) = p(0) + \int_\sigma^0 H_z \rho g d\sigma'$$

The horizontal component x of the pressure gradient may be written as:

$$GP_x = \frac{\partial}{\partial x}\left[p(0) + \int_\sigma^0 H_z \rho g d\sigma'\right]$$

or :

$$GP_x = \frac{\partial p(0)}{\partial x} + \frac{\partial}{\partial x}\left[\int_\sigma^0 H_z \rho g d\sigma'\right]$$

Considering transformation (1.33), we have:

$$GP_x = \frac{\partial p(0)}{\partial x} + \left(\frac{\partial}{\partial x}\right)_\sigma \left[\int_\sigma^0 H_z \rho g d\sigma'\right] - \frac{1}{H_z}\left(\frac{\partial z}{\partial x}\right)_\sigma \frac{\partial}{\partial \sigma}\left[\int_\sigma^0 H_z \rho g d\sigma'\right]$$

with :

$$-\frac{1}{H_z}\left(\frac{\partial z}{\partial x}\right)_\sigma \frac{\partial}{\partial \sigma}\left[\int_\sigma^0 H_z \rho g d\sigma'\right] = \left(\frac{\partial z}{\partial x}\right)_\sigma \rho g \left[H_z\right]_\sigma^0 = \left(\frac{\partial z}{\partial x}\right)_\sigma \rho g$$

Introducing buoyancy b:

$$b = g\frac{(\rho_0 - \rho)}{\rho_0} \tag{1.44}$$

adding and substracting the following quantity :

$$\left(\frac{\partial}{\partial x}\right)_\sigma \left[\int_\sigma^0 H_z \rho_0 g d\sigma'\right]$$

and then dividing by ρ_0, gives:

$$\frac{1}{\rho_0} GP_x = \frac{1}{\rho_0}\frac{\partial p_a}{\partial x} + \left(\frac{\partial}{\partial x}\right)_\sigma \left[\int_\sigma^0 H_z \frac{\rho - \rho_0}{\rho_0} g d\sigma'\right] + \left(\frac{\partial z}{\partial x}\right)_\sigma \frac{\rho}{\rho_0} g + \left(\frac{\partial}{\partial x}\right)_\sigma \left[\int_\sigma^0 H_z g d\sigma'\right]$$

where p_a is the air-sea level pressure.

Introducing (1.37) in the last term of this form leads to the expression :

$$\frac{1}{\rho_0}GP_x = \frac{1}{\rho_0}\frac{\partial P_a}{\partial x} - \left(\frac{\partial}{\partial x}\right)_\sigma \left[\int_\sigma^0 H_z b d\sigma'\right] + \left(\frac{\partial z}{\partial x}\right)_\sigma \frac{\rho}{\rho_0} g + \left(\frac{\partial}{\partial x}\right)_\sigma \int_\sigma^0 (\frac{\partial z}{\partial \sigma'}) g d\sigma'$$

where z is a function of σ. Integrating the last term of this expresion gives:

$$GP_x = \frac{1}{\rho_0}\frac{\partial P_a}{\partial x} - \left(\frac{\partial}{\partial x}\right)_\sigma \left[\int_\sigma^0 H_z b d\sigma'\right] + \left(\frac{\partial z}{\partial x}\right)_\sigma \frac{\rho}{\rho_0} g + \left(\frac{\partial}{\partial x}\right)_\sigma g\,[z]_\sigma^0$$

also :

$$GP_x = \frac{1}{\rho_0}\frac{\partial P_a}{\partial x} - \left(\frac{\partial}{\partial x}\right)_\sigma \left[\int_\sigma^0 H_z b d\sigma'\right] + \left(\frac{\partial z}{\partial x}\right)_\sigma \left(\frac{\rho}{\rho_0}\right) g + g\frac{\partial \zeta}{\partial x} - g\frac{\rho_0}{\rho_0}\left(\frac{\partial z}{\partial x}\right)_\sigma$$

Using the definition (1.44) for b, finally we get:

$$GP_x = \frac{1}{\rho_0}\frac{\partial P_a}{\partial x} - \left(\frac{\partial}{\partial x}\right)_\sigma \left[\int_\sigma^1 H_z b d\sigma'\right] - b\left(\frac{\partial z}{\partial x}\right)_\sigma + g\frac{\partial \zeta}{\partial x}$$

For convenience, we define:

$$-GP_x = -\frac{1}{\rho_0}\frac{\partial p_a}{\partial x} - g\frac{\partial \zeta}{\partial x} + \Pi_x \qquad \Pi_x = \left(\frac{\partial}{\partial x}\right)_\sigma \left[\int_\sigma^0 H_z b d\sigma'\right] - b\left(\frac{\partial z}{\partial x}\right)_\sigma \tag{1.45}$$

Generally Π_x in not zero at the sea surface ($\sigma = 0$).

Similary, for the y component we have:

$$-GP_y = -\frac{1}{\rho_0}\frac{\partial p_a}{\partial y} - g\frac{\partial \zeta}{\partial \partial x} + \Pi_y \qquad \Pi_y = \left(\frac{\partial}{\partial y}\right)_\sigma \left[\int_\sigma^0 H_z b d\sigma'\right] - b\left(\frac{\partial z}{\partial y}\right)_\sigma \tag{1.46}$$

1.4.3 Equations

In the σ coordinates, eqs. (1.23 to 1.26) become :

$$\frac{\partial u}{\partial t} + L(u) - fv = -g\frac{\partial \zeta}{\partial x} - \frac{1}{\rho_0}\frac{\partial p_a}{\partial x} + \Pi_x + \frac{1}{\rho_0 H_z}\frac{\partial \tau_{xz}}{\partial \sigma} + \mathcal{F}_x \tag{1.47}$$

$$\frac{\partial v}{\partial t} + L(v) + fu = -g\frac{\partial \zeta}{\partial y} - \frac{1}{\rho_0}\frac{\partial p_a}{\partial y} + \Pi_y + \frac{1}{\rho_0 H_z}\frac{\partial \tau_{yz}}{\partial \sigma} + \mathcal{F}_y \tag{1.48}$$

$$\frac{1}{H_z}\frac{\partial p}{\partial \sigma} = -\rho g \tag{1.49}$$

$$\frac{\partial \zeta}{\partial t} + \frac{\partial (H_z u)}{\partial x} + \frac{\partial (H_z v)}{\partial y} + \frac{\partial (H_z \tilde{w})}{\partial \sigma} = h\phi \tag{1.50}$$

where :

$$L(A) = u\frac{\partial A}{\partial x} + v\frac{\partial A}{\partial y} + \tilde{w}\frac{\partial A}{\partial \sigma} \tag{1.51}$$

A term ϕ was added to the right-hand of the continuity equation to denote a river discharge in the model.

$\mathcal{F}_x$ and $\mathcal{F}_y$ are horizontal friction terms.

1.4.4 Advection-diffusion equation

We adopt a uniform formalism to write the advection-diffusion equation for any constituent c (also the thermodynamic variables T (temperature) and S (salinity).

In the σ coordinates, for a constituent c, the MARS model solves the following equation:

$$\frac{\partial(H_z c)}{\partial t}+\frac{\partial}{\partial x}\left[H_z\left(uc-\kappa_H\frac{\partial c}{\partial x}\right)\right]+\frac{\partial}{\partial y}\left[H_z\left(vc-\kappa_H\frac{\partial c}{\partial y}\right)\right]+\frac{\partial}{\partial \sigma}\left[H_z\left(\tilde{w}c\right)\right]-\frac{1}{H_z}\frac{\partial}{\partial \sigma}\left(\frac{\kappa_V}{H_z}\frac{\partial c}{\partial \sigma}\right)=H_z(s^c-p^c) \tag{1.52}$$

Chapter 2

Parameterizations and closures

Owing to the RANS decomposition (*cf.* sect. 1.2.1) a tensor of turbulent fluctuations $\overline{u_i' u_j'}$ appears in the momentum equations. These terms are called "turbulent fluxes of momentum". In practice, a "turbulence closure" is a procedure used to express these correlations.

From semi-empirical theories, it appears that equations of momentum can be solved using an expression relating the Reynolds stress given in (1.21), in terms of the mean velocity field. Following Boussinesq, we write :

$$-\rho_0 \overline{u\prime_i u\prime_j} = \nu_{(i,j)} \left(\frac{\partial \overline{u_i}}{\partial x_j} + \frac{\partial \overline{u_j}}{\partial x_i} \right) \tag{2.1}$$

where ν (the eddy viscosity) depends on the conditions of the flow. The eddy viscosity relation (2.1) implies that the local gradient of velocity determines the flux of momentum.

In the ocean the horizontal scales of turbulent flows are quite different to the vertical ones. Therefore, we adopt two coefficients : ν_H to describe the effect of the horizontal gradients and ν_V to descibe the vertical gradients.

For $i = j$, we write:

$$\rho_0 \overline{u'^2} = -2\nu_H \frac{\partial \overline{u}}{\partial x} \quad ; \quad \rho_0 \overline{v'^2} = -2\nu_H \frac{\partial \overline{v}}{\partial y} \quad ; \quad \rho_0 \overline{w'^2} = -2\nu_V \frac{\partial \overline{w}}{\partial z} \tag{2.2}$$

Introducing the Reynolds' tensions, on the vertical axe we write:

$$\frac{\tau_{xz}}{\rho_0} = \nu_V \frac{\partial u}{\partial z} \qquad \frac{\tau_{yz}}{\rho_0} = \nu_V \frac{\partial v}{\partial z} \qquad F_z^c = \kappa_V \frac{\partial c}{\partial z} \tag{2.3}$$

Similar expressions for the horizontal coordinates are given in section 2.1.4.

There is no progress unless we can formulate a rational method for finding the eddy viscosity ν from other known parameters of a turbulent flow. The formulation of an eddy viscosity relation is called a "turbulence closure scheme".

A hierachy of turbulence closure models has been proposed by Mellor & Yamada, (1974) [23].

2.1 Turbulence models

Three classes of turbulent closure models have been included in the MARS modelling system.

2.1.1 Algebraic formulations

Numerous models based on algebraic relations exist. The following formulations are actually implemented in the MARS model code.

Constants coefficient

Regarding ν_V and κ_V, in the MARS modelling system we recommend a constant viscosity between 10^{-4} (kinematic viscosity) and $10^{-1}\, m^2/s$ (the largest value measured *in situ*)

Prandtl's law

Prandtl derived the logarithmic velocity distribution near a solid surface by using a mixing length theory :

$$\frac{u}{u^*} = \frac{1}{\kappa} \ln \frac{z}{z_0} \tag{2.4}$$

where $\kappa = 0.41$ is Karman constant. z_0 is a thickness used to depict the roughness of the sea bottom.

u^*, the "friction velocity", is given by:

$$u_* = (\tau_b/\rho_0)^{1/2} \tag{2.5}$$

τ_b is the bottom stress (*cf.* § 2.3).

In the MARS code, u^* is computed while assuming that the first σ level (close to the sea bed) is situated in the logarithmic layer:

$$u_* = \frac{\kappa u}{\ln \frac{z}{z_0}}$$

where u is the velocity at the first σ level σ_1 given by eq. (1.29). At the distance l from the sea bottom, we take:

$$\nu_V \propto u_* l = \frac{\kappa u}{\ln \frac{z}{z_0}}\ l$$

This concept deals with the bottom induced turbulence. Nevertheless, it does not reflect the effect of the density stratification. Moreover, it does not concern the mixing coefficient κ_V (set at a constant value).

Quetin

This model, based on density stratification, consists of the following formulations:

$$l = \kappa z (1 - 0.7 \frac{z}{h})$$

$$\nu_V = \frac{l^2 M}{\sqrt{1+10Ri}}$$
$$\kappa_V = l^2 M \exp^{-0.6Ri}$$

Ri is the Richardson number (cf. Eq. 2.6). In case of unsteady stratification, R_i is restricted as: $Ri > -0.09$. M^2 is define by :

$$M^2 = \left(\frac{\partial u}{\partial z}\right)^2 + \left(\frac{\partial v}{\partial z}\right)^2$$

Pacanowski & Philander

Pacanowski & Philander, (1981) [28] suggested the following relations :

$$\nu_V = 10^{-2}\left(\frac{1}{1+5\cdot Ri}\right)^2 + \nu_{bg}$$
$$\kappa_V = \nu_V\left(\frac{1}{1+5\cdot Ri}\right) + \kappa_{bg}$$

Ri is the Richardson number, defined as:

$$Ri = N^2/M^2 \quad \text{where} N^2 = \frac{\partial b}{\partial z} \tag{2.6}$$

N^2 is the Brunt-Väisälä frequency. b, the buoyancy, is defined by eq. (1.44). ν_{bg} and κ_{bg} are background viscosity and diffusivity.

In case of unsteady stratification:

$$\nu_V < 0.030\, m^2/s \quad \text{where} \quad \kappa_V < 0.052\, m^2/s$$

2.1.2 Single equation models

With this approach, the eddy viscosity (resp. the diffusivity) is set as a function of a turbulent velocity $\mathcal{V}$ and a mixing length l_m :

$$\nu_V, \kappa_V \propto \mathcal{V}\cdot l_m \tag{2.7}$$

This scheme includes a single prognostic equation for the Turbulent Kinetic Energy (TKE).

Turbulent Kinetic Energy

The turbulent velocity $\mathcal{V}$ is the square root of the TKE (e). The TKE equation is given in appendix A. Hereafter, we consider the simple form :

$$\frac{\mathrm{D}e}{\mathrm{D}t} = \frac{\partial F_z^e}{\partial z} + S^e - P^e - \epsilon \tag{2.8}$$

In eq. (2.8), the TKE flux is given by:

$$F_z^e = \frac{\nu_V}{s_e}\frac{\partial e}{\partial z}$$

where s_e is a coefficient for TKE diffusion.

$$\nu_V = C_M e^{1/2} l_m \tag{2.9}$$

C_M is a constant. GASPAR et *al.* (1990) [12] proposed: $C_M \simeq 0.1$

TKE is producted by the velocity shear :

$$S^e = \nu_V M^2$$

M^2 is given by (2.6). The "loss" of TKE by the Archimedes' effect is written as:

$$P^e = \kappa_V \frac{\partial b}{\partial z}$$

This term is a sink for a steady stratification. It becomes a source for an unsteady stratification.

The viscous dissipation of TKE is parameterized following KOLMOGOROV, (1941) [17] :

$$\epsilon = C_\epsilon \frac{e^{3/2}}{l_\epsilon} \tag{2.10}$$

From *in situ* experiments, we get: $C_\epsilon \simeq 0.7$.

Mixing length

[12] proposed the mixing lengths l_m and l_ϵ :

$$l_\epsilon = (l_u l_d)^{1/2} \tag{2.11}$$

and :

$$l_m = min(l_u, l_d) \tag{2.12}$$

where l_u and l_d are given by :

$$\frac{g}{\rho_r} \int_z^{z+l_u} \left[\rho(z) - \rho(z')\right] \, dz' = e(z) \tag{2.13}$$

$$\frac{g}{\rho_r} \int_z^{z-l_d} \left[\rho(z) - \rho(z')\right] \, dz' = e(z) \tag{2.14}$$

$z + l_u$ and $z - l_d$ are bounded by sea surface and sea bed.

This formulation has distinct advantages:

1. The lengths scale l_u and l_d have a simple physical interpretation: They are the distances traveled upwards (l_u) or downwards (l_d) by a fluid particle in converting all of its original TKE into potential energy.
2. The definitions (2.13) and (2.14) take into account the most general case of variable stratification. In a stably stratified fluid with a constant density gradient, they yield to : $l_u = l_d = \sqrt{2} l_b$ where l_b is a usual buoyancy length scale: $l_b = \sqrt{e}/N$

2.1.3 Two equations models

This class of model is based on a second prognostic equation for a mixing scale kl, the dissipation ϵ or a generic length scale (ψ) related to TKE k (in the standard notation) and l by the general formulation $\psi = (C_\mu^0)^p e^m l^n$) (*cf.* WARNER et *al.* [36]). C_μ^0 is the stability coefficient based on experimental data.

The $k-kl$ (MELLOR & YAMADA, 1982 [24]), $k-\epsilon$ (RODI, 1993 [32]) and $k-\omega$ with $\omega = \epsilon/k$ (WILCOX, 1998 [37]) are popular two eqs. turbulence models. Recently, UMLAUF & BURCHARD, (2003) [34] suggested a genelerization of the different approaches that yields to a family of differential equations typically used in marine Reynolds' stress models. The most well-known ocean turbulence models can be directly recovered as special cases of parameters m, n and p.

However, a prognostic equation may be established for the dissipation ϵ (BURCHARD, 2001 [6]).

Acccording to [34]) ψ is given by the following form:

$$\frac{\partial \psi}{\partial t} + u_i \frac{\partial \psi}{\partial x_i} = \frac{\partial}{\partial z}\left(\frac{\nu_V}{s_\psi}\frac{\partial \psi}{\partial z}\right) + \frac{\psi}{e}\left(c_1 Prod + c_3 Buoy - c_2 \epsilon\right). \tag{2.15}$$

where $Prod$ represents the effects of shear production and $Buoy$ the buoyant production. The parameters c_n are significant scaling constants of the shear production, stratification and dissipation. The numerical values have to be consistent with the Karman constant and with experimental observations of turbulence ([37]). The parameter c_3 takes on the values c_3^- in stable stratified flows and c_3^+ in unstable flows. The parameter s_ψ is the turbulence Schmidt number for ψ.

The generic length scale (GLS) formalism is used to write the same equations for each model using similar formulations based on n, p and m parameters.

Equations

The MARS model is based on the following turbulence equations:

$$\frac{\partial e}{\partial t} = \frac{\partial}{\partial z}\left(\frac{\nu_V}{s_e}\frac{\partial e}{\partial z}\right) + Prod + Buoy - \epsilon \tag{2.16}$$

$$\frac{\partial \psi}{\partial t} = \frac{\partial}{\partial z}\left(\frac{\nu_V}{s_\psi}\frac{\partial \psi}{\partial z}\right) + \frac{\psi}{e}\left(c_1 Prod + c_3 Buoy - c_2 \epsilon F_{wall}\right), \tag{2.17}$$

F_{wall} is a "wall" proximity function to ensure a positive value for the diffusion coefficient in the $k-kl$ model.

ψ relates the TKE e and the mixing length l according to the general formulation:

$$\psi = ({c_\mu}^o)^p \, e^m l^n, \tag{2.18}$$

where $0.5270 \leq {c_\mu}^o \leq 0.5544$.
The following relation is included for completeness:

$$l = ({c_\mu}^o)^3 \, e^{3/2} \epsilon^{-1}. \tag{2.19}$$

Then, the turbulente viscosity and diffusivity are given by the general formulations:

$$\nu_V = le^{1/2} S_M \tag{2.20}$$
$$\kappa_V = le^{1/2} S_H, \tag{2.21}$$

S_M and S_H are called "stability functions".

Stability functions

Stability functions are derived algebraically from the transport equations for the Reynolds stresses after parameterization of third-order moments and pressure strain correlations.

Kantha & Clayson [KC]: The KANTHA & CLAYSON, (1994) [15] quasi-equilibrum stability functions are expressed as:

$$S_M = \frac{a_0 + a_1 G_H}{1 + b_1 G_H + b_2 G_M + b_3 {G_H}^2 + b_4 G_M G_H} \tag{2.22}$$

$$S_H = \frac{a_4 + a_5 G_M + a_6 G_H}{1 + b_1 G_H + b_2 G_M + b_3 {G_H}^2 + b_4 G_M G_H} \tag{2.23}$$

Parameter values of a_i and b_i are given in table 2.1. G_M and G_H are given by :

$$G_H = \frac{l^2}{2e} N^2, \tag{2.24}$$
$$G_M = \frac{l^2}{2e} M^2, \tag{2.25}$$

The upper limits $G_H \leq 0.033$ and $G_M \leq 0.825 - 25 * G_H$ was suggested by [KC].

Table 2.1: [KC] stability function parameters

a_0	a_1	a_4	a_5	a_6	b_1	b_2	b_3	b_4
0.699	-11.259	0.74	0.90	-4.53	-32.23	5.08	159.96	-83.59

In a quasi steady-state homogeneous shear ($Prod + Buoy - \epsilon = 0$), we have :

$$S_M G - S_H G_H = 1$$

Then we get the new stability functions: (*see* WARNER et *al.*, 2005 [36] :

$$S_H = \frac{A_2 \left(1 - 6A_1/B_1\right)}{1 - 3A_2 G_H \left(6A_1 + B_2 \left(1 - C_3\right)\right)}, \tag{2.26}$$

$$S_M = \frac{{B_1}^{-1/3} + \left(18A_1 A_1 + 9A_1 A_2 \left(1 - C_2\right)\right)}{1 - 9A_1 A_2 G_H}, \tag{2.27}$$

with :

$$G_H = \frac{G_{hu} - \left(G_{hu} - G_{hcrit}\right)^2}{G_{hu} + G_{h0} - 2G_{hcrit}}, \tag{2.28}$$

where $G_{hu} = -N^2 l^2/(2e)$. G_H is limited as $G_{hmin} < G_H < G_{h0}$. Parameter values are given in table 2.2.

Table 2.2: [KC] quasi-equilibrum stability function parameters

A_1	A_2	B_1	B_2	C_2	C_3	G_{h0}	G_{hcrit}	G_{hmin}
0.92	0.74	16.6	10.1	0.7	0.2	0.0233	0.02	-0.28

Galperin [GK]: Galperin et *al.*, (1988) [11] proposed to motidify the [MY] formulations with $C_2 = C_3 = 0$. Then, in a quasi-equilibrum state:

$$S_H = \frac{A_2\left(1 - 6A_1/B_1\right)}{1 - 3A_2 G_H\left(6A_1 + B_2\right)}, \tag{2.29}$$

$$S_M = A_1 \frac{1 - 3C_1 - 6A_1/B_1 - 3A_2 G_H\left[\left(B_2 - 3A_2\right)\left(1 - 6A_1/B_1\right) - 3C_1\left(B_2 + 6A_1\right)\right]}{\left[1 - 3A_2 G_H\left(6A_1 + B_2\right)\right]\left(1 - 9A_1 A_2 G_H\right)}, \tag{2.30}$$

where $G_H = -N^2 l^2/e$ is limited as: $-0.28 < G_H < 0.0233$. Parameter values are given in table table 2.3.

Burchard & Petersen, 1999 [5] [BP] proposed to improve the [GK] stability functions as follows :

$$S_H = \frac{A_3}{1 + B_3\alpha_N}, \tag{2.31}$$

$$S_M = A_1 \frac{A_1 + A_2\alpha_N}{1 + B_1\alpha_N + B_2{\alpha_N}^2}, \tag{2.32}$$

with $\alpha_N = N^2 l^2/e$. Parameter values are given in table 2.4. α_N is bounded as : $-0.0466 < \alpha < 0.0233$.

Canuto [CH]: Canuto et *al.* (2001) [8] proposed a general set of stability functions to represent the turbulence production. Shear, buoyancy and vorticity effects are included in a global formulation of the Reynolds stresses. Moreover, the vorticity effect is added in the expression of the turbulent heat fluxes.

Then we get the following relations in [BD] (Burchard & Deleersnijder, 2001 [7]):

$$S_H = \frac{s_0 + s_1 G_H + s_2 G_M}{1 + t_1 G_H + t_2 G_M + t_3 {G_H}^2 + t_4 G_H G_M + t5 {G_M}^2}, \tag{2.33}$$

$$S_M = A_1 \frac{s_4 + s_5 G_H + s_6 G_M}{1 + t_1 G_H + t_2 G_M + t_3 {G_H}^2 + t_4 G_H G_M + t5 {G_M}^2}, \tag{2.34}$$

Table 2.3: [GK] stability function parameters

A_1	A_2	B_1	B_2	C_1
0.92	0.74	16.6	10.1	0.08

Table 2.4: [BP] stability function parameters

A_1	A_2	A_3	B_1	B_2	B_3
0.5562	2.182	0.6985	20.40	53.12	17.34

G_H and G_M are given by eqs. (2.24) and (2.25). Parameters values t_n and s_n are given in table 2.5

Table 2.5: [CH] stability function parameters

s_1	s_2	s_3	s_4	s_5	s_6
0.5168	-7.848	-0.0545	0.5412	-2.04	0.3964
t_1	t_2	t_3	t_4	t_5	
-23.84	2.68	75.574	-45.48	-0.2937	

with $G_H < 0.0673$. The upper limit of G_M is given by:

$$G_M{}^{lim} = \alpha \frac{1 + t_1 G_H + t_2 G_H{}^2}{t_2 + t_4 G_H}, \tag{2.35}$$

where $\alpha \simeq 1$.

In the previous paragraphs, the stability function G_M and G_H are expressed as TKE (e) and mixing length (l) relations. [BB] (Burchard & Bolding, 2001 [6]) proposed to specify the stabilty functions using TKE (e) and the dissipation rate (ϵ) :

$$G_M = \frac{e^2}{\epsilon^2} M^2 \tag{2.36}$$

$$G_H = \frac{e^2}{\epsilon^2} N^2 \tag{2.37}$$

In the comparison above the [CH] stability functions given in eqs. (2.33) and (2.34) remain valid but the parameter values should be quite different. Parameter values are given for two cases :

1) In table 2.6 [BB] formulations with (2.36) and (2.37) ;
2) In table 2.7 [CH] formulations with (2.25) and (2.24).

Table 2.6: [CH] stability function parameters by [BB]

s_1	s_2	s_3	s_4	s_5	s_6
0.1120	0.004519	0.00088	0.1070	0.01741	-0.00012
t_1	t_2	t_3	t_4	t_5	
0.2555	0.02872	0.008677	0.005222	-0.0000337	

Table 2.7: [CH] stability function parameters

s_1	s_2	s_3	s_4	s_5	s_6
0.1190	0.00429	0.00066	0.1270	0.01526	-0.00016
t_1	t_2	t_3	t_4	t_5	
0.1977	0.03154	0.005832	0.004127	-0.000042	

Note: The stability functions presented in the previous sections have been included in the MARS modelling system. In practice, these formulations allow us to take into account higher Richardson numbers, from $R_i = 0.19$ for the basic formulation [MY] to $R_i = 0.85$ for the [CH] formulations.

Therefore, the MARS model should be efficient in the oceanic regions of intense mixing

2.1.4 Horizontal diffusion

Regarding the horizontal turbulence, we adopt the following approach: the numerical model must solve the instantaneous patterns of the flow that are larger than the grid size. Thus we need to introduce a parameterization of the small scale effects.

Following eq. (2.2) the horizontal fluxes of momentum are expressed as a function of the local gradient of velocity:

$$\begin{aligned} \frac{\tau_{xx}}{\rho_0} &= \nu_H \frac{\partial u}{\partial x} \qquad \frac{\tau_{xy}}{\rho_0} = \nu_H \frac{\partial u}{\partial y} \\ \frac{\tau_{yx}}{\rho_0} &= \nu_H \frac{\partial v}{\partial x} \qquad \frac{\tau_{yy}}{\rho_0} = \nu_H \frac{\partial v}{\partial y} \end{aligned} \tag{2.38}$$

Regarding the diffusivity, we have :

$$F_x^c = \kappa_H \frac{\partial c}{\partial x} \qquad F_y^c = \kappa_H \frac{\partial c}{\partial y} \tag{2.39}$$

In practice ν_H and κ_H are expressed in terms of the grid size of the model (Smagorinsky, 1963 [33], Okubo, 1974 [27]). This kind of parameterization is proposed by the MARS model.

The following formulation is commonly employed in the MARS modelling system:

$$\nu_H = \kappa_H = f_{visc} \cdot 0.01 \cdot \Delta y^{1.15}$$

2.2 Air-sea interactions

The thermal structure of the upper ocean layer is quite complex due to the time and space variability of wind stress and heat fluxes. The heat fluxes at the sea surface, combined with the wind, induced turbulent mixing near surface layer cause temperature variations within the upper layers and consequently, density stratification.

Significant heat is exchanged across the ocean surface by four processes :

1 - Short wave radiation is received from the sun : Q_{sol}
2 - Radiative heat in the infrared spectrum is exchange between the atmosphere and ocean : Q_{ther}
3 - Heat is lost by the surface due to the latent heat of evaporation : Q_{lat}
4 - Heat is exchanged between the atmosphere and the ocean through conduction whenever there is a temperature difference between air and sea : Q_{sen}

Therefore, the net heat flux Q_{net} across a horizontal surface is given by :

$$Q_{net} = Q_{sol} + Q_{ther} + Q_{lat} + Q_{sen} \tag{2.40}$$

Nowadays our understanding of the physical processes which control the transfer of heat across the air-ocean interface is more advanced than our knowledge of the value of the different terms.

2.2.1 Radiative fluxes

Solar radiation

Three theoretical laws are useful in describing the main physical processes present at the air-sea interface: Planck's law, Wien's law and Stefan-Boltzmann law.

In physics, Planck's law describes the spectral radiance of electromagnetic radiation at all wavelengths from a black body at temperature T. As a function of wavelength, Planck's law is written as:

$$B_\lambda(T) = \frac{2hc^2}{\lambda^5 \left(\exp\left(hC/\lambda kT\right) - 1\right)} \tag{2.41}$$

where : $h = 6.626\ 10^{34}\ J.s$ is the Planck constant, $k = 1.38\ 10^{-23}\ J.K^{-1}$ is the Boltzmann constant. $C = 2.998\ 10^{-23}\ m.s^{-1}$ is the speed of light, λ the wavelength (m) and T temperature (K).

Wien's displacement law states that that there is an inverse relationship between the wavelength of the peak of the emission of a black body and its temperature :

$$\lambda_{max} = \frac{a}{T} \tag{2.42}$$

with : $a = 2897\ \mu m.K$. a is called the Wien's displacement constant.

The sun radiates as a black body with a temperature of $\simeq 5800\ K$. Some 50% of the energy is in the visible range $[0.4 - 0.7]\ \mu m$. The maximum energy is about $\lambda_{max} \simeq 0.48\ \mu m$

(Kidder & Vonder Haar, 1995 [16]).

All bodies with a temperature above absolute zero radiate heat energy. Thus, the ocean also loses heat trough radiation. The amount is proportional to the fourth power of the abolute temperature (Stefan-Boltzmann law):

$$Q = c_s T^4 \tag{2.43}$$

where $c_s = 5.67\ 10^{-8}\ W.m^{-2}.K^{-4}$ is the Stefan-Boltzmann constant. From Wien's law, at a temperature of $285\,^oK$ ($12\,^oC$) the peak wavelenghth of the maximum of the sea surface is about 10 μm (infrared range).

Along the way from the outer edge of the atmosphere to the surface of the earth, the energy of the sun can be attenued by one or more processes. The radiation can be reflected back into space. Only about half of the total radiation makes its way through the atmosphere where it can be absorbed by the ocean. Of that which does not reach the earth's surface, 30% is reflected back into space and the remaining 20% is absorbed within the atmosphere.

The short wave budget is writen as follows :

$$Q_{sol} = S_0 \sin(z) \underbrace{(1 - \chi + T_r)}_{(1)} \underbrace{(1 - c_1\eta + c_2\beta)}_{(2)} \underbrace{(1 - \alpha)}_{(3)} \tag{2.44}$$

where S_0 is the solar flux at the outer edge of the atmosphere. The distribution of the sun's energy on the outer atmposphere is not constant. There is slighlty more incoming radiation during the summer months and less in the winter months.

The sun altitude is defined by the following expression:

$$\sin(z) = \sin\varphi \sin\delta + \cos\varphi \cos\delta \cos\left(\frac{2\pi}{T} t\right) \tag{2.45}$$

where φ is latitude, δ is the sun declination, t is time and $T = 86400\ s$ (one day).

The underlined term (1) denotes the solar flux at the top of the atmosphere. χ is a gaz absorption coefficient commonly expressed as a function of the atmospheric constituents (Goody & Young, 1989 [53]). The diffusion coefficient (T_r) depends on the ratio of the particle size and the wavelength.

The second term (2) stands for solar extinction. η means the cloud density. β is the sun altitude at midday. c_1 and c_2 are constants.

The last factor $(1 - \alpha)$ represents the fraction of the incident solar enegy absorbed by the oceanic upper layers. α is the albedo. The albedo of an object is the percent of radiation reflected from its surface.

Solar fluxes in the MARS code

The MARS model is forced using outputs of the French forecasting systems Aladin & Arpege devised by Météo-France. These models are weather layered models that describe a three-dimensional grid field of the radiative budget in the short wavelength spectrum.

Otherwise when the true solar fluxes can not be specified, we used two parameterizations in the MARS code:

1 - NOMADS-2 (Gill, 1982 [52]) ;
2 - MAST-3 (Luyten et *al.*, 1992 [62]).

The default option is MAST-3 parameterization.

NOMADS-2: NOMADS-2 relation follows the general form (2.44) with $S_0 = 1368\ W/m^2$. The sun declination is defined as:

$$\delta = 25\,^o5' \frac{pi}{180} \cos\left(\frac{2\pi}{T_1} - 2.95\right)$$

T_1 is the number of hours in a year consisting of 365.24 *days* : $T_1 = 8735.76\ h$. In the form (2.45) T is the number of hours in one day (24).

In the form (2.44) we have $(1 - \chi + T_r) = 0.76$ with $c_1 = 0.4$, $c_2 = 0.38$. Furthermore: $\beta = \eta^2$ and $\alpha = 0.06$

MAST-3: [62] proposed to follow the general formulation (2.44) with $S_0 = 1368\ W/m^2$. A correction P is formulated to take into account the elliptical path of the earth in relation to the the sun radiation S_0P :

$$P = 1 + k_1 \cos(j' - 2.8)$$

with : $j' = k_2 j$; $k_1 = 0.03344$ and $k_2 = 0.9856$. j is the number of days in a year (in radian rd). $sin(z)$ is given by (2.45).

The sun declination is given by:

$$\delta = \delta_0 + \sum_{n=1}^{3} \left[a_n \cos(nj') + b_n \sin(nj')\right]$$

with $\delta_0 = 0.33281$

The parameter values a_n and b_n are $(-22.984,\ -0.34990,\ -0.13980)$ and $(3.7872,\ 0.03205,\ 0.07187)$ respectively. Regarding the time t, we have:

$$t = t_h - 12 + T_E + \theta$$

θ is the longitude in hour (divided by 15). T_E is the time equation:

$$TE = \sum_{n=1}^{3} \left[d_n \cos(nj') + e_n \sin(nj')\right]$$

The parameter values d_n and e_n are $(0.0072,\ -0.0528,\ -0.0012)$ and $(-0.1229,\ -0.1565,\ -0.0041)$ respectively. Following Rosati & Miyakoda (1998), [65], the first term of eq. (2.44) is divided

by 2. The absorption coefficient is $\chi = 0.09$ and $T_r = \exp(-\tau)$ where $\tau = mD_rT_L$ is the extinction coefficient proposed by Dogniaux (1985), [**?**]. The optical air mass is given by:

$$m = \left[\sin z + 0.15(z + 3.885)^{-1.253}\right]^{-1}$$

with $D_r = (0.9m + 9.4)^{-1}$ the Rayleigh optical thickness and $T_L = (0.02 * lz + 3.55)$ the Linke turbidity factor.

In the second term of eq. (2.44), the parameter value c_1 and c_2 are 0.62 and 0.0019 respectively.
To complete this approach, we take $\beta = 90 - \varphi + \delta$ with φ latitude and $\alpha = 0.07$

Thermal infrared budget

The ocean is not a true black body[1]. Thus, the Stefan-Boltzmann law (2.43) is written :

$$Q_{iro} = \epsilon_0 \sigma T_0^4$$

where ϵ_0 is the *emissivity* is the ratio of energy radiated by the upper ocean to energy radiated by a black body. T_0 is the sea surface temperature (SST). For the upper layer of the ocean we have $\epsilon_0 \simeq 0.985$

Much of the long wave radiation from the sea surface is absorbed by the clouds and water vapor in the air and then reradiated back to the sea by the low atmosphere. Thus, to establish the thermal infrared budget the useful term is not the back radiation as calculated by the Stefan-Boltzmann law, but the *effective back radiation*. This is defined as the *net* long wave radiation loss from the sea surface minus the reradiated amount back to the sea by the low atmosphere.

Thermal fluxes in the MARS code

As the solar fluxes, the MARS code may be forced by the thermal fluxes issued from the forecasting systems Aladin & Arpege. Otherwise, when the true thermal fluxes can not be specified in the MARS code, we use four formulations :

Luyten & De Mulder (1992), [62] ;
Clark et *al.* (1995), [**?**] ;
EDF [**?**] ;
Bignami et *al.* (1995), [41].

Luyten & De Mulder (1992) [LDM92]: This formulation was originally introduced by Gill (1992), [52]. It can be expressed as follows :

$$Q_{ther} = -\epsilon\sigma T_0^4(0.39 - 0.05\sqrt{e_a})(1 - \lambda\eta^2) \tag{2.46}$$

where e_a is the saturation vapor pressure at the air temperature and λ the cloud cover coefficient given by Budyko (1974), [42]. This coefficient depends on latitude. Luyten & De Mulder (1992), [62] suggested the following relation: $\lambda = 0.6\eta$ (η : cloud cover)
This formulation deals with only the infrared energy loss from the sea surface. This term varies depending on the vapor in the air and the level of cloud cover.

[1] In physics, a black body is an idealized object that absorbs all electromagnetic radiation that falls on it. No electromagnetic radiation passes through it and none is reflected

Clark et *al.*, (1995) [CAL95]: According to the preceding formulation, we write :

$$Q_{ther} = -\epsilon\sigma T_0^4(0.39 - 0.05\sqrt{e_a}) \tag{2.47}$$

[EDF] : The thermal flux is given by:

$$Q_{ther} = -\epsilon\sigma T_a^4(0.937\ 10^{-5}T_a^2)(1 + \lambda\eta^2) - \epsilon\sigma T_0^4 \tag{2.48}$$

with $\lambda = 0.3$.

This formulation takes into account the reradiated amount back to the sea by the low atmosphere. But this part is highly reduced (by the power -5).

Bignami & *al.*, (1995) [BAL95]: With this formulation the amount reradiated back to the sea by the low atmosphere is of the same order as the energy loss from the sea surface:

$$Q_{ther} = -\epsilon\sigma T_a^4(0.653 + 0.00535e_a)(1 + \lambda\eta^2) - \epsilon\sigma T_0^4 \tag{2.49}$$

where $\lambda = 0.1762$

Berliand & Berliand (1952) [BEB52]: Following LDM92, BEB52 added a suitable contribution function of the temperature difference in the air-sea boundary layer :

$$Q_{ther} = -\epsilon\sigma T_0^4(0.39 + 0.05\sqrt{e_a})(1 + \lambda\eta^2) - 4\epsilon\sigma T_a^3(T_0 - T_a) \tag{2.50}$$

Hastenrath & Lamb (1978) [HAL78]: Following BEB52, HAL78 proposed the form :

$$Q_{ther} = -\epsilon\sigma T_0^4(0.39 + 0.056\sqrt{e_a})(1 + \lambda\eta^2) - 4\epsilon\sigma T_a^3(T_0 - T_a) \tag{2.51}$$

Ayina (2008) [MOC08]: Following BAL95, MOC08 proposed the form:

$$Q_{ther} = -\epsilon\sigma T_0^4(0.653 + 0.0535e_a)(1 + \lambda\eta^2) - \epsilon\sigma T_a^3(T_0 - T_a) \tag{2.52}$$

2.2.2 Turbulent fluxes

According to eq. (1.21) the turbulent fluxes at the air-sea interface are written as:

$$\begin{aligned} \overline{u'w'} &= \frac{\tau_{ij}}{\rho} \\ \overline{q'w'} &= \frac{Q_{lat}}{\rho L_v} \\ \overline{\theta'w'} &= \frac{Q_{sen}}{\rho C_p} \end{aligned} \tag{2.53}$$

where τ, Q_{lat} and Q_{ses} are the Reynolds stresses of momentum, latent heat and sensible heat respectively. u', w', q' and θ' are turbulent fluctuations of velocity, specific humidity and potential temperature at the air-sea interface. L_v is the specific latent heat for sea water ($L_v = 2.45\ 10^{-6}\ J/Kg$) and C_p the specific heat capacity ($C_p = 1005\ J/Kg$).

These turbulent fluxes are estimated using a *bulk* method. The bulk method states that

the Reynolds stresses my be formulated in terms of the mean variables in the atmospheric surface layer (the lowest 10% of the atmospheric boundary layer). The bulk method is based on the Monin-Obukhov (1954), [63] theory (MOST). The MOST theory is a relationship describing the vertical behavior of nondimensionalized mean flow and turbulence properties within the atmospheric surface layer as a function of the Monin-Obukov parameters. These key parameters can be used to define a set of dimensional scales u_* (*cf.* eq. 2.5), q_* and θ_* as follows :

$$\begin{aligned} \frac{\tau_{ij}}{\rho_a} &= u_*^2 \\ \frac{Q_{lat}}{\rho_a L_v} &= -u_* q_* \\ \frac{Q_{sen}}{\rho C_p} &= -u_* \theta_* \end{aligned} \tag{2.54}$$

Theses key scales can then be used in a dimensional analysis to express all surface-layer flow properties as a dimensionless universal functions of z/L (L is the Monin-Obukhov length). For example the mean surface wind shear in a quasi-stationary, locally homogeneous surface layer can be written as:

$$\frac{\kappa z}{u_*}\frac{\partial u}{\partial z} = C^{ste} \tag{2.55}$$

κ is the von Karman constant. In a stratified layer, the preceding relation (2.55) becomes :

$$\frac{\kappa z}{u_*}\frac{\partial u}{\partial z} = \phi_u(\varsigma) \tag{2.56}$$

where $\phi_u(\varsigma) = 1$ for $\varsigma = 0$.

ς is the ratio between the buoyancy forces and the kinematic surface stress:

$$\varsigma = \frac{z}{L}\frac{\frac{g}{\theta_v}\overline{\theta_v' w'}}{u_*^3} \tag{2.57}$$

where: $\theta_v = \theta(1 + 0.61q)$ is the *virtual* temperature. Thus we have: $\varsigma < 0$ for an unsteady layer and $\varsigma > 0$ for a steady state.

Integrating (2.56) for the three key parameters gives:

$$\begin{aligned} u_* &= \kappa \left[\log\frac{z}{z_{u0}} - \Psi_u(\varsigma)\right]^{-1}(u_z - u_s) \\ q_* &= \kappa \left[\log\frac{z}{z_{q0}} - \Psi_q(\varsigma)\right]^{-1}(q_z - q_s) \\ \theta_* &= \kappa \left[\log\frac{z}{z_{\theta 0}} - \Psi_\theta(\varsigma)\right]^{-1}(\theta_z - \theta_s) \end{aligned} \tag{2.58}$$

Introducing these forms in (2.54) leads to:

$$\begin{aligned} \tau &= \rho_a C_D (u_z - u_s) \\ Q_{lat} &= -\rho_a L_v C_E (u_z - u_s)(q_z - q_s) \\ Q_{sen} &= -\rho_a C_p C_H (u_z - u_s)(\theta_z - \theta_s) \end{aligned} \tag{2.59}$$

Parameters suffixed (s) are significant of the sea surface and those indexed (z) indicate the height above sea level where the turbulent fluxes are estimated. C_D, C_E and C_H are drag coefficients. They are defined as follows:

$$\begin{aligned} C_D &= \kappa^2 \left[\log \frac{z}{z_{u0}} - \Psi_u(\varsigma)\right]^{-2} \\ C_E &= \kappa^2 \left[\log \frac{z}{z_{u0}} - \Psi_u(\varsigma)\right]^{-1} \left[\log \frac{z}{z_{q0}} - \Psi_q(\varsigma)\right]^{-1} \\ C_H &= \kappa^2 \left[\log \frac{z}{z_{u0}} - \Psi_u(\varsigma)\right]^{-1} \left[\log \frac{z}{z_{\theta 0}} - \Psi_\theta(\varsigma)\right]^{-1} \end{aligned} \tag{2.60}$$

z_{u0}, z_{q0} and $z_{\theta 0}$ are roughness thickness for momentum, humidity and temperature. They are relevant to the height above sea level where wind, humidity and temperature effects are more important than viscosty.

Three functions Ψ_u, Ψ_q and Ψ_θ are introduced to represent the stability parameter ς. They are commonly derived from in situ measurements. The Monin-Obukhov length is given by :

$$L = \frac{T_v (u_z - u_s)^2 C_D^{3/2}}{g\kappa \left[C_H(\theta_z - \theta_s) + 0.61 T_{as} C_E (q_z - q_s)\right]} \tag{2.61}$$

For a steady state ($\varsigma > 0$), we have:

$$\begin{aligned} &\Psi_u(\varsigma) = C_1 \varsigma \qquad \text{avec } C_1 = C^{ste} \\ &\Psi_q(\varsigma) = \Psi_\theta(\varsigma) = \Psi_u(\varsigma) \end{aligned}$$

In an unsteady layer ($\varsigma > 0$):

$$x = (1 - 16\varsigma)^{1/4} \tag{2.62}$$

$$\Psi_u(\varsigma) = 2\log\left(\frac{1}{2}(1+x)\right) + \log\left(\frac{1}{2}(1+x^2)\right) - 2\arctan x + \frac{\pi}{2} \tag{2.63}$$

$$\Psi_q(\varsigma) = \Psi_\theta(\varsigma) = 2\log\left(\frac{1}{2}(1+x^2)\right) \tag{2.64}$$

The global system composed of eqs. (2.58) to (2.60) can not be solved analytically. The turbulent fluxes are generally estimated using a simple iteration algorithm.

Otherwise, some parameterizations of turbulent fluxes have been proposed in the past. Hereafter, two main classes of theses methods are explained: the neutral direct, and, the equivalent neutral iterative methods.

Neutral direct

In this type of method, the exchange coefficients are derived from the observed wind velocity at 10 m (Smith & Banke, 1975 [66] ; Smith, 1988 [67]). The simplest expressions are constant coefficients.

Equivalent neutral iterative

This method, based on empirical formulae for calculating the *neutral* exchange coefficients at 10 m, is iterative.

Two methodolgies are used to express the three coefficients defined in (2.60)

I - Invariant parameter ($u = u_N$): The neutral coefficients are supposed dependent on wind velocity at 10 m. The roughness is first estimated and the *non neutral* coefficients are then expressed from the neutral ones assuming that wind (for ex. : $u = u_N$), temperature and humidity are constant in two different states. Large & Pond, (1981) [60], Geernaert, (1990) [51] and Luyten & De Mulder, (1992) [62] adopted this method.

The relations between non-neutral and equivalent-neutral conditions are obtained by writing C_D/C_{DN}, C_E/C_{EN} and C_H/C_{HN} using eqs. (2.58) (2.60):

$$\begin{aligned} C_D &= C_{DN}\left\{1+\frac{C_{DN}^{1/2}}{\kappa}\left[\log\left(\frac{z_0 n}{z_0}\right)-\Psi_u\right]\right\}^{-2} \\ C_E &= C_{EN}\left[1-\frac{1}{\kappa}\left(C_{EN}C_{DN}^{1/2}\Psi_q+\frac{1}{\kappa}C_{DN}^{1/2}\right)+\frac{C_{EN}}{\kappa^2}\Psi_u\Psi_q\right]^{-1} \\ C_H &= C_{HN}\left[1-\frac{1}{\kappa}\left(C_{HN}C_{DN}^{1/2}\Psi_\theta+\frac{1}{\kappa}C_{DN}^{1/2}\right)+\frac{C_{HN}}{\kappa^2}\Psi_u\Psi_\theta\right]^{-1} \end{aligned} \tag{2.65}$$

The drag coefficients C_D, C_E et C_H are then estimated using a simple iterative method from the neutral parameter values, the wind velocity at 10 m and the functions Ψ_u, Ψ_q and Ψ_θ.

II - Constant flux ($u_* = u_{*N}$): With this method the neutral coefficients at 10 m above sea level are defined from wind velocity. Roughness characteristics are unknown, thus the non-neutral coefficients at wind level are estimated from the neutral values at 10 m assuming that turbulents fluxes are constant (for ex. : $u_* = u_{*N}$) (Dupuis et *al.*, 1997 [47], Large & Yeager, 2004 [61]). First, the wind velocity is computed at the reference 10 m level, and then temperature and humidity can be assessed :

$$\begin{aligned} u_N(10\ m) &= u\left\{1+\frac{C_{DN}^{1/2}}{\kappa}\left[\log\left(\frac{z_u}{10_0}\right)-\Psi_u(\varsigma_u)\right]\right\}^{-2} \\ q(z_u) &= q(z_q)-\frac{q_*}{\kappa}\left[\log\left(\frac{z_q}{z_u}\right)+\Psi_q(\varsigma_u)-\Psi_q(\varsigma_q)\right]^{-1} \\ \theta(z_u) &= \theta(z_\theta)-\frac{\theta_*}{\kappa}\left[\log\left(\frac{z_\theta}{z_u}\right)+\Psi_\theta(\varsigma_u)-\Psi_\theta(\varsigma_\theta)\right]^{-1} \end{aligned} \tag{2.66}$$

Following the previous method (2.65), the non-neutral drag coefficients are deduced from the neutral-equivalent ones. We can therefore write:

$$\begin{aligned} C_D &= C_{DN}\left\{1+\frac{C_{DN}^{1/2}}{\kappa}\left[\log\left(\frac{z_u}{10_0}\right)-\Psi_u(\varsigma_u)\right]\right\}^{-2} \\ C_E &= C_{EN}\frac{C_D^{1/2}}{C_{DN}^{1/2}}\left\{1+\frac{C_{EN}}{\kappa C_{DN}^{1/2}}\left[\log\left(\frac{z_u}{10}\right)+\Psi_q(\varsigma_u)\right]\right\}^{-1} \end{aligned} \tag{2.67}$$

$$C_E = C_{EN}\frac{C_D^{1/2}}{C_{DN}^{1/2}}\left\{1+\frac{C_{EN}}{\kappa C_{DN}^{1/2}}\left[\log\left(\frac{z_u}{10}\right)+\Psi_\theta(\varsigma_u)\right]\right\}^{-1}$$

$\varsigma_u = z_u/L$ is the stability parameter at the level z_u. The drag coefficients C_D, C_E et C_H are then estimated using a simple iterative method from the neutral parameter values, the wind velocity at 10 m and from the functions Ψ_u, Ψ_q and Ψ_θ.

Turbulent fluxes in the MARS code

In the MARS code, the turbulent fluxes are estimated in terms of wind velocity, air relative humidity and surface temperature. Each flux deals with two computational methods:

. Latente flux : Clark et *al.* (1995), [**?**] and Luyten & De Mulder (1992), [62] ;
. Sensible flux : Elliott & Clarke (1990), [**?**] and Luyten & De Mulder (1992), [62].

Clark et *al.* (1995) [CAL95]: This parameterization is based on a neutral-direct approach. The specific humidity q is given by :

$$q = rh\frac{0.622e}{p-0.378e} \tag{2.68}$$

p is the surface pressure $(mBar)$

$$e = \exp\left[2.304\left(\frac{7.5T}{T+273.}+0.7858\right)\right] \tag{2.69}$$

is the vapor pressure at temperature T :
The heat transfer coefficient is a function of the wind velocity U:

$$C_E = 1.2\ 10^{-3}\left(1+\frac{1}{U}\right) \tag{2.70}$$

Elliot & Clarke (1990) [ECL90]: The sensible heat coefficient is given by the form:

$$C_E = 1.2\ 10^{-3}\left(1+\frac{1}{U}\right) \tag{2.71}$$

Luyten & De Mulder (1992) [LDM92]: This parameterization is based on a neutral-equivalent iterative method assuming that temperature and specific humidity are constant in neutral and non-neutral conditions. Specific humidity is given by:

$$q = \frac{0.622e}{p-0.38e} \tag{2.72}$$

The vapor pressure at temperature T:

$$e = rh\ 10^{\frac{0.7859+0.3477T}{1+0.00412T}} \tag{2.73}$$

The drag coefficients are estimated using eq. (4.11). The momentum roughness is given by Charnock, (1955) [44]) :

$$z_0 = \alpha\frac{u_*}{g} \tag{2.74}$$

That yields :

$$\frac{z_{0n}}{z_0} = \frac{C_{DN}}{C_D}$$

C_{DN} is related to the wind velocity. Many forms of this drag coefficient have been proposed in the past:

LARGE & POND (1981) $\quad C_{DN} = \begin{cases} 1.2\ 10^{-3} & \text{si} \quad U < 11 m/s \\ 10^{-3}(0.63 + 0.066U) & \text{si} \quad U \geq 11 m/s \end{cases}$

SMITH & BANKE (1975) $\quad C_{DN} = 10^{-3}(0.63 + 0.066U)$

GEERNAERT et *al.* (1986) $\quad C_{DN} = 10^{-3}(0.43 + 0.097U)$

with: $C_{EN} = C_{HN} = 1.13\ 10^{-3}$

Stability functions are defined in **4.10 ???** (BUSINGER et *al.* 1971, [43]) with $C_1 = -5$. The coefficients C_D, C_E and C_H are estimated using a bilinear interpolation method from eqs. (2.65).

Large & Yeager (2004) [LAY04]: This parameterization is based on a neutral-equivalent iterative method assuming constant fluxes. The specific humidity of sea water is defined as:

$$q = rh\rho_a q_1 \exp(q_2/SST) \tag{2.75}$$

where: $q_1 = 640380\ kg/m^3$, $q_2 = -5107.4\ K$ and $rh = 0.98$ (KRAUS, 1972 [59]).

The drag coefficients are computed at the level z_u using the forms (2.66) and (2.67). Stability functions are identical to those proposed by LUYTEN & DE MULDER, (1995) [**?**]. Neutral coefficients are related to wind velocity at 10 m above the sea level:

$C_{DN} = \dfrac{2.7}{u_{n10}} + 0.142 + \dfrac{u_{n10}}{13.09}$ where u_{n10} is wind velocity at 10 m in neutral conditions

$C_{EN} = 34.6\ 10^{-3}\sqrt{C_{DN}}$

$C_{DN} = \begin{cases} 18.\ 10^{-3}\sqrt{C_{DN}} & \text{si} \quad \varsigma > 0 \quad \text{(stable)} \\ 327.\ 10^{-3}\sqrt{C_{DN}} & \text{si} \quad \varsigma < 0 \quad \text{(unstable)} \end{cases}$

Fairall et *al.* (2003) [FAL03]: This parameterization was employed in the TOGA-COARE experiment in a wide range of climatic conditions.

The wind velocity is reduced as follows :

$$u = \sqrt{u_z^2 + w_g^2}$$
$$w_g = \beta_{gust}\,(bf.z_{bf})^{1/3}$$
$$bf = \max\left(0, \frac{-hu_*T_{v_*}}{T}\right)$$
$$T_{v_*} = T_*\left[1 + q\left(\frac{R_v}{R_a} - 1\right)\right] + Tq_*\left(\frac{R_v}{R_a} - 1\right)$$
$$\beta_{gust} = 1.2 \qquad \text{(from JABOUILLE \& AL. (1996), [57])}$$
$$z_{bf} = 600\ m \qquad \text{(height of the atmospheric boundary layer)}$$

R_v and R_a are gas constants for air and water vapor. The vapor pressure of sea water is reduced by 2% following KRAUS (1972), [59]. The roughness is estimated by SMITH, (1988) [67] or by using other formulations (OOST et *al.*, 2002 [64] and TAYLOR & YELLAND 2001, [68]). Following [67], we have :

$$z_0 = \alpha \frac{u_*}{g} + \beta \frac{\nu}{u_*} \qquad \text{with} \quad \beta = 0.11$$

where :

$$\alpha = \begin{cases} 0.011 & \text{if} \quad U \leq 10\ m/s \\ (0.011 + 0.007(U-10)) & \text{if} \quad 0 < U \leq 18\ m/s \\ 0.018 & \text{if} \quad U > 18\ m/s \end{cases} \qquad \text{(HARE et } al.\text{, 1999 [55])}$$

Following [64] we get :

$$\begin{aligned} z_0 &= \frac{25}{\pi} L_{wv} \left(\frac{u_*}{C_{wv}} \right)^{4.5} + \beta \frac{\nu}{u_*} \qquad \text{avec} \qquad \beta = 0.11 \\ L_{wv} &= \frac{g}{2\pi} (0.729U)^2 \\ C_{wv} &= \frac{g}{2\pi} (0.729U) \end{aligned}$$

C_{wv} is the peak wavelength (crest) of waves. Following TAYLOR & YELLAND (2001), [68]:

$$\begin{aligned} z_0 &= 1200 H_{wv} \left(\frac{H_{wv}}{L_{wv}} \right)^{4.5} + \beta \frac{\nu}{u_*} \\ L_{wv} &= \frac{g}{2\pi} (0.729U)^2 \\ H_{wv} &= 0.018 U^2 (1 + 0.015U) \end{aligned}$$

H_{wv} is the significant height of waves. The roughness for latent heat and sensible heat are written as:

$$z_{0q} = z_{0\theta} = \min \left\{ 1.15\ 10^{-4}, 5.5\ 10^{-3} \left(\frac{\nu}{z_0 u_*} \right)^{0.6} \right\}$$

Stability functions are defined as:

A - In a stable layer ($\varsigma > 0$):

$$\begin{aligned} \Psi_u(\varsigma) &= -(1+\varsigma) - 0.6667 \frac{(\varsigma - 14.28)}{\exp \Gamma} - 8.525 \\ \Psi_q(\varsigma) = \Psi_\theta(\varsigma) &= -\left(1 + \frac{2}{3}\varsigma \right)^{3/2} - 0.6667 \frac{(\varsigma - 14.28)}{\exp \Gamma} - 8.525 \\ \Gamma &= \min 50, 0.35\varsigma \end{aligned}$$

B - In an unstable layer ($\varsigma < 0$) :

$$\Psi_u(\varsigma) = (1-f)\Psi_{ub} + \Psi_{uC} \qquad \text{et} \qquad \Psi_q(\varsigma) = \Psi_\theta(\varsigma)(1-f)\Psi_{qb} + \Psi_{qC}$$

Ψ_{ub} et Ψ_{qb} are the functions defined in (2.62) by Businger et *al.* (1971) [43]. We have:

$$\Psi_{uC}(\varsigma) = \frac{3}{2}\log\left(\frac{y^2+y+1}{3}\right) - \sqrt{3}\arctan\left(\frac{2y+1}{\sqrt{3}}\right) + \sqrt{3} \quad \text{where} \quad y = (1-10.15\varsigma)^{1/3}$$
$$\Psi_{qC}(\varsigma) = \frac{3}{2}\log\left(\frac{y^2+y+1}{3}\right) - \sqrt{3}\arctan\left(\frac{2y+1}{\sqrt{3}}\right) + \sqrt{3} \quad \text{where} \quad y = (1-34.15\varsigma)^{1/3}$$

Intense rainfall enhances surface cooling, (and therefore the sensible heat), creating a high heat transfer stress.

Regarding the wind stress, following Fairall et *al.* (1996), [49]:

$$\tau_p = \frac{RU}{3600}$$

The sensible heat flux is given by the form:

$$Q_{sensp} = \tilde{R}C_{pr}\varepsilon(T_a - T_s)\left(1+\frac{1}{B}\right) \quad \left.\begin{array}{l} R(mm/h) \\ \tilde{R}(kg/s) \end{array}\right\} \quad \text{rainfall rate}$$

where $C_{pr} = 4186\ J/kg/K$ is the heat capacity of water and $B = C_p\Delta T/L_v\Delta Q$ is the Bowen ratio. The dew factor ε is given by the formula :

$$\varepsilon = \frac{1}{\left(1+\frac{R_a}{R_v}\frac{L_v d_v}{C_p d_h}\frac{dq_s}{dT}\right)}$$

d_v and d_h are vapor and heat diffusivities.

The Webb correction is added to the latent heat flux (Webb et *al.* 1980 [69]) :

$$Q_{latwebb} = \rho_a L_v \overline{wq} \quad \text{where} \quad \bar{w} = 1.61uq + (1+1.61q)\frac{u_* T_*}{T}$$

Ayina & Bentamy (2007) [MOC08]: This parameterization is commonly used by the Laboratoire d'Océanographie Spatiale (LOS-IFREMER). The specific humidity is related to surface salinity and gravity waves effects are included to specify the roughness of momentum.

Following [67], surface roughness is given by: $z_0 = \alpha\frac{u_*}{g} + \beta\frac{\nu}{u_*}$ where $\beta = 0.11$

Then, according to [64] we take:

$$z_0 = \frac{25}{\pi}L_{wv}\left(\frac{u_*}{C_{wv}}\right)^{4.5} + \beta\frac{\nu}{u_*} \qquad \text{where}$$
$$L_{wv} = \frac{g}{2\pi}(0.729U)^2$$
$$C_{wv} = \frac{g}{2\pi}(0.729U)$$

C_{wv} is the peak wavelength (crest) of waves.

Following [68] we get:

$$z_0 = 1200 H_{wv} \left(\frac{H_{wv}}{L_{wv}}\right)^{4.5} + \beta \frac{\nu}{u_*}$$
$$L_{wv} = \frac{g}{2\pi}(0.729U)^2$$
$$H_{wv} = 0.018U^2(1 + 0.015U)$$

The roughness for latent and sensible heat exchange is defined as:

$$z_{0q} = \frac{10}{\exp\left(\frac{\kappa^2}{C_E \log \frac{10}{z_{u0}}}\right)}$$
$$z_{0\theta} = \frac{10}{\exp\left(\frac{\kappa^2}{C_H \log \frac{10}{z_{u0}}}\right)}$$

Stability functions are defined in **4.10 ???** (Businger et *al.*, 1971) with $C_1 = -7$ in stable stratification.

MOC-2008 is a useful two step method used to compute turbulent fluxes at the air-sea interface. This method deals with the importance of including the air-sea stratification effect in the computation of turbulent fluxes. In the first step, the air temperature is derived from satellite data. The second step is based on using an iterative aerodynamic approach (bulk) to estimate the turbulent fluxes by taking into account the effect of air-sea stability and by respecting the coherence in the estimation of these three fluxes

2.3 Vertical boundary conditions

Vertical boundary conditions can be desribed as follows:

2.3.1 Bottom

For $\sigma = -1$:

$$\tilde{w}_b = 0$$

$$\nu_V \frac{\partial u}{\partial z}\bigg|_b = \frac{\tau_{bx}}{\rho_0} \qquad \nu_V \frac{\partial v}{\partial z}\bigg|_b = \frac{\tau_{by}}{\rho_0}$$

$$\kappa_V \frac{\partial T}{\partial z}\bigg|_b = 0 \qquad \kappa_V \frac{\partial S}{\partial z}\bigg|_b = 0$$

where:

$$(\tau_{bx}, \tau_{by}) = \rho_0 C_d^b \|\overrightarrow{u_b}\|(u_{bx}, v_{by}) \tag{2.76}$$

$$C_d^b = \left(\frac{\kappa}{\ln\left(\frac{z}{z_0}\right)}\right)^2 \tag{2.77}$$

$\overrightarrow{u_b}$ is the velocity at the first σ level above the sea bed and z_0 is the bottom roughness.

2.3.2 Surface

For $\sigma = 0$:

$$\tilde{w}_s = 0 \tag{2.78}$$

$$\nu_V \frac{\partial u}{\partial z}\bigg|_s = \frac{\tau_{sx}}{\rho_0} \qquad \nu_V \frac{\partial v}{\partial z}\bigg|_s = \frac{\tau_{sy}}{\rho_0}$$

$$\kappa_V \frac{\partial T}{\partial z}\bigg|_s = \frac{Q}{\rho_0 C_p} \qquad \kappa_V \frac{\partial S}{\partial z}\bigg|_s = 0$$

with:

$$(\tau_{sx}, \tau_{sy}) = \rho_a C_d^s \|\overrightarrow{W}\|(W_x, W_y) \tag{2.79}$$

where the $\rho_a = 1.2\ kg/m^3$ is the air density and $C_d^s = 0.016$ is the wind induced drag coefficient.

(W_x, W_y) is wind velocity at 10 m above the sea level.

Q is the vertical heat flux at the air-sea interface, $C_p = 4200\ J.kg^{-1}.K^{-1}$.

2.4 Open boundary conditions

Numerical models of finite coastal regions inevitably involve the treatment of open boundaries where the numerical grid ends. Ideal open boundaries are "transparent" to motions which are generated within the computational domain and which are "felt" at the open boundaries. There is no numerical treatment of open boundaries which achieves this ideal. A large number of open boundary conditions have been proposed in the past (Palma & Matano, 1998 [29]). Due to the essentially hyperbolic nature of the incompressible, hydrostatic primitive equations, external data is required for only inward boundary fluxes. The outward fluxes may be treated with an algorithm for two-dimensional radiation. In the MARS model the prescription of the Open Boundary Conditions (OBCs) is based on the method of characteristics.

2.4.1 The method of characteristics

This method is only applicable to hyperbolic Partial Differential Equations (PDE).

The primitive equations (1.23) to (1.26) are a set of non-hyperbolic equations, thus hereafter, assuming a linearized "mean state" (h_0, u_0, v_0), we only consider the "dynamical" part of this system for an homogeneous fluid.

Let us consider *Shallow Water* (SW) equations :

$$\begin{aligned}
&\frac{\partial \mathcal{U}}{\partial t} + u_0\frac{\partial \mathcal{U}}{\partial x} + v_0\frac{\partial \mathcal{U}}{\partial y} - f\mathcal{V} + g\frac{\partial h}{\partial x} = F_{\mathcal{U}} \\
&\frac{\partial \mathcal{V}}{\partial t} + u_0\frac{\partial \mathcal{V}}{\partial x} + v_0\frac{\partial \mathcal{V}}{\partial y} + f\mathcal{U} + g\frac{\partial h}{\partial y} = F_{\mathcal{V}} \\
&\frac{\partial h}{\partial t} + u_0\frac{\partial h}{\partial x} + v_0\frac{\partial h}{\partial y} + h_0\left(\frac{\partial \mathcal{U}}{\partial x} + \frac{\partial \mathcal{V}}{\partial y}\right) = 0
\end{aligned} \tag{2.80}$$

ζ is the sea surface elevation, H is the depth and $h = H + \zeta$ the instantaneous depth.

2.4.2 Barotropic characteristics

Hereafter we consider the case of an eastern boundary.

The SW matrix in the normal direction of the boundary is :

$$\begin{pmatrix} u_0 & 0 & g \\ 0 & u_0 & 0 \\ h_0 & 0 & u_0 \end{pmatrix}$$

The left-hand side eigenvectors $w_1 = \mathcal{U} + h\sqrt{g/h_0}$, $w_2 = \mathcal{V}$ and $w_3 = \mathcal{U} - h\sqrt{g/h_0}$ are called the *characteristics* variables of sys. (2.80). The corresponding eigenvalues are : $\lambda_1 = u_0 + c$, $\lambda_2 = u_0$ and $\lambda_3 = u_0 - c$, where $c = \sqrt{gh_0}$ is the gravity wave celerity.

Using these characteristics, sys. (2.80) can be rewritten as:

$$\frac{\partial w_1}{\partial t} + (u_0 - c)\frac{\partial w_1}{\partial x} + v_0\frac{\partial w_1}{\partial y} - c\frac{\partial \mathcal{V}}{\partial y} - f\mathcal{V} = F_{\mathcal{U}}$$

$$\begin{aligned}
&\frac{\partial w_2}{\partial t} + u_0\frac{\partial w_2}{\partial x} + v_0\frac{\partial w_2}{\partial y} + \frac{c}{2}\frac{\partial (w_3 - w_1)}{\partial y} + \frac{f}{2}(w_1 + w_3) = F_{\mathcal{V}} \\
&\frac{\partial w_3}{\partial t} + (u_0 + c)\frac{\partial w_3}{\partial x} + v_0\frac{\partial w_3}{\partial y} - c\frac{\partial \mathcal{V}}{\partial y} - f\mathcal{V} = F_{\mathcal{U}}
\end{aligned} \tag{2.81}$$

and :

$$\begin{aligned}
&\frac{\partial w_3}{\partial t} + \lambda_3\frac{\partial w_3}{\partial x} + v_0\frac{\partial w_3}{\partial y} - c\frac{\partial \mathcal{V}}{\partial y} - f\mathcal{V} = F_{\mathcal{U}} \\
&\frac{\partial w_2}{\partial t} + \lambda_2\frac{\partial w_2}{\partial x} + v_0\frac{\partial w_2}{\partial y} + \frac{c}{2}\frac{\partial (w_1 - w_3)}{\partial y} + \frac{f}{2}(w_1 + w_3) = F_{\mathcal{V}} \\
&\frac{\partial w_1}{\partial t} + \lambda_1\frac{\partial w_1}{\partial x} + v_0\frac{\partial w_1}{\partial y} - c\frac{\partial \mathcal{V}}{\partial y} - f\mathcal{V} = F_{\mathcal{U}}
\end{aligned} \tag{2.82}$$

In case $\lambda_k > 0$ $(k = 1, 2, 3)$ the characteristic w_k would be outward; inward in the opposite.

w_1 is an outgoing characteristic due to the fact that $u_0 << c$. Then w_3 is an ingoing characteristic.

On the open boundary, the following conditions should be applied:

If $u_0 > 0$: w_3 inward, w_2 and w_1 outward

Provide $B_1 w_3 = B_1 w_3^{ext}$; extrapolate w_2 and w_1.

If $u_0 < 0$: w_3 et w_2 inward, w_1 outward

Provide $B_2 w_3 = B_2 w_3^{ext}$ and $B_3 w_2 = B_3 w_2^{ext}$; extrapolate w_1.

Regarding the operator B_i, the following simple solution is choosen: $B_i = Id$.

2.5 Moving boundaries

In shallow coastal areas, some areas may dry up at low water level, which means that we have moving boundaries. The definition of these boundaries would appear to be rather straightforward : the instantaneous water depth $h = 0$ (h is defined by eq. (1.31)). Several techniques have been developed to track the moving boundaries. However, there are some difficulties involved in applicable numerical models.

In the MARS model, the wetting and drying processes have been cleared up by introducing a water depth H on each side of a grid cell (Fig. 2.1).

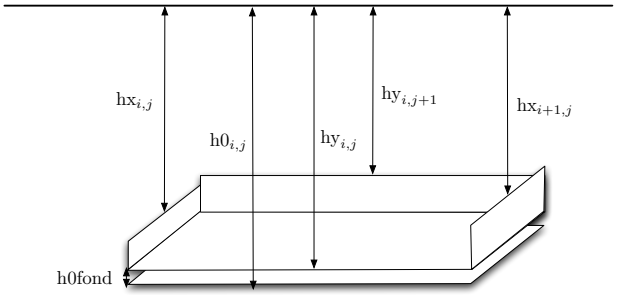

Figure 2.1: Spatial repatition of water depths on a grid cell

A *central* depth is introduced:

$$h0_{i,j} = \max\left(hx_{i,j}, hx_{i+1,j}, hy_{i,j}, hy_{i,j+1}\right) + h0fond \tag{2.83}$$

$h0fond$ is a minimum depth.

The instantaneous depths $\mathrm{hx} + \eta, \mathrm{hy} + \eta$ are used to solve momentum equations (1.23) and (1.24). In the meantime, the global advection-diffusion equation (1.27) is solved by introducing the central depth $\mathrm{h0} + \eta$. Then, in cells where the instantaneous depth becomes negative, $\mathrm{h0} + \eta$ remains positive.

Wetting and drying areas rely on the parameter $h0fond$. This problem will be adressed in section 3.5.

Chapter 3

Numerical techniques

The governing equations for coastal flows are so complicated that an exact solution is unavailable and it is computational solutions are necessary.

Computational techniques replace the governing partial differential equations with systems of algebraic equations, so that a computer can be used to obtain the solution. This chapter will deal with the computational techniques employed in the MARS modelling system for obtaining and solving the final systems of algebraic equations.

For local methods, like the finite difference employed in the MARS modelling system, the algebraic equations link together values of dependent variables at adjacent grid points. Under these conditions, it is understood that a grid of discrete points is distributed throughout the computational domain, in both time and space.

3.1 Barotropic-baroclinic splitting

The pressure terms of the momentum equations (1.47-1.48) are written (*cf.* § 1.4.2) :

$$GP_x = -\frac{1}{\rho_0}\frac{\partial p_a}{\partial x} - g\frac{\partial \zeta}{\partial x} + \Pi_x \tag{3.1}$$

$$GP_y = -\frac{1}{\rho_0}\frac{\partial p_a}{\partial y} - g\frac{\partial \zeta}{\partial y} + \Pi_y \tag{3.2}$$

where Π_x and Π_y are given by eqs. (1.45) and (1.46). The first two terms of each component are depth independent. Together they compose a contribution to the motion called the *barotropic mode* (*i.e.*: the *external mode*). In coastal areas, the barotropic mode may be larger than the *baroclinc mode* (*i.e.*: the *internal mode*) associated to the second part Π_x (resp. Π_y) of the pressure gradient.

Numerical models of ocean circulation typically include moving external gravity waves, which are essentially two-dimensional, and a variety of other internal motions which are much slower and generally three-dimensional. In a number of ocean models, the computational problems resulting from the multiple time scales are addressed by splitting the fast and slow dynamics into separate subproblems that are solved by different techniques.

The fast external motions can be modelled accurately with a two-dimensional barotropic subsystem dealing with the shallow water equations for a homogeneous fluid. The remaining slow motions can be modelled by a three-dimensional baroclinic subsystem.

The MARS approach uses the same dependent variables as in the original unsplit system, but at the end of each baroclinic time step it adjusts these variables to maintain consistency with the results computed using the barotropic equations.

3.1.1 Vertical discretization

The vertical extension $-1 < \sigma < 0$ is staggered into k_{max} ($\sigma_k,\ k = 1 \cdots k_{max}$) levels. The σ distribution is given by eq. (1.29). Then, for each σ_k level we can define a "water slice" $\Delta\sigma_k$ satisfying the condition:

$$\sum_{k=1}^{k_{max}} \Delta\sigma_k = 1 \tag{3.3}$$

3.1.2 Vertical summing

Introducing (3.1) and (3.2) in the momentum equations (1.47) and (1.48) gives:

$$\begin{aligned}
\frac{\partial u_k}{\partial t} + u_k\frac{\partial u_k}{\partial x} + v_k\frac{\partial u_k}{\partial y} + \tilde{w}_k\frac{\partial u_k}{\partial \sigma} - fv_k &= -\frac{1}{\rho_0}\frac{\partial p_a}{\partial x} - g\frac{\partial \zeta}{\partial x} + \Pi_{x,k} + \frac{1}{\rho_0}\left(\frac{\partial \tau_{xx,k}}{\partial x} + \frac{\partial \tau_{xy,k}}{\partial y}\right) \\
&\quad + \frac{1}{\rho_0 H_z}\frac{\tau_{xz,k+1/2} - \tau_{xz,k-1/2}}{\Delta\sigma_k} \\
\frac{\partial v_k}{\partial t} + u_k\frac{\partial v_k}{\partial x} + v_k\frac{\partial v_k}{\partial y} + \tilde{w}_k\frac{\partial v_k}{\partial \sigma} + fu_k &= -\frac{1}{\rho_0}\frac{\partial p_a}{\partial y} - g\frac{\partial \zeta}{\partial y} + \Pi_{y,k} + \frac{1}{\rho_0}\left(\frac{\partial \tau_{yx,k}}{\partial x} + \frac{\partial \tau_{yy,k}}{\partial y}\right) \\
&\quad + \frac{1}{\rho_0 H_z}\frac{\tau_{yz,k+1/2} - \tau_{xz,k-1/2}}{\Delta\sigma_k}
\end{aligned}$$

where $\tau_{xz,k+1/2}$ ($\tau_{xz,k-1/2}$) is the vertical friction term along x at the top (bottom) of the cell k of thickness $\Delta\sigma_k$.

Introducing the vertical sum operator $\bar{a}$:

$$A = \bar{a} \equiv \sum_{k=1}^{k_{max}} a_k \Delta\sigma_k \tag{3.4}$$

gives:

$$\begin{aligned}
\frac{\partial U}{\partial t} + \underbrace{\overline{u\frac{\partial u}{\partial x} + v\frac{\partial u}{\partial y} + \tilde{w}\frac{\partial u}{\partial \sigma}}}_{ADX} - f\bar{v} &= -\frac{1}{\rho_0}\frac{\partial p_a}{\partial x} - g\frac{\partial \zeta}{\partial x} + \overline{\Pi}_x + \underbrace{\frac{1}{\rho_0}\overline{\left(\frac{\partial \tau_{xx}}{\partial x} + \frac{\partial \tau_{xy}}{\partial y}\right)}}_{DHX} \\
&\quad + \frac{\tau_{sx} - \tau_{bx}}{\rho_0 h} \qquad (3.5) \\
\frac{\partial V}{\partial t} + \underbrace{\overline{u\frac{\partial v}{\partial x} + v\frac{\partial v}{\partial y} + \tilde{w}\frac{\partial v}{\partial \sigma}}}_{ADY} + f\bar{u} &= -\frac{1}{\rho_0}\frac{\partial p_a}{\partial y} - g\frac{\partial \zeta}{\partial y} + \overline{\Pi}_y + \underbrace{\frac{1}{\rho_0}\overline{\left(\frac{\partial \tau_{yx}}{\partial x} + \frac{\partial \tau_{yy}}{\partial y}\right)}}_{DHY} \\
&\quad + \frac{\tau_{sy} - \tau_{by}}{\rho_0 h} \qquad (3.6)
\end{aligned}$$

The continuity equation becomes:

$$\frac{\partial \zeta}{\partial t} + \frac{\partial (h u_k)}{\partial x} + \frac{\partial (h v_k)}{\partial y} + \frac{h(\tilde{w}_{k+1/2} - \tilde{w}_{k-1/2})}{\Delta\sigma_k} = h\phi_k$$

The vertical sum gives:

$$\frac{\partial \zeta}{\partial t} + \frac{\partial (hU)}{\partial x} + \frac{\partial (hV)}{\partial y} = h\bar{\phi} \tag{3.7}$$

The system being solved is now composed of eqs. (3.5-3.7) associated with eqs. (1.47-1.50) *via* :

- the advection terms ADX and ADY
- the horizontal diffusion terms DHX and DHY
- the baroclinic pressure gradient components $(\overline{\Pi}_x, \overline{\Pi}_y)$
- the bottom friction (τ_{bx}, τ_{by})

3.1.3 2Dh model

Assuming $\partial u/\partial\sigma \approx 0$, *i.e.* $u_k = U\ \forall k$, likewise for v, then eqs. (3.5) and (3.6) become:

$$\begin{aligned}
\frac{\partial U}{\partial t} + U\frac{\partial U}{\partial x} + V\frac{\partial V}{\partial y} + g\frac{\partial \zeta}{\partial x} - fV &= -\frac{1}{\rho_0}\frac{\partial p_a}{\partial x} + \overline{\Pi}_x + DHX + \frac{\tau_{sx} - \tau_{bx}}{\rho_0 h} \qquad (3.8) \\
\frac{\partial V}{\partial t} + U\frac{\partial V}{\partial x} + V\frac{\partial V}{\partial y} + g\frac{\partial \zeta}{\partial y} + fU &= -\frac{1}{\rho_0}\frac{\partial p_a}{\partial y} + \overline{\Pi}_y + DHY + \frac{\tau_{sy} - \tau_{by}}{\rho_0 h} \qquad (3.9)
\end{aligned}$$

Assuming a parameterization of the turbulent horizontal diffusion based on the velocity components U and V, the system composed of eqs. (3.7) to (3.9) is a *self-sufficient* system. Then the MARS model is running in a 2Dh configuration.

The bottom friction is given by the Strickler formulation:

$$(\frac{\tau_{bx}}{\rho_0 h}, \frac{\tau_{by}}{\rho_0 h}) = \frac{g \cdot \|U\|}{S_t^2 \cdot h^{4/3}} \ (U, V) \tag{3.10}$$

where

$$\|U\| = \sqrt{U^2 + V^2} \tag{3.11}$$

S_t is the Strickler parameter.

3.1.4 2D-3D model

Let us introduce the shorthand systems:

Baroclinic mode :

$$\frac{\partial u}{\partial t} = -g\frac{\partial \zeta}{\partial x} + G_u \tag{3.12}$$

$$\frac{\partial v}{\partial t} = -g\frac{\partial \zeta}{\partial y} + G_v \tag{3.13}$$

with:

$$G_u = fv - L(u) - \frac{1}{\rho_0}\frac{\partial p_a}{\partial x} + \Pi_x + \frac{1}{H_z}\frac{\left(\frac{\nu_z}{H_z}\frac{\partial u}{\partial \sigma}\right)}{\partial \sigma} + \mathcal{F}_x \tag{3.14}$$

$$G_v = -fu - L(v) - \frac{1}{\rho_0}\frac{\partial p_a}{\partial y} + \Pi_y + \frac{1}{H_z}\frac{\left(\frac{\nu_z}{H_z}\frac{\partial v}{\partial \sigma}\right)}{\partial \sigma} + \mathcal{F}_y \tag{3.15}$$

Barotropic mode:

$$\frac{\partial U}{\partial t} = -g\frac{\partial \zeta}{\partial x} + \bar{G}_u \tag{3.16}$$

$$\frac{\partial V}{\partial t} = -g\frac{\partial \zeta}{\partial y} + \bar{G}_v \tag{3.17}$$

$$\tag{3.18}$$

with:

$$\bar{G}_u = \sum_{k=1}^{k_{max}} (fv_k - L(u)_k + \pi_{xk} + \mathcal{F}_{xk})\,\Delta\sigma_k - \frac{1}{\rho_0}\frac{\partial p_a}{\partial x} + \Pi_x + \frac{\tau_{sx} - \tau_{bx}}{\rho_0 h^u} \tag{3.19}$$

$$\bar{G}_v = \sum_{k=1}^{k_{max}} (-fu_k - L(v)_k + \pi_{yk} + \mathcal{F}_{yk})\,\Delta\sigma_k - \frac{1}{\rho_0}\frac{\partial p_a}{\partial y} + \Pi_y + \frac{\tau_{sy} - \tau_{by}}{\rho_0 h^v} \tag{3.20}$$

The depths h^u and h^v are defined at the u and v points (*cf.* § 3.3)

3.2 Numerical schemes

The aim of this section is to provide some information about the finite difference schemes in both space and time proposed by the MARS model for updating ζ, U, V, u and v

From time step n (t_n) to t_{n+1}, the time scheme is based on a two-time level method :

1 - at an intermediate time step $t_{n+1/2}$, the variables (ζ, U, u) then (ζ, V, v) are first updated ;
2 - then at time step t_{n+1}, variables (ζ, V, v) and (ζ, U, u).

3.2.1 2D time scheme

Neglecting the right hand sides in eqs. (3.7) to (3.9):

First step

$$\begin{cases} U^{n+\frac{1}{2},*} = U^n - \frac{1}{2}\Delta t \left(g\frac{\partial \zeta^n}{\partial x} + fV^n + U^n\frac{\partial U^n}{\partial x} + V^n\frac{\partial U^n}{\partial y} \right) \\ V^{n+\frac{1}{2},*} = V^n - \frac{1}{2}\Delta t \left(g\frac{\partial \zeta^n}{\partial y} - fU^n + U^n\frac{\partial V^n}{\partial x} + V^n\frac{\partial V^n}{\partial y} \right) \end{cases} \tag{3.21}$$

$$\begin{cases} \zeta^{n+\frac{1}{2},*} = \zeta^n - \frac{1}{2}\Delta t \left(\frac{\partial h^n U^{n+\frac{1}{2}}}{\partial x} + \frac{\partial h^n V^{n+\frac{1}{2},*}}{\partial y} \right) \\ U^{n+\frac{1}{2}} = U^n - \frac{1}{2}\Delta t \left(g\frac{\partial \zeta^{n+\frac{1}{2},*}}{\partial x} + fV^{n+\frac{1}{2},*} + U^{n+\frac{1}{2},*}\frac{\partial U^{n+\frac{1}{2},*}}{\partial x} + V^{n+\frac{1}{2},*}\frac{\partial U^{n+\frac{1}{2},*}}{\partial y} \right) \end{cases} \tag{3.22}$$

$$\begin{cases} \zeta^{n+\frac{1}{2}} = \zeta^n - \frac{1}{2}\Delta t \left(\frac{\partial h^{n+\frac{1}{2},*} U^{n+\frac{1}{2}}}{\partial x} + \frac{\partial h^{n+\frac{1}{2},*} V^{n+\frac{1}{2}}}{\partial y} \right) \\ V^{n+\frac{1}{2}} = V^n - \frac{1}{2}\Delta t \left(g\frac{\partial \zeta^{n+\frac{1}{2}}}{\partial y} - fU^{n+\frac{1}{2}} + U^{n+\frac{1}{2}}\frac{\partial V^{n+\frac{1}{2},*}}{\partial x} + V^{n+\frac{1}{2},*}\frac{\partial V^{n+\frac{1}{2},*}}{\partial y} \right) \end{cases} \tag{3.23}$$

Second step

$$\begin{cases} U^{n+1,*} = U^{n+\frac{1}{2}} - \frac{1}{2}\Delta t \left(g\frac{\partial \zeta^{n+\frac{1}{2}}}{\partial x} + fV^{n+\frac{1}{2}} + U^{n+\frac{1}{2}}\frac{\partial U^{n+\frac{1}{2}}}{\partial x} + V^{n+\frac{1}{2}}\frac{\partial U^{n+\frac{1}{2}}}{\partial y} \right) \\ V^{n+1,*} = V^{n+\frac{1}{2}} - \frac{1}{2}\Delta t \left(g\frac{\partial \zeta^{n+\frac{1}{2}}}{\partial y} - fU^{n+\frac{1}{2}} + U^{n+\frac{1}{2}}\frac{\partial V^{n+\frac{1}{2}}}{\partial x} + V^{n+\frac{1}{2}}\frac{\partial V^{n+\frac{1}{2}}}{\partial y} \right) \end{cases} \tag{3.24}$$

$$\begin{cases} \zeta^{n+1,*} = \zeta^{n+\frac{1}{2}} - \frac{1}{2}\Delta t \left(\frac{\partial h^{n+\frac{1}{2}} U^{n+1,*}}{\partial x} + \frac{\partial h^{n+\frac{1}{2}} V^{n+1}}{\partial y} \right) \\ V^{n+1} = V^{n+\frac{1}{2}} - \frac{1}{2}\Delta t \left(g\frac{\partial \zeta^{n+1,*}}{\partial y} - fU^{n+1,*} + V^{n+1,*}\frac{\partial V^{n+1,*}}{\partial y} \right) \end{cases} \tag{3.25}$$

$$\left\{ \begin{array}{l} \zeta^{n+1} = \zeta^{n+\frac{1}{2}} - \dfrac{1}{2}\Delta t \left(\dfrac{\partial h^{n+1,*} U^{n+1}}{\partial x} + \dfrac{\partial h^{n+1,*} V^{n+1}}{\partial y} \right) \\ \\ U^{n+1} = U^{n+\frac{1}{2}} - \dfrac{1}{2}\Delta t \left(g \dfrac{\partial \zeta^{n+1}}{\partial x} + f V^{n+1} + U^{n+1,*} \dfrac{\partial U^{n+1,*}}{\partial x} + V^{n+1} \dfrac{\partial U^{n+1,*}}{\partial y} \right) \end{array} \right. \tag{3.26}$$

Among the precedings forms, steps (3.21) and (3.24) are explicit updates of the barotropic velocity components U and V. This first step was included to reduce the artificial diffusivity induced by the finite difference representation of the nonlinear terms.

The following forms (3.22) and (3.23) then (3.25) and (3.26) are semi-implicit updates.

This algoritm requires four linear systems to be solved at each time step (*cf.* appendix D).

3.2.2 2D-3D time scheme

Introducing $G_u(u,v)$ eq. (3.14) and $G_v(u,v)$ eq. (3.15) and the depth integrated forms $\bar{G}_u(u,v)$ eq. (3.19) and $\bar{G}_v(u,v)$ eq. (3.20), the 2D-3D time scheme is written as :

First step

$$\left\{ V^{n+\frac{1}{2},*} = V^n - \frac{1}{2}\Delta t \left(g \frac{\partial \zeta^n}{\partial y} + \bar{G}_v(u^{n-\frac{1}{2}}, v^{n-\frac{1}{2}}) \right) \right. \tag{3.27}$$

$$\left\{ \begin{array}{l} \zeta^{n+\frac{1}{2},*} = \zeta^n - \dfrac{1}{2}\Delta t \left(\dfrac{\partial h^n U^{n+\frac{1}{2}}}{\partial x} + \dfrac{\partial h^n V^{n+\frac{1}{2},*}}{\partial y} \right) \\ \\ U^{n+\frac{1}{2}} = U^n - \dfrac{1}{2}\Delta t \left(g \dfrac{\partial \zeta^{n+\frac{1}{2},*}}{\partial x} + \bar{G}_u(u^n, v^n) \right) \\ \\ u^{n+\frac{1}{2}} = u^n - \dfrac{1}{2}\Delta t \left(g \dfrac{\partial \zeta^{n+\frac{1}{2},*}}{\partial x} + G_u(u^n, v^n) \right) \end{array} \right. \tag{3.28}$$

$$\left\{ \begin{array}{l} \zeta^{n+\frac{1}{2}} = \zeta^n - \dfrac{1}{2}\Delta t \left(\dfrac{\partial h^{n+\frac{1}{2}} U^{n+\frac{1}{2},*}}{\partial x} + \dfrac{\partial h^{n+\frac{1}{2}} V^{n+\frac{1}{2},*}}{\partial y} \right) \\ \\ V^{n+\frac{1}{2}} = V^n - \dfrac{1}{2}\Delta t \left(g \dfrac{\partial \zeta^{n+\frac{1}{2}}}{\partial y} + \bar{G}_v(u^{n+\frac{1}{2}}, v^n) \right) \\ \\ v^{n+\frac{1}{2}} = v^n - \dfrac{1}{2}\Delta t \left(g \dfrac{\partial \zeta^{n+\frac{1}{2}}}{\partial y} + G_v(u^{n+\frac{1}{2}}, v^n) \right) \end{array} \right. \tag{3.29}$$

For a constituent T (*cf.* eq. 1.27) :

$$\left\{ h^{n+\frac{1}{2}}T^{n+\frac{1}{2}} = h^nT^n - \frac{1}{2}\Delta t\left(\frac{\partial h^{n+\frac{1}{2},*}u^{n+\frac{1}{2}}T^n}{\partial x} + \frac{\partial h^{n+\frac{1}{2},*}v^{n+\frac{1}{2}}T^n}{\partial y} + \frac{\partial h^{n+\frac{1}{2},*}w^{n+\frac{1}{2}}T^{n+\frac{1}{2}}}{\partial z}\right) \right. \tag{3.30}$$

Second step

$$\left\{ U^{n+1,*} = U^{n+\frac{1}{2}} - \frac{1}{2}\Delta t\left(g\frac{\partial \zeta^{n+\frac{1}{2}}}{\partial x} + \bar{G}_v(u^n, v^n)\right) \right. \tag{3.31}$$

$$\left\{ \begin{array}{l} \zeta^{n+1,*} = \zeta^{n+\frac{1}{2}} - \frac{1}{2}\Delta t\left(\frac{\partial h^{n+\frac{1}{2}}U^{n+1,*}}{\partial x} + \frac{\partial h^{n+\frac{1}{2}}V^{n+1}}{\partial y}\right) \\ V^{n+1} = V^{n+\frac{1}{2}} - \frac{1}{2}\Delta t\left(g\frac{\partial \zeta^{n+1,*}}{\partial y} + \bar{G}_v(u^{n+\frac{1}{2}}, v^{n+\frac{1}{2}})\right) \\ v^{n+1} = v^{n+\frac{1}{2}} - \frac{1}{2}\Delta t\left(g\frac{\partial \zeta^{n+1,*}}{\partial y} + G_v(u^{n+\frac{1}{2}}, v^{n+\frac{1}{2}})\right) \end{array} \right. \tag{3.32}$$

$$\left\{ \begin{array}{l} \zeta^{n+1} = \zeta^{n+\frac{1}{2}} - \frac{1}{2}\Delta t\left(\frac{\partial h^{n+1,*}U^{n+1}}{\partial x} + \frac{\partial h^{n+1,*}V^{n+1}}{\partial y}\right) \\ U^{n+1} = U^{n+\frac{1}{2}} - \frac{1}{2}\Delta t\left(g\frac{\partial \zeta^{n+1}}{\partial x} + \bar{G}_u(u^{n+\frac{1}{2}}, v^{n+1})\right) \\ u^{n+1} = v^{n+\frac{1}{2}} - \frac{1}{2}\Delta t\left(g\frac{\partial \zeta^{n+1}}{\partial x} + G_u(u^{n+\frac{1}{2}}, v^{n+1})\right) \end{array} \right. \tag{3.33}$$

$$\left\{ h^{n+1}T^{n+1} = h^{n+\frac{1}{2}}T^{n+\frac{1}{2}} - \frac{1}{2}\Delta t\left(\frac{\partial h^{n+1,*}u^{n+1}T^{n+\frac{1}{2}}}{\partial x} + \frac{\partial h^{n+1,*}v^{n+1}T^{n+\frac{1}{2}}}{\partial y} + \frac{\partial h^{n+1,*}w^{n+1}T^{n+1}}{\partial z}\right) \right. \tag{3.34}$$

In the first step, updates $U^{n+\frac{1}{2},*}$ and $V^{n+1,*}$ are omitted. In order to turn down the artificial diffusivity problem induced by the nonlinear terms representation, these terms have been included in the depth integrated terms $\bar{G}_u$, $\bar{G}_v$ which are computed at each intermediate time step.

Some numerical tests proved that this *two step* method provides accurate solutions (u,v) according to the depth integrated variables (U,V).

3.2.3 Automatic time step control

The Courant-Friedrichs-Lewy condition (CFL condition) is a necessary condition for convergence while solving partial differential equations. The condition $CFL < 1$ applies, generally, to explicit schemes for hyperbolic partial differential equations. Physically, the CFL condition indicates that a particle of fluid should not travel more than one saptail step-size Δx in one time-step ΔT. The CFL condition ($CFL < 1$) is not a necessary condition for both the explicit and semi-implicit

schemes used in the MARS model.

Nevertheless there is a stability condition related to the nonlinear terms. This constraint was empirically formulated following a CFL condition:

$$\frac{u\Delta t}{\Delta x} < CFL_{crit}$$

where Δx is the grid size in the x direction. Typically we have $CFL_{crit} = 0.7$

The following method has been implemented in MARS to adapt the time step to local hydrodynamical conditions:

1. $CFL_{ref} \leftarrow 0 \qquad t_{ref} \leftarrow t$
2. Compute CFL criterion at surface level ($k = k_{max}$) at time t : CFL_{max}
3. If $CFL_{max} < CFL_{crit}$, go to **6**
4. Compute Δt where $CFL_{max} = 0.5$
5. If $\Delta t < 10\,s$: Stop
6. $CFL_{ref} \leftarrow \max(CFL_{max}, CFL_{ref})$
7. If $t < (t_{ref} + t_{obs})$, go to **2** at the next time step
8. In case $CFL_{ref} < 0.84 \cdot CFL_{crit}$, time step is increased : $\Delta t \leftarrow 1.2 \cdot \Delta t$ then go to **1** (at the next time step)

Regarding the 2Dh model, the time step is adjusted as follows:

1. Compute the maximum CFL number at time t : CFL_{max}
2. In case $CFL_{max} < CFL_{crit}$ the "correction factor" $facor$ will be :

$$facor = \min(1 + 5\left(1 - \frac{CFL_{max}}{CFL_{crit}}\right), 1.02)$$

   otherwise :

$$facor = \max(1 - 10\left(\frac{CFL_{max}}{CFL_{crit}} - 1\right), 0.8)$$

3. Compute the new time step Δt : $\Delta t \leftarrow facor \cdot \Delta t$
4. If $\Delta t < 3\,s$: Stop.

3.2.4 Advection schemes

Let us consider a scalar field q associating a scalar value to every point in a space. The transport equation of this quantity by a velocity field $\mathbf{u}$ is given by the general advective form :

$$\frac{\partial q}{\partial t} + \mathbf{u}.\nabla q = 0 \tag{3.35}$$

For an incompressible fluid, the divergence of the velocity is zero everywhere (*cf.* §1.1) then eq. (3.35) may be rewritten in the conservative form :

$$\frac{\partial q}{\partial t} + \nabla.(\mathbf{u}q) = 0 \tag{3.36}$$

A typical bidimensional finite difference time scheme of the preceding form is given by:

$$q_{i,j}^{n+1} = q_{i,j}^{n} - \frac{\Delta t}{\Delta x}\left(F^{u}_{i+\frac{1}{2},j}[q^n] - F^{u}_{i-\frac{1}{2},j}[q^n]\right) - \frac{\Delta t}{\Delta y}\left(F^{v}_{i,j+\frac{1}{2}}[q^n] - F^{v}_{i,j-+\frac{1}{2}}[q^n]\right) \tag{3.37}$$

Δx and Δy are grid size parameters (*cf.* sect. 3.3). F^u and F^v are q fluxes on both sides of a cell centered at $(x_i, y_j) = (i\Delta x, j\Delta y)$. Repeated use of (3.37) generates the solution at all interior grid points (i, j) at time level $(n + 1)$. Incrementing n and substituting the values $q_{i,j}^{n+1}$ into the right hand side of (3.37) allows the discrete solution to be marched forward in time.

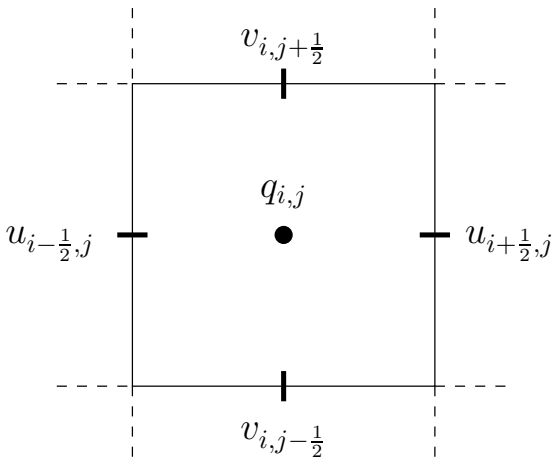

Figure 3.1: Horizontal grid

The horizontal arrangement of variables used in MARS is equivalent to the well known Arakawa C grid (*cf.* Fig. 3.2.4). The horizontal velocity component u is defined at points $(x_{i+\frac{1}{2}}, y_j)$ (resp.: v at points $(x_i, y_{j+\frac{1}{2}})$).

On the right side of a cell (i, j) we can write:

$$F^{u}_{i+\frac{1}{2},j} = u_{i+\frac{1}{2},j}\hat{q}_{i+\frac{1}{2},j,n} \tag{3.38}$$

where $\hat{q}_{i+\frac{1}{2},j,n}$ is an estimate of q at point $(i + \frac{1}{2}, j)$.

The finite difference scheme (3.37) does not consider the cross derivatives. Therefore, the final numerical representation should be a first-order scheme of eq. (3.36), whatever the order of the algorithm used to estimate (3.38).

An alternative method for obtaining a better order scheme is the two-step method (MACHO) developed by IFREMER:

1 - First step : the advective form (3.35) is used to compute a prediction $q_{i,j}^{AX}$ (in x direction ;
2 - Second step : the general scheme (3.37) is used to solve the conservative form (3.36) at time step $n+1$.

$$\begin{cases} q_{i,j}^{AX} = q_{i,j}^{n} - \dfrac{\Delta t}{\Delta x} u_{i,j}^{a} \left(\hat{q}_{i+\frac{1}{2},j}^{n} - \hat{q}_{i-\frac{1}{2},j}^{n} \right) \\ q_{i,j}^{n+1} = q_{i,j}^{n} - \dfrac{\Delta t}{\Delta x} \left(F_{i+\frac{1}{2},j}^{u}[q^{n}] - F_{i-\frac{1}{2},j}^{u}[q^{n}] \right) - \dfrac{\Delta t}{\Delta y} \left(F_{i,j+\frac{1}{2}}^{v}[q^{AX}] - F_{i,j-\frac{1}{2}}^{v}[q^{AX}] \right) \end{cases} \tag{3.39}$$

$u_{i,j,}^{a}$ is the mean velocity component u in the cell (i,j). Thus, in y direction y we have:

$$\begin{cases} q_{i,j}^{AY} = q_{i,j}^{n} - \dfrac{\Delta t}{\Delta y} v_{i,j}^{a} \left(\hat{q}_{i,j+\frac{1}{2}}^{n} - \hat{q}_{i,j-\frac{1}{2}}^{n} \right) \\ q_{i,j}^{n+1} = q_{i,j}^{n} - \dfrac{\Delta t}{\Delta x} \left(F_{i+\frac{1}{2},j}^{u}[q^{AY}] - F_{i-\frac{1}{2},j}^{u}[q^{AY}] \right) - \dfrac{\Delta t}{\Delta y} \left(F_{i,j+\frac{1}{2}}^{v}[q^{n}] - F_{i,j-\frac{1}{2}}^{v}[q^{n}] \right) \end{cases} \tag{3.40}$$

Some properties of numerical schemes

Let us note:

$$C_x = u_{i+\frac{1}{2},j} \frac{\Delta t}{\Delta x} \qquad C_y = v_{i,j+\frac{1}{2}} \frac{\Delta t}{\Delta y} \qquad CFL = \max\left(|C_x|, |C_y|\right) \tag{3.41}$$

C_x and C_y are horizontal Courant numbers for the u, v grid points. CFL is the global Courant number .

Asuming a stationary field, eq. (3.37) may be written :

$$q_{i,j}^{n+1} = q_{i,j}^{n} - C_x \left(\hat{q}_{i+\frac{1}{2},j} - \hat{q}_{i-\frac{1}{2},j} \right) - Cy \left(\hat{q}_{i,j+\frac{1}{2}} - \hat{q}_{i,j-\frac{1}{2}} \right) \tag{3.42}$$

Assuming $v = 0$, the preceding form becomes:

$$q_{i,j}^{n+1} = q_{i,j}^{n} - C_x \left(\hat{q}_{i+\frac{1}{2},j} - \hat{q}_{i-\frac{1}{2},j} \right) \tag{3.43}$$

Order

Let us consider $u(x,y,t) = u_0$, then the truncation error:

$$err = \frac{1}{\Delta t} \left(q_{i,j}^{n+1} - q(x_i, y_j, t^{n+1}) \right) = \mathrm{O}\left(\Delta x^{l}, \Delta t^{m} \right) \tag{3.44}$$

where $q_{i,j}^{n+1}$ is the computational solution at time $n+1$ and $q(x_i, y_j, t^{n+1})$ the true solution. l and m are integers related to space and time orders of the numerical scheme.

Under the CFL condition $CFL < 1$, the space parameters Δx and Δt are linked by the relationship $u_0 \Delta t = CFL.\Delta x$. A global numerical error in space and time is given by:

$$err = \mathrm{O}\left(\Delta x^l\right) + \mathrm{O}\left(\Delta t^m\right) + \sum_{p=1}^{r-1} \mathrm{O}\left(\Delta x^{r-p} \Delta t^p\right) = \mathrm{O}\left(\Delta t^m\right) \tag{3.45}$$

where $r = \min l, m$ is the global order of the scheme.

Stability

The stability of numerical schemes is closely associated with numerical error. The stability of a numerical scheme can be investigated by performing the Von Neumann stability analysis. The von Neumann stability analysis provides the amplitude ratio :

$$A = \left| \frac{q_{i,j}^{n+1}}{q_{i,j}^{n}} \right| \tag{3.46}$$

The necessary and sufficient condition for the error to remain bounded is that $A \leq 1$.

Euler-Quickest

The *Quickest* [1] scheme originally developed by Leonard (1979), [19] is based on a three-point upstream-weight quadratic interpolation:

$$q_{i+\frac{1}{2},j}^{qst} = \begin{cases} q_{i,j} + \tilde{\alpha}_1(q_{i+1,j} - q_{i,j}) + \tilde{\alpha}_2(q_{i,j} - q_{i-1,j}) & \text{if} \quad u > 0 \\ \\ q_{i+1,j} + \tilde{\alpha}_1(q_{i,j} - q_{i+1,j}) + \tilde{\alpha}_2(q_{i+2,j} - q_{i+1,j}) & \text{if} \quad u < 0 \end{cases} \tag{3.47}$$

with $\alpha_1 = \frac{1}{6}(1 - CFL)(2 - CFL)$ and $\alpha_2 = \frac{1}{6}(1 - CFL)(1 + CFL)$. The truncation error may be written:

$$\begin{aligned} err^{qst} &= -\frac{1}{24}\delta_x^4 q u_0 \left(2\Delta x^3 - u_0 \Delta t \Delta x^2 - 2(u_0 \Delta t)^2 \Delta x + (u_0 \Delta t)^3\right) \\ &\quad + \mathrm{O}\left(\Delta x^4\right) + \mathrm{O}\left(\Delta x^2 \Delta t^2\right) + \mathrm{O}\left(\Delta t^4\right) \\ &= -\frac{1}{24}\delta_x^4 q u_0 \left(2 - CFL - 2CFL^2 + CFL^3\right) \Delta x^3 + \mathrm{O}\left(\Delta x^4\right) \end{aligned}$$

This results in a third-order convective differencing scheme. The amplification factor is given by:

$$A^{qst} = 1 - \frac{1}{24} CFL(CFL-1)(CFL-2)(CFL+1) k^4 \Delta x^4 + \mathrm{O}\left(k^6 \Delta x^6\right)$$

The truncation error is equivalent to a fourth-order numerical diffusion. The Quickest scheme is stable under the condition: $CFL \in [0, 1]$

[1] QUICKEST : Quadratic Upstream Interpolation for Convective Kinematics with Estimated Streaming Terms

Ultimate-Quickest

The Quickest scheme given in eq. (3.47) can be written as :

$$q^{qst}_{i+\frac{1}{2},j} = \begin{cases} q_{i,j} + (q_{i+1,j} - q_{i,j})\psi_{i+\frac{1}{2},j} & \text{if} \quad u > 0 \\ \\ q_{i+1,j}(q_{i,j} - q_{i+1,j})\psi_{i+\frac{1}{2},j} & \text{if} \quad u < 0 \end{cases} \tag{3.48}$$

where $\psi_{i+\frac{1}{2},j} = \tilde{\alpha}_1 + \tilde{\alpha}_2\theta_{i+\frac{1}{2},j}$ and :

$$\theta_{i+\frac{1}{2},j} = \begin{cases} \dfrac{(q_{i,j} - q_{i-1,j})}{(q_{i+1,j} - q_{i,j})} & \text{si} \quad u > 0 \\ \\ \dfrac{(q_{i+1,j} - q_{i+2,j})}{(q_{i,j} - q_{i+1,j})} & \text{si} \quad u < 0 \end{cases} \tag{3.49}$$

Even though the Quickest scheme is third-order accurate, it still suffers from numerical oscillations when discontinuities exist. Leonard (1991), [20] proposed a *monotonising* universal limiter (*i.e.* the *ultimate* algorithm) for the advection problem to eliminate unphysical oscillations without corrupting the expected accuracy of the underlying method. In the preceding condition (3.48), the quantity $\psi_{i+\frac{1}{2},j}$ is subsituted by a limited estimation $\psi^l_{i+\frac{1}{2},j}$ defined as:

$$\psi^l_{i+\frac{1}{2},j} = \max\left(0, \min\left(1, psi_{i+\frac{1}{2},j}, \frac{1-CFL}{CFL}\theta_{i+\frac{1}{2},j}\right)\right) \tag{3.50}$$

that yields :

$$q^{lqst}_{i+\frac{1}{2},j} = \begin{cases} q_{i,j} + (q_{i+1,j} - q_{i,j})\psi^l_{i+\frac{1}{2},j} & \text{si} \quad u > 0 \\ \\ q_{i+1,j}(q_{i,j} - q_{i+1,j})\psi^l_{i+\frac{1}{2},j} & \text{si} \quad u < 0 \end{cases} \tag{3.51}$$

Then we get a monotonic scheme with the same stability properties as the scheme without limiter.

A series of numerical tests were carried out to verify the performance of the Ultimate-Quickest scheme.

1D tests

To illustrate the behaviour of the two preceding schemes, we consider the propagation of 1D profiles at constant velocity:

1. A rectangle
2. An demi-ellipse
3. A gaussian

The Quickest scheme produces numerical oscillations (*cf.* Fig. 3.2., However the local discontinuities are greatly dampened using the Ultimate Quickest scheme. Moreover, the limiter maintains the amplitude of the profile.

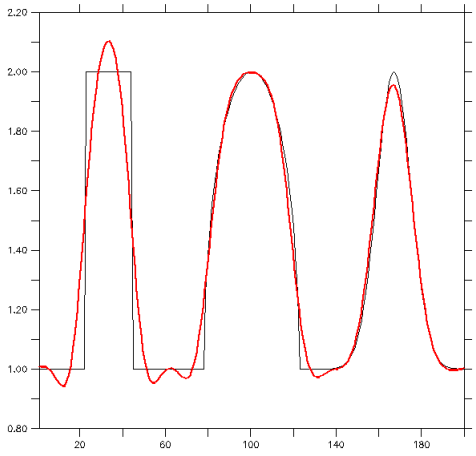

(c) Quickest ($CFL = 0.10$)

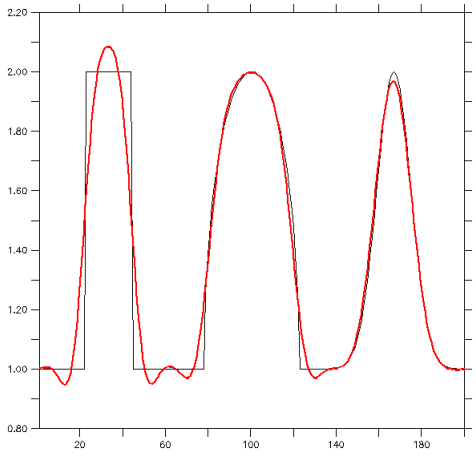

(d) Quickest ($CFL = 0.45$)

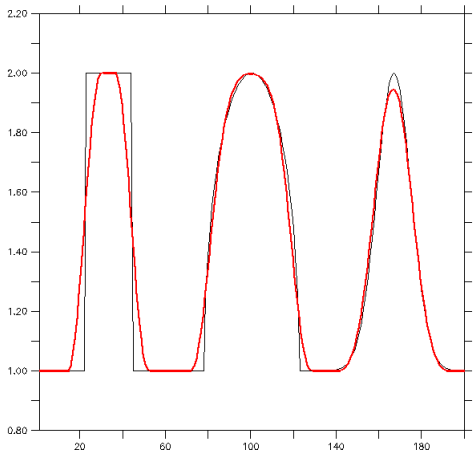

(e) Ultimate Quickest ($CFL = 0.10$)

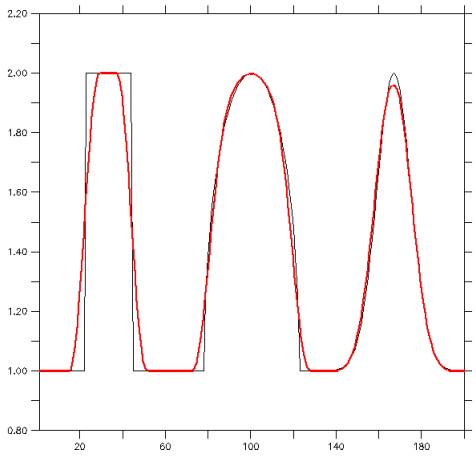

(e) Ultimate Quickest ($CFL = 0.45$)

Figure 3.2: Advection of 1D profiles at constant velocity. Quickest and Ultimate Quickest schemes.

2D tests

The pure advection of a gaussian column concentration distribution in a uniform 2-D flow field was studied (*cf.* Figs. 3.3 & 3.4)

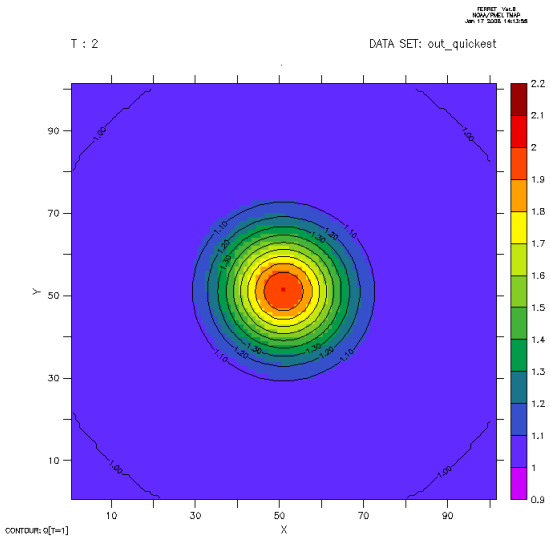

(a) Quickest ($CFL = 0.1$)

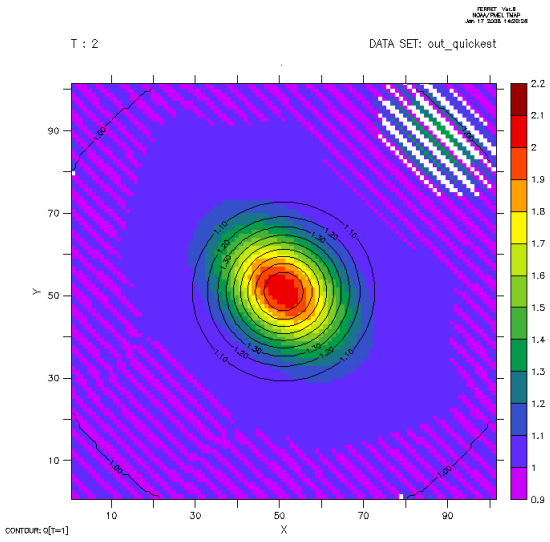

(b) Quickest ($CFL = 0.4$)

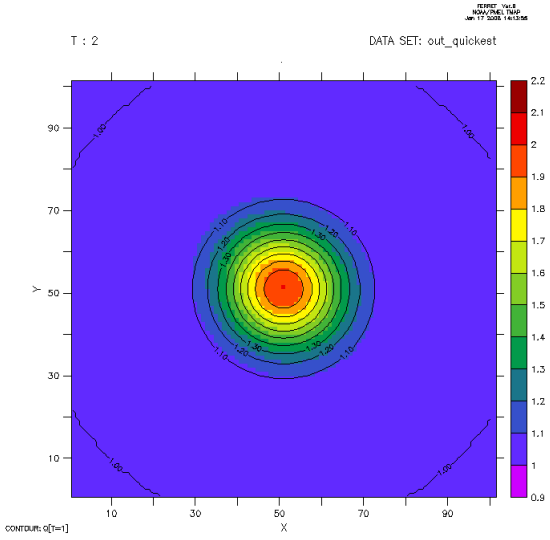

(a) Ultimate Quickest ($CFL = 0.1$)

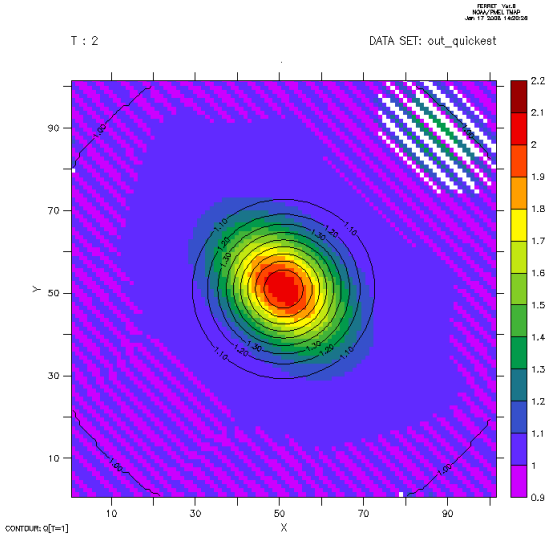

(b) Ultimate Quickest ($CFL = 0.4$)

Figure 3.3: Cas-test 2D-1. Advection of a gaussian column using the simple method (3.37).

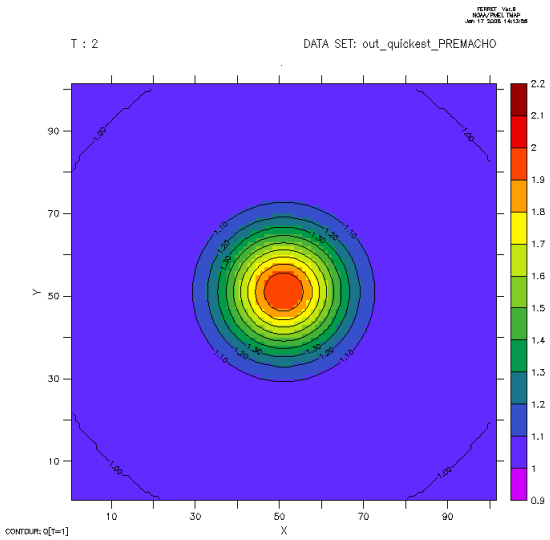

(a) Quickest ($CFL = 0.1$)

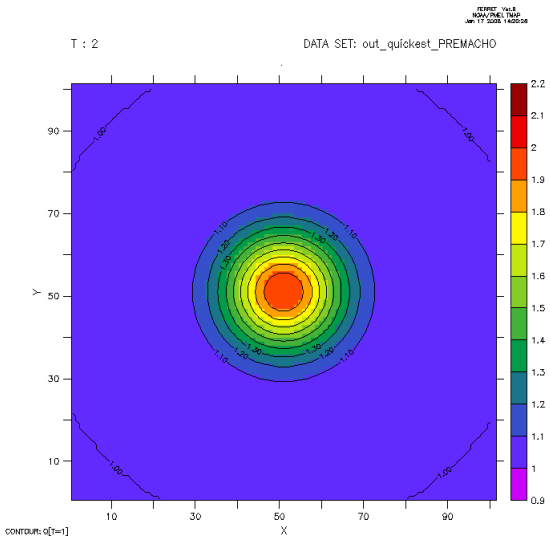

(b) Quickest ($CFL = 0.4$)

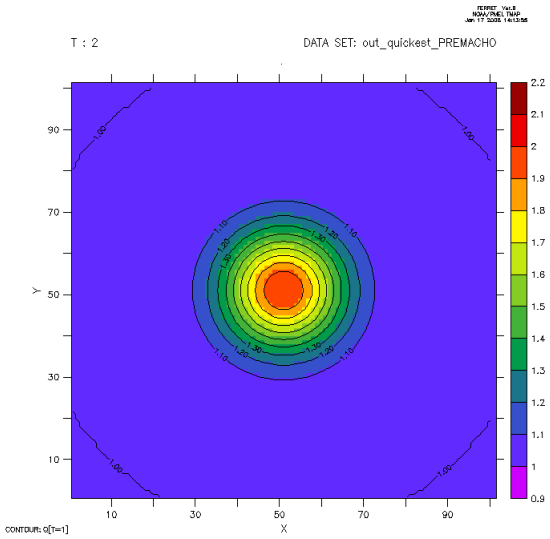

(a) Ultimate Quickest ($CFL = 0.1$)

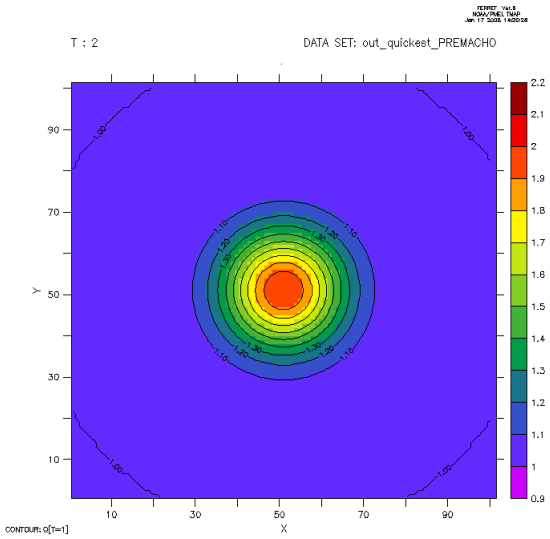

(b) Ultimate Quickest ($CFL = 0.4$)

Figure 3.4: Cas-test 2D-2. Advection a gaussian column using the MACHO method (3.39).

3.3 Vertical and horizontal discretization

The equations described above must be converted into corresponding algebraic equations in order to obtain the computational solution.

To convert the governing partial differential equations to a system of algebraic equations, a number of choices are available: finite difference, finite element, *etc.* In pratice, time derivatives are discretized almost exclusively using the finite difference method. In the MARS modelling system, the spatial derivatives are also approximated using finite difference.

3.3.1 Horizontal grid

The model domain is decomposed into cells. A cell is the basic unit of domain decomposition. The grid spacing can be set *via* two scalars : Δx and Δy. The indexing are i along x coordinate (from west to east) and j along y coordinate (from south to north). Within each cell, the horizontal arrangement of variables is shown in figure 3.5. This is equivalent to the well known Arakawa C grid (see Tab. 3.1).

The depth $H(x, y)$ must be specified at u and v points, locations where the horizontal velociy components are computed.

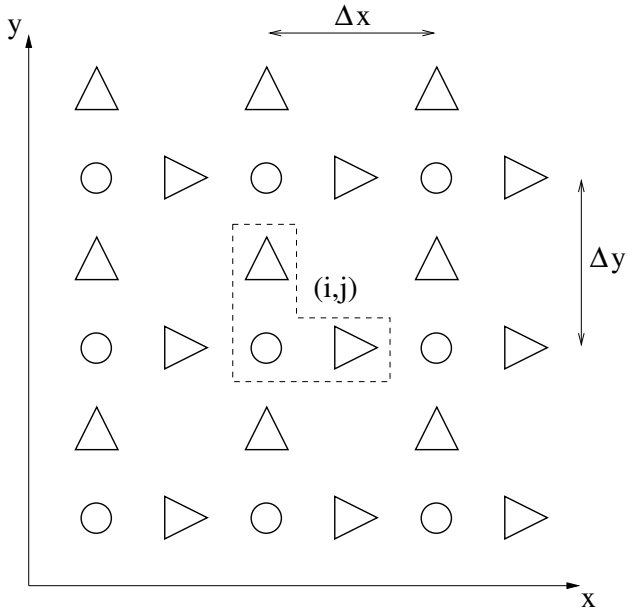

Figure 3.5: MARS-2D & 3D horizontal grid and variables arrangement in a cell.

symbols	variables
○	ζ, ρ, c, ν_H, ν_V, κ_V, k, $\tilde{w}$, p_a
▷	U, u, H^u
△	V, v, H^v

Table 3.1: List of variables in a cell (*cf.* Fig. 3.5)

3.3.2 Vertical grid

The model also uses a finite difference representation on the vertical axe (Fig. 3.6 and Tab. 3.2). The barotropic variables ζ, U and V are not considered here since they are depth-integrated variables. On the other hand, v points are not mentioned in Table 3.2 because the Figure 3.6 shows a transect across u points in figure 3.5.

A similar drawing should be obtain in the $(y\sigma)$ vertical plane.

The σ_k levels are distributed on points ρ and u ($\circ, \triangleright$) in figure 3.6; then the $\tilde{w}$ points ($\triangle$) are stagggered at levels:

$$\sigma_k^w = \frac{\sigma_k + \sigma_{k+1}}{2}$$

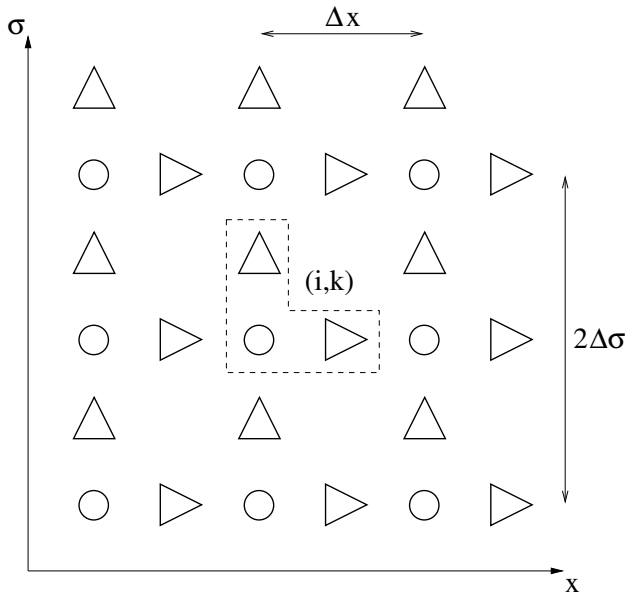

Figure 3.6: MARS-3D. Vertical grid and variables arrangement in a cell.

symbol	variable
$\circ$	ρ, c
$\triangleright$	u
$\triangle$	ν_V, κ_V, k, $\tilde{w}$

Table 3.2: List of variables in a cell (*cf.* Fig. 3.6)

3.4 Turbulence schemes

First we use a 1Dv (vertical) model to state the several turbulence schemes embedded in the MARS modelling system.

3.4.1 1Dv model

In a 1DV representation, the derivatives $\partial/\partial x$ and $\partial/\partial y$ are omitted in the primitive equations. Thus, we have to solve the simple forms:

$$\frac{\partial u_i}{\partial t} + 2\Omega \wedge u = \frac{\partial}{\partial z}\left(n_z \frac{\partial u_i}{\partial z}\right) + F \tag{3.52}$$

$$\frac{\partial T}{\partial t} = \frac{\partial}{\partial z}\left(k_z \frac{\partial T}{\partial z}\right) \tag{3.53}$$

F is an external forcing.

Computational grid

Figure 3.7 shows the vertical standard arrangement which can be used in one-dimensional numerical ocean models.

Discretisation

Equations (3.52) and (3.53) are solved using a fractional step method:

Step 1: *Diffusion step.* From t to $t+dt/2$: the following simple equation is considered:

$$\frac{\partial u_i}{\partial t} = \frac{\partial}{\partial z}\left(n_z \frac{\partial u_i}{\partial z}\right), \tag{3.54}$$

where u_i means u and v successively. This equation is solved using a semi-implicite method :

$$\begin{aligned}
\frac{{u_z}^{n+1/2,1}(k)^n_{u_i}(k)}{0.5\Delta t} &= \frac{\theta}{h^2 dsigu(k)}\left[n_z(k)\frac{{u_z}^{n+1/2}(k+1)-{u_z}^{n+1/2}(k)}{dsigw(k)}\right. \\
&- \left. n_z(k-1)\frac{{u_z}^{n+1/2}(k)-{u_z}^{n+1/2}(k-1)}{dsigw(k-1)}\right] \\
&+ \frac{1-\theta}{h^2 dsigu(k)}\left[n_z(k)\frac{{u_z}^{n}(k+1)-{u_z}^{n}(k)}{dsigw(k)}\right. \\
&- \left. n_z(k-1)\frac{{u_z}^{n}(k)-{u_z}^{n}(k-1)}{dsigw(k-1)}\right],
\end{aligned} \tag{3.55}$$

$$\begin{aligned}
\frac{{v_z}^{n+1/2,1}(k)^n_{v_i}(k)}{0.5\Delta t} &= \frac{\theta}{h^2 dsigu(k)}\left[n_z(k)\frac{{v_z}^{n+1/2}(k+1)-{v_z}^{n+1/2}(k)}{dsigw(k)}\right. \\
&- \left. n_z(k-1)\frac{{v_z}^{n+1/2}(k)-{v_z}^{n+1/2}(k-1)}{dsigw(k-1)}\right] \\
&+ \frac{1-\theta}{h^2 dsigu(k)}\left[n_z(k)\frac{{v_z}^{n}(k+1)-{v_z}^{n}(k)}{dsigw(k)}\right. \\
&- \left. n_z(k-1)\frac{{v_z}^{n}(k)-{v_z}^{n}(k-1)}{dsigw(k-1)}\right],
\end{aligned} \tag{3.56}$$

where θ is the implicit coefficient ($\theta = 1/2$). The suffix $n + 1/2, 1$ means the first estimate at time step $n + 1/2$.

Step 2 : *Coriolis step.*

$$u_z{}^{n+1/2,2}(k) = cos\,(fcor 0.5\Delta t)\, u_z{}^{n+1/2,1}(k) + sin\,(fcor 0.5\Delta t)\, v_z{}^{n+1/2,1}(k), \quad (3.57)$$
$$v_z{}^{n+1/2,2}(k) = -sin\,(fcor 0.5\Delta t)\, u_z{}^{n+1/2,1}(k) + cos\,(fcor 0.5\Delta t)\, v_z{}^{n+1/2,1}(k) \quad (3.58)$$

3.4.2 Turbulence equations discretization

The MARS-3D model is based on the two prognostic turbulence equations given in section 2.1.3 :

1 - TKE eq. (2.16);
2 - ψ parameter eq. (2.17).

Note: The advection terms have been neglected in these equations.

TKE discretisation

The following finite difference representation of the TKE equation is adopted:

$$\begin{aligned} \frac{e_k{}^{n+1} - e_k{}^n}{\delta t} &= \frac{1}{dsigw(k)} \left[\frac{n_{zms}(k)}{\sigma_{ect}} \frac{\left(e_{k+1}{}^{n+1} - e_k{}^{n+1}\right)}{h^2 dsigu(k+1)} \right. \\ &- \left. \frac{n_{zmi}(k)}{\sigma_{ect}} \frac{\left(e_k{}^{n+1} - e_{k-1}{}^{n+1}\right)}{h^2 dsigu(k)} \right] \\ &+ Prod^n(k) + Dest^n(k) - \frac{\epsilon^n(k)}{e_k{}^n} \left[\gamma e_k{}^{n+1} + (1-\gamma)\, e_k{}^n \right], \end{aligned} \quad (3.59)$$

σ_{ect} is the Schmidt number for TKE. γ is an implicit coefficient for turbulent dissipation ($\gamma = 1$ for this class of model).

The shear production $Prod$ and the buoyancy effect $Dest$ are represented as follows:

$$\begin{aligned} Prod(k) &= \frac{1}{2} n_z(k) \left[(u_z(k+1,i,j) - u_z(k,i,j))^2 \right. \\ &+ (u_z(k+1,i-1,j) - u_z(k,i-1,j))^2 \\ &+ (v_z(k+1,i,j) - v_z(k,i,j))^2 \\ &+ \left. (u_z(k+1,i,j-1) - u_z(k,i,j-1))^2 \right] / (hdsigw(k))^2, \end{aligned} \quad (3.60)$$

$$Dest(k) = k_z(k)\, (bz(k+1,i,j) - bz(k,i,j)) \,/\, [h * (sig(k+1) - sig(k))]\,. \quad (3.61)$$

$Prod$ is centered in space. In the buoyancy formulation, $bz(k)$ is located at the center of the cell. The buoyancy is defined by eq. (1.44).

$n_{zms}(k)$ and $n_{zmi}(k)$ are the eddy viscosity coefficients:

$$n_{zms}(k) = \frac{dsigw(k+1) n_z(k) + dsigw(k) n_z(k+1)}{2 dsigu(k+1)}, \quad (3.62)$$

$$n_{zmi}(k) = \frac{dsigw(k) n_z(k-1) + dsigw(k-1) n_z(k)}{2 dsigu(k)}. \quad (3.63)$$

ψ parameter

The following finite difference representation of the ψ parameter equation is adopted :

$$\begin{aligned}\frac{{\psi_k}^{n+1}-{\psi_k}^{n}}{\delta t} &= \frac{1}{dsigw(k)}\left[\frac{n_{zms}(k)}{\sigma_\psi}\frac{\left({\psi_{k+1}}^{n+1}-{\psi_k}^{n+1}\right)}{h^2 dsigu(k+1)}\right. \\ &- \left.\frac{n_{zmi}(k)}{\sigma_\psi}\frac{\left({\psi_k}^{n+1}-{\psi_{k-1}}^{n+1}\right)}{h^2 dsigu(k)}\right] \\ &+ \frac{\psi_k^n}{E_k^{n+1}}\left[c_1 Prod(k)+c_3 Dest(k)\right] \\ &- c_2 F_{wall}\epsilon^n(k)\left[\gamma{\psi_k}^{n+1}+(1-\gamma){\psi_k}^{n}\right]/E_k^{n+1},\end{aligned} \tag{3.64}$$

The following terms: $n_{zms}(k)$, $n_{zmi}(k)$, $Prod$ and $Dest$ are identical to those employed to solve the TKE equation.

The Schmidt number σ_ψ is scheme-dependent.

The scaling constants c_1, c_2 and c_3 are given in table 3.3).

Boundary conditions

Therefore, for a well-posed computation it is necessary that auxiliary conditions are well-posed at the boundaries (sea- surface and bottom).

For (3.60) and (3.64), there is two ways to prescribed appropriate boundary conditions :

1 - Specify (e and ψ) (Dirichlet boundary condition)
2 - Specify the incoming fluxes ($\partial e/\partial z$) and/or ($\partial\psi/\partial z$)

Appropriate conditions would be the Dirichlet condition for the TKE equation and Flux specification for ψ parameter. Thus we write :

$$e_b = \frac{({u_b}^*)^2}{(c_{\mu o})^2}, \tag{3.65}$$

k-kl

$$\psi = \frac{({u_b}^*)^2\,\kappa h_1}{(c_{\mu o})^2}, \tag{3.66}$$

k-ϵ

$$\psi = \frac{({u_b}^*)^3}{\kappa h_1}, \tag{3.67}$$

k-ω

$$\psi = \frac{1}{c_{\mu o}\kappa h_1}, \tag{3.68}$$

Gen

$$\psi = \frac{({u_b}^*)}{(\kappa h_1)^{2/3}}, \tag{3.69}$$

${u_b}^*$ is the friction velocity on the bottom, h_1 is the bottom boundary layer thickness.

In the code, ${u_b}^*$ is specified as follows:

$$\begin{aligned} {u_b}^* &= C_d \left[\frac{1}{2} \left(uz(k,i,j)^2 + uz(k,i-1,j)^2 \right) \right. \\ &\left. + \frac{1}{2} \left(vz(k,i,j)^2 + vz(k,i-1,j)^2 \right) \right]^{1/2}, \end{aligned} \tag{3.70}$$

The drag coefficient on the sea-bed C_d is given by:

$$C_d = \left(\frac{\kappa}{ln\left(h_1/z_o\right)} \right)^2$$

z_o is a thickness to depict the bottom roughness.

Physical processes near the air-sea interface are also turbulent (*see* sect. 2.2.2). The friction velocity becomes ${u_s}^*$:

$${u_s}^* = \left(\frac{\tau_s}{\rho} \right)^{1/2} \tag{3.71}$$

τ_s is the wind stress.

In case of a flux condition, at the bottom the TKE flux is zero.
Regarding the ψ parameter, the formulation is scheme-dependent:

k-kl

$$\left(\frac{\partial \psi}{\partial z} \right)_b = \frac{({u_b}^*)^2 \, \kappa}{(c_{\mu o})^2}, \tag{3.72}$$

k-ϵ

$$\left(\frac{\partial \psi}{\partial z} \right)_b = -\frac{({u_b}^*)^3}{\kappa {h_1}^2}, \tag{3.73}$$

k-ω

$$\left(\frac{\partial \psi}{\partial z} \right)_b = -\frac{1}{c_{\mu o} \kappa {h_1}^2}, \tag{3.74}$$

Gen

$$\left(\frac{\partial \psi}{\partial z} \right)_b = -\frac{2}{3} \frac{({u_b}^*)}{\kappa^{2/3} {h_1}^{5/3}}. \tag{3.75}$$

At the first computational level close to the surface, the TKE flux is zero. The ψ parameter is defined through the generating expressions:

k-kl

$$\left(\frac{\partial \psi}{\partial z}\right)_b = -\frac{{u_b^*}^2 \kappa}{{(c_{\mu o})}^2}, \tag{3.76}$$

k-ϵ

$$\left(\frac{\partial \psi}{\partial z}\right)_b = \frac{{u_b^*}^3}{\kappa {h_1}^2}, \tag{3.77}$$

k-ω

$$\left(\frac{\partial \psi}{\partial z}\right)_b = \frac{1}{c_{\mu o} \kappa {h_1}^2}, \tag{3.78}$$

Gen

$$\left(\frac{\partial \psi}{\partial z}\right)_b = \frac{2}{3} \frac{(u_b^*)}{\kappa^{2/3} {h_1}^{5/3}}, \tag{3.79}$$

Closures

The turbulent length scale l and viscous dissipation ϵ can be specified as functions of e and ψ.

k-kl :

$$\epsilon^{n+1}(k) = {c_{\mu o}}^3 \frac{\left({E_k}^{n+1}\right)^{5/2}}{{\psi_k}^{n+1}}, \tag{3.80}$$

$$l^{n+1}(k) = \frac{{\psi_k}^{n+1}}{{E_k}^{n+1}}. \tag{3.81}$$

k-ϵ :

$$\epsilon^{n+1}(k) = {\psi_k}^{n+1}, \tag{3.82}$$

$$l^{n+1}(k) = {c_{\mu o}}^3 \frac{\left({E_k}^{n+1}\right)^{3/2}}{\epsilon^{n+1}(k)}. \tag{3.83}$$

k-ω :

$$\epsilon^{n+1}(k) = {c_{\mu o}}^4 {e_k}^{n+1} {\psi_k}^{n+1}, \tag{3.84}$$

$$l^{n+1}(k) = {c_{\mu o}}^3 \frac{\left({e_k}^{n+1}\right)^{3/2}}{\epsilon^{n+1}(k)}. \tag{3.85}$$

Gen

$$\epsilon^{n+1}(k) = \left({\psi_k}^{n+1}\right)^{3/2}, \tag{3.86}$$

$$l^{n+1}(k) = {c_{\mu o}}^3 \frac{\left({e_k}^{n+1}\right)^{3/2}}{\epsilon^{n+1}(k)}. \tag{3.87}$$

Table 3.3: Generic length scale values

	k-kL	k-ϵ	k-ω	Gen
σ_e	2.44	1.00	2.00	0.80
σ_ψ	2.44	1.00	2.00	1.07
c_1	0.9	1.44	0.555	1.00
c_2	0.5	1.92	0.833	1.22
${c_3}^+$	1.0	1.00	1.00	1.00
E_{min}	1.0e-8	1.0e-8	1.0e-8	1.0e-8
ψ_{min}	1.0e-12	1.0e-12	1.0e-12	1.0e-12

3.4.3 Generic length scale values

Parameter values are given in table 3.3. More informations can be found in (Warner et *al.* 2005, [36].
${c_3}^+$ indicates c_3 when the buoyancy term *Dest* is positive. Parameter c_3^- values are given in table 3.4

Table 3.4: Generic parameter ${c_3}^-$ values. KC: Kantha & Clayson, G: Galperin, C,CA & CB: Canuto. ND: not determined

	K-KL	K-ϵ	K-ϵ	Gen
KC, G	2.53	-0.52	-0.58	0.10
C, CA	2.38	-0.63	-0.64	0.05
CB	ND	-0.57	ND	ND

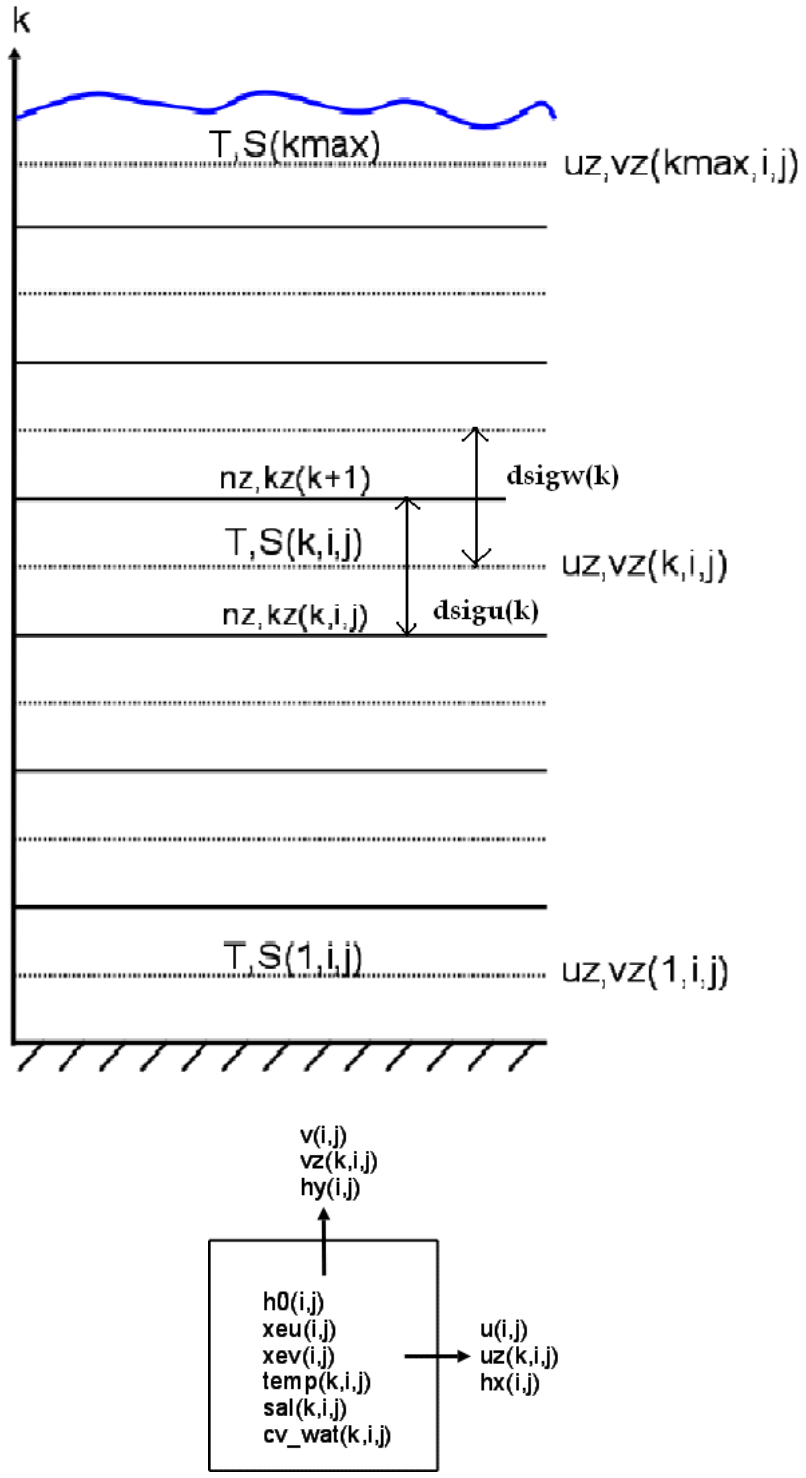

Figure 3.7: Vertical and horizontal variable arrangements in MARS-3D.

3.5 Wetting and drying scheme

3.5.1 An FCT approach

In shallow water models, wetting and drying (WAD) areas are determined by the total water depth $h = 0$ for "dry" and $h > 0$ for "wet". There are two popular ways to treat WAD. One is to reconfigure boundary each time new dry and/or wet cells appear. An other way is to test for dry or wet cells at each time step, then apply blocking conditions for fluxes at cell's interfaces. MARS follows this second method by using a WAD scheme based on a *positive definite* advection scheme.

A positive definite advection scheme is a method that never generates a negative value. Many attempts to construct positive definite advection schemes involved "filling algorithm" in which the solution obtained after each time step is corrected by filling in any negative value. In order to conserve the total mass of water, negatives cannot simply bet set to zero; compensating mass must removed from positive regions. There are a variety of filling algorithms designed for this purpose. Some filling algorithm attempt to fill local negative regions from adjacent positive areas. This requires a great deal of logical testing that cannot be performed efficiently on vector computers. A much better approach can be obtained using a FCT (Flux Corrected Transport) method.

The WAD scheme embedded in the MARS model defines dry cells as regions where remain a thin "film" of fluid O (cm).

FCT 1D (Boris & Book)

Let us consider the one-dimensional flux form of eq. (3.13):

$$u_j^{n+1} = u_j^n - \frac{\Delta t}{\Delta x}\left(F_{j+1/2} - F_{j-1/2}\right)$$

One way to obtain a positive definite advection scheme is to apply an anti-diffusive correction to a previously computed monotonic solution.

In order to introduce the FCT approach in a simple way, we assume two solutions :

1 - $F^l_{j\pm1/2}$ a first-order monotone approximation;

2 - $F^h_{j\pm1/2}$ a high-order approximation.

The *anti-diffusif* flux is written:

$$A_{j+1/2} = F^h_{j+1/2} - F^l_{j+1/2}$$

Now consider the following algorithm:

- Compute a monotonic solution for u_j^{n+1} :

$$u_j^l = u_j^n - \frac{\Delta t}{\Delta x}\left(F^l_{j+1/2} - F^l_{j-1/2}\right)$$

- Compute a correction:

$$u_j^{n+1} = u_j^l - \frac{\Delta t}{\Delta x}\left(A^c_{j+1/2} - A^c_{j-1/2}\right), \quad \text{with} \qquad A^c_{j+1/2} = C_{j+1/2}A_{j+1/2}$$

In case $C = 1$ we get a high-order scheme, $C = 0$ gives the monotonic scheme.

Then, to avoid increasing extremes over time, the flux-limiting scheme can be expressed by the form:

$$A^c_{j+1/2} = S_{j+1/2}\max\left\{0, \min\left[|A_{j+1/2}|, S_{j+1/2}(u^l_{j+2} - u^l_{j+1})\frac{\Delta x}{\Delta t}, S_{j+1/2}(u^l_j - u^l_{j-1})\frac{\Delta x}{\Delta t}\right]\right\}$$

where $S_{j+1/2}$ is the sign of $A_{j+1/2}$:

$$S_{j+1/2} = \frac{A_{j+1/2}}{|A_{j+1/2}|}$$

In case $A_{j+1/2} > 0$ the anti-diffusif flux is given by:

$$\frac{\Delta t}{\Delta x}A^c_{j+1/2} = \max\left\{0, \min\left[\frac{\Delta t}{\Delta x}A_{j+1/2}, (u^l_{j+2} - u^l_{j+1}), (u^l_j - u^l_{j-1})\right]\right\}$$

Let us consider a standard case, figure (3.8), the "anti-diffusif velocity" is directed to the right hand side of the local gradient. Thus, the second term in the minimum operator of the preceding expression ensures u_{j+1} greater than u_{j+2}. We can write:

$$u^{n+1}_{j+1} = u^l_{j+1} - \frac{\Delta t}{\Delta x}\left(A^c_{j+3/2} - A^c_{j+1/2}\right) \leq u^l_{j+2} \tag{3.88}$$

Assuming $A_{j+3/2} > 0$ in this example, we get:

$$u^l_{j+1} + \frac{\Delta t}{\Delta x}A^c_{j+1/2} \leq u^l_{j+2} \tag{3.89}$$

finally:

$$\frac{\Delta t}{\Delta x}A^c_{j+1/2} \leq (u^l_{j+2} - u^l_{j+1})$$

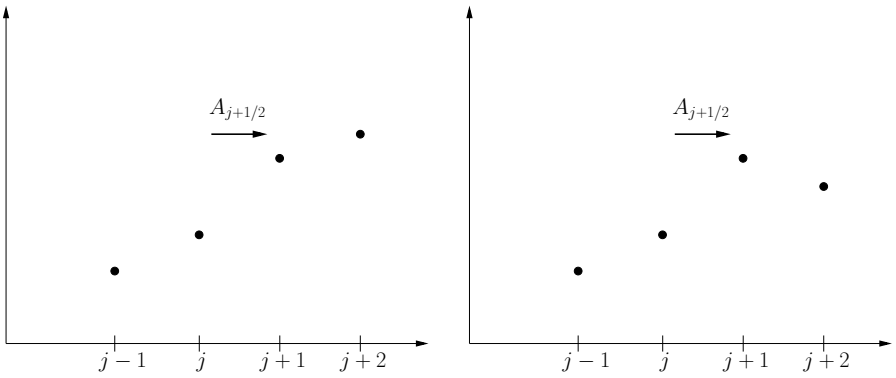

Figure 3.8: An illustration of the anti-diffusive algorithm, the original flux is limited on the left and set to zero on the right hand side of a cell

Boris & Book (1973), [4] developped the flux-corrected transport approach as a general technique

of *predictor/corrector* tye in which large diffusion is introduced in the predictor stage and an equal (almost) amount of diffusion is introduced in the corrector stage. However, the anti-diffusion is limited so that no new maxima or minima can appear in the solution. The limiting step is important as it maintains the positivity of the solution.

Zalesak limiter

Assuming the two following solutions:

$$1 \text{ - } F^l_{j+1/2} = \frac{a}{2}\left(u_j + u_{j+1}\right) - \frac{|a|}{2}\left(u_{j+1} - u_j\right) \text{ (Upstream)}$$

$$2 \text{ - } F^h_{j+1/2} = \frac{a}{2}\left(u_j + u_{j+1}\right) - \frac{a^2\Delta t}{2\Delta x}\left(u_{j+1} - u_j\right) \text{ (Lax-Wendroff)}$$

Zalesak (1979), [38] proposed to improve the FCT method.

The Zalesak algorithm consists of the following six steps:

1. Evaluate the range of permissible values:

$$u_j^{\max} = \max(u^n_{j-1}, u^n_j, u^n_{j+1}, u^l_{j-1}, u^l_j, u^l_{j+1})$$
$$u_j^{\min} = \min(u^n_{j-1}, u^n_j, u^n_{j+1}, u^l_{j-1}, u^l_j, u^l_{j+1})$$

2. Compute the sum of all (incoming) anti-diffusive fluxes in the cell j:

$$P_j^+ = \max(0, A_{j-1/2}) - \min(0, A_{j+1/2})$$

3. Compute the net anti-diffusif flux (*i.e.* : $-(A^c_{j+1/2} - A^c_{j-1/2})$) the maximum flux to ensure the monotonicity : $u_j^{n+1} \leq u_j^{\max}$

$$Q_j^+ = (u_j^{\max} - u_j^l)\frac{\Delta x}{\Delta t}$$

4. Limit the anti-diffusive flux:

$$R_j^+ = \begin{cases} \min(1, Q_j^+/P_j^+) & \text{if } P_j^+ > 0, \\ 0 & \text{if } P_j^+ = 0 \end{cases}$$

5. Compute the outgoing fluxes:

$$P_j^- = \max(0, A_{j+1/2}) - \min(0, A_{j-1/2})$$
$$Q_j^- = (u_j^l - u_j^{\min})\tfrac{\Delta x}{\Delta t}$$
$$R_j^- = \begin{cases} \min(1, Q_j^-/P_j^-) & \text{if } P_j^- > 0, \\ 0 & \text{if } P_j^- = 0 \end{cases}$$

6. Compute the correction $C_{j+1/2}$

$$C_{j+1/2} = \begin{cases} \min(R_{j+1}^+, R_j^-) & \text{si } A_{j+1/2} > 0 \\ \min(R_j^+, R_{j+1}^-) & \text{si } A_{j+1/2} < 0 \end{cases}$$

FCT 2D

In two dimension, the Zalesak method should be written as follows:

$$P^+_{i,j} = \max(0, A_{i-1/2,j}) - \min(0, A_{i+1/2,j}) + \max(0, A_{i,j-1/2}) - \min(0, A_{i,j+1/2})$$
$$P^-_{i,j} = \max(0, A_{i+1/2,j}) - \min(0, A_{i-1/2,j}) + \max(0, A_{i,j+1/2}) - \min(0, A_{i,j-1/2})$$

Thus :

$$u^a_{i,j} = \max(u^n_{i,j}, u^l_{i,j}) \quad ; \quad u^b_{i,j} = \min(u^n_{i,j}, u^l_{i,j})$$

The extremum values are defined as:

$$u^{\max}_{i,j} = \max\left(u^a_{i,j}, u^a_{i,j-1}, u^a_{i,j+1}, u^a_{i-1,j}, u^a_{i+1,j}\right)$$
$$u^{\min}_{i,j} = \min\left(u^b_{i,j}, u^b_{i,j-1}, u^b_{i,j+1}, u^b_{i-1,j}, u^b_{i+1,j}\right)$$

One way to obtain the monotone fluxes is to use an *upstream* differencing.

3.5.2 Upholding a positive depth

The FCT algrithm is used to keep a positive depth in each WAD cell. This method should only be applied in the WAD areas in modelling applications.

The FCT algorithm is a monotonicity preserving scheme. Hereafter, the scheme is used in a more simple form to maintain positive depths (or greater than a threshold).

Let us consider the one dimensional form of the continuity equation:

$$\eta^{n+1}_j = \eta^n_j - \frac{\Delta t}{\Delta x}\left(F_{j+1/2} - F_{j-1/2}\right)$$

The fluxes $F^l_{j\pm1/2}$ are derived from a second-order monotone scheme. The anti-diffusive flux is given by the form:

$$A_{j+1/2} = F_{j+1/2} - F^l_{j+1/2}$$

Then, a straightforward algorithm may be written :

- Compute the monotone solution :

$$\eta^l_j = \eta^n_j - \frac{\Delta t}{\Delta x}\left(F^l_{j+1/2} - F^l_{j-1/2}\right)$$

- Calculate the correction :

$$\eta^{n+1}_j = \eta^l_j - \frac{\Delta t}{\Delta x}\left(A^c_{j+1/2} - A^c_{j-1/2}\right), \qquad A^c_{j+1/2} = C_{j+1/2}A_{j+1/2}$$

Let *hmin* be the minimum depth in a cell : $\mathrm{h0}_{i,j} + \eta_{i,j} \geq \mathrm{hmin}, \quad \forall(i,j)$, then the Zalesak original method becomes the following two step algorithm :

1 - Compute the outgoing fluxes :

$$P_j^- = \max(0, A_{j+1/2}) - \min(0, A_{j-1/2})$$
$$Q_j^- = (\eta_j - (\mathrm{hmin} - \mathrm{h0}_{i,j}))\frac{\Delta x}{\Delta t}$$
$$R_j^- = \begin{cases} \min(1, Q_j^-/P_j^-) & \text{si } P_j^- > 0, \\ 0 & \text{si } P_j^- = 0 \end{cases}$$

2 - Compute $C_{j+1/2}$

$$C_{j+1/2} = \begin{cases} R_j^- & \text{si } A_{j+1/2} > 0 \\ R_{j+1}^- & \text{si } A_{j+1/2} < 0 \end{cases}$$

Chapter 4

Numerical formulations

4.1 2Dh formulations

The bottom friction (*cf.* 2.76) is written using a semi-explicit formulation.

From n to $n+1/2$:

$$\begin{aligned}
(1+ft\beta_2\Delta t)u^{n+\frac{1}{2},*} &= u^n - \Delta t\left(u^n\frac{\partial u^n}{\partial x}+v^n\frac{\partial u^n}{\partial y}\right) - g\Delta t\frac{\partial \zeta^n}{\partial x} + \Delta t f v^n \\
&\quad + \Delta t\left[\frac{\partial}{\partial x}\left(\nu_H\frac{\partial u^n}{\partial x}\right)+\frac{\partial}{\partial y}\left(\nu_H\frac{\partial u^n}{\partial y}\right)\right] \\
&\quad + \Delta t\frac{\tau_{sx}}{\rho h^n} - \frac{\Delta t}{\rho}\frac{\partial p_a}{\partial x} - \Delta t f t\beta_1 u^n \\
(1+ft\beta_2\Delta t)v^{n+\frac{1}{2},*} &= v^n - \Delta t\left(u^n\frac{\partial v^n}{\partial x}+v^n\frac{\partial v^n}{\partial y}\right) - g\Delta t\frac{\partial \zeta^n}{\partial y} - \Delta t f u^n \\
&\quad + \Delta t\left[\frac{\partial}{\partial x}\left(\nu_H\frac{\partial v^n}{\partial x}\right)+\frac{\partial}{\partial y}\left(\nu_H\frac{\partial v^n}{\partial y}\right)\right] \\
&\quad + \Delta t\frac{\tau_{sy}}{\rho h^n} - \frac{\Delta t}{\rho}\frac{\partial p_a}{\partial y} - \Delta t f t\beta_1 v^n
\end{aligned}$$

$$\begin{aligned}
\zeta^{n+\frac{1}{2},*} &= \zeta^n - \Delta t\frac{\partial}{\partial x}\left[h^n\left(\alpha\, u^n + (1-\alpha)\, u^{n+\frac{1}{2}}\right)\right] \\
&\quad - \Delta t\frac{\partial}{\partial y}\left[h^n\left(\alpha\, v^n + (1-\alpha)\, v^{n+\frac{1}{2},*}\right)\right]
\end{aligned}$$

$$\begin{aligned}
(1+ft\beta_2\Delta t)u^{n+\frac{1}{2}} &= u^n - g\Delta t\frac{\partial}{\partial x}\left(\alpha\,\zeta^n + (1-\alpha)\,\zeta^{n+\frac{1}{2},*}\right) + \Delta t f v^{n+\frac{1}{2},*} - \Delta t f t\beta_1 u^n \\
&\quad - \Delta t u^{n+\frac{1}{2},*}\frac{\partial}{\partial x}\left(\alpha\, u^n + (1-\alpha)\, u^{n+\frac{1}{2},*}\right) \\
&\quad - \Delta t v^{n+\frac{1}{2},*}\frac{\partial}{\partial y}\left(\alpha\, u^n + (1-\alpha)\, u^{n+\frac{1}{2},*}\right) \\
&\quad + \Delta t\left[\frac{\partial}{\partial x}\left(\nu_H\frac{\partial u^n}{\partial x}\right)+\frac{\partial}{\partial y}\left(\nu_H\frac{\partial u^n}{\partial y}\right)\right] \\
&\quad + \Delta t\frac{\tau_{sx}}{h^n\rho} - \frac{\Delta t}{\rho}\frac{\partial p_a}{\partial x}
\end{aligned}$$

$$\begin{aligned}
\zeta^{n+\frac{1}{2}} &= \zeta^n - \Delta t\frac{\partial}{\partial x}\left[\left(\alpha h^n + (1-\alpha)h^{n+\frac{1}{2},*}\right)\left(\alpha\, u^n + (1-\alpha)\, u^{n+\frac{1}{2}}\right)\right] \\
&\quad - \Delta t\frac{\partial}{\partial y}\left[\left(\alpha h^n + (1-\alpha)h^{n+\frac{1}{2},*}\right)\left(\alpha\, v^n + (1-\alpha)\, v^{n+\frac{1}{2}}\right)\right] \\
(1+ft\beta_2\Delta t)v^{n+\frac{1}{2}} &= v^n - g\Delta t\frac{\partial}{\partial y}\left(\alpha\,\zeta^n + (1-\alpha)\,\zeta^{n+\frac{1}{2}}\right) - f\Delta t u^{n+\frac{1}{2}} - \Delta t f t\beta_1 v^n \\
&\quad - \Delta t u^{n+\frac{1}{2},*}\frac{\partial}{\partial x}\left(\alpha\, v^n + (1-\alpha)\, v^{n+\frac{1}{2},*}\right) \\
&\quad - \Delta t v^{n+\frac{1}{2},*}\frac{\partial}{\partial y}\left(\alpha\, v^n + (1-\alpha)\, v^{n+\frac{1}{2},*}\right) \\
&\quad + \Delta t\left[\frac{\partial}{\partial x}\left(\nu_H\frac{\partial v^n}{\partial x}\right)+\frac{\partial}{\partial y}\left(\nu_H\frac{\partial v^n}{\partial y}\right)\right]
\end{aligned}$$

$$+\Delta t\frac{\tau_{sy}}{\rho\left(\alpha\, h^{n}+(1-\alpha)\, h^{n+\frac{1}{2},*}\right)}-\frac{\Delta t}{\rho}\frac{\partial p_a}{\partial y}$$

From $n+1/2$ to $n+1$:

$$\begin{aligned}
(1+ft\beta_2\Delta t)u^{n+1,*} &= u^{n+\frac{1}{2}}-\Delta t\left(u^{n+\frac{1}{2}}\frac{\partial u^{n+\frac{1}{2}}}{\partial x}+v^{n+\frac{1}{2}}\frac{\partial u^{n+\frac{1}{2}}}{\partial y}\right)-g\Delta t\frac{\partial \zeta^{n+\frac{1}{2}}}{\partial x}+\Delta t f v^{n+\frac{1}{2}}\\
&\quad+\Delta t\left[\frac{\partial}{\partial x}\left(\nu_H\frac{\partial u^{n+\frac{1}{2}}}{\partial x}\right)+\frac{\partial}{\partial y}\left(\nu_H\frac{\partial u^{n+\frac{1}{2}}}{\partial y}\right)\right]\\
&\quad+\Delta t\frac{\tau_{sx}}{\rho h}-\Delta t-\frac{\rho}{\rho}\frac{\partial p_a}{\partial x}-\Delta t f t\beta_1 u^{n+\frac{1}{2}}\\
(1+ft\beta_2\Delta t)v^{n+1,*} &= v^{n+\frac{1}{2}}-\Delta t\left(u^{n+\frac{1}{2}}\frac{\partial v^{n+\frac{1}{2}}}{\partial x}+v^{n+\frac{1}{2}}\frac{\partial v^{n+\frac{1}{2}}}{\partial y}\right)-g\Delta t\frac{\partial \zeta^{n+\frac{1}{2}}}{\partial y}-\Delta t f u^{n+\frac{1}{2}}\\
&\quad+\Delta t\left[\frac{\partial}{\partial x}\left(\nu_H\frac{u^n p h}{x}\right)+\frac{\partial}{\partial y}\left(\nu_H\frac{v^n p h}{y}\right)\right]\\
&\quad+\Delta t\frac{\tau_{sy}}{\rho h}-\frac{\Delta t}{\rho}\frac{\partial p_a}{\partial y}-\Delta t f t\beta_1 v^{n+\frac{1}{2}}
\end{aligned}$$

$$\begin{aligned}
\zeta^{n+1,*} &= \zeta^{n+\frac{1}{2}}-\Delta t\frac{\partial}{\partial x}\left[h^{n+\frac{1}{2}}\left(\alpha\, u^{n+\frac{1}{2}}+(1-\alpha)\, u^{n+1,*}\right)\right]\\
&\quad-\Delta t\frac{\partial}{\partial y}\left[h^{n+\frac{1}{2}}\left(\alpha\, v^{n+\frac{1}{2}}+(1-\alpha)\, v^{n+1}\right)\right]\\
(1+ft\beta_2\Delta t)v^{n+1} &= v^{n+\frac{1}{2}}-g\Delta t\frac{\partial}{\partial y}\left(\alpha\,\zeta^{n+\frac{1}{2}}+(1-\alpha)\,\zeta^{n+1,*}\right)-f\Delta t u^{n+1,*}-\Delta t f t\beta_1 v^{n+\frac{1}{2}}\\
&\quad-\Delta t u^{n+1,*}\frac{\partial}{\partial x}\left(\alpha\, v^{n+\frac{1}{2}}+(1-\alpha)\, v^{n+1,*}\right)\\
&\quad-\Delta t v^{n+1,*}\frac{\partial}{\partial y}\left(\alpha\, v^{n+\frac{1}{2}}+(1-\alpha)\, v^{n+1,*}\right)\\
&\quad+\Delta t\left[\frac{\partial}{\partial x}\left(\nu_H\frac{\partial v^{n+\frac{1}{2}}}{\partial x}\right)+\frac{\partial}{\partial y}\left(\nu_H\frac{\partial v^{n+\frac{1}{2}}}{\partial y}\right)\right]\\
&\quad+\Delta t\frac{\tau_{sy}}{\rho h^{n+\frac{1}{2}}}-\frac{\Delta t}{\rho}\frac{\partial Pa}{\partial y}
\end{aligned}$$

$$\begin{aligned}
\zeta^{n+1} &= \zeta^{n+\frac{1}{2}}-\Delta t\frac{\partial}{\partial x}\left[\left(\alpha h^{n+\frac{1}{2}}+(1-\alpha)h^{n+1,*}\right)\left(\alpha\, u^{n+\frac{1}{2}}+(1-\alpha)\, u^{n+1}\right)\right]\\
&\quad-\Delta t\frac{\partial}{\partial y}\left[\left(\alpha h^{n+\frac{1}{2}}+(1-\alpha)h^{n+1,*}\right)\left(\alpha\, v^{n+\frac{1}{2}}+(1-\alpha)\, v^{n+1}\right)\right]\\
(1+ft\beta_2\Delta t)u^{n+1} &= u^{n+\frac{1}{2}}-g\Delta t\frac{\partial}{\partial x}\left(\alpha\,\zeta^{n+\frac{1}{2}}+(1-\alpha)\,\zeta^{n+1}\right)+\Delta t f v^{n+1}-\Delta t f t\beta_1 u^{n+\frac{1}{2}}\\
&\quad-\Delta t u^{n+1,*}\frac{\partial}{\partial x}\left(\alpha\, u^{n+\frac{1}{2}}+(1-\alpha)\, u^{n+1,*}\right)\\
&\quad-\Delta t v^{n+1,*}\frac{\partial}{\partial y}\left(\alpha\, u^{n+\frac{1}{2}}+(1-\alpha)\, u^{n+1,*}\right)
\end{aligned}$$

$$+ \Delta t \left[\frac{\partial}{\partial x} \left(\nu_H \frac{\partial un + \frac{1}{2}}{\partial x} \right) + \frac{\partial}{\partial y} \left(\nu_H \frac{\partial u^{n+\frac{1}{2}}}{\partial y} \right) \right]$$
$$+ \Delta t \frac{\tau_{sx}}{\rho \left(\alpha h^{n+\frac{1}{2}} + (1-\alpha) h^{n+1,*} \right)} - \frac{\Delta t}{\rho} \frac{\partial p_a}{\partial x}$$

4.2 2D-3D formulations

From n to $n+1/2$:

The first explicit formulation of $V^{n+\frac{1}{2},*}$ is:

$$V^{n+\frac{1}{2},*} = V^n - \Delta t \left[\bar{G}_v \left(u^{n-\frac{1}{2}}, v^{n-\frac{1}{2}} \right) + g \frac{\partial \zeta^n}{\partial y} \right]$$

Then, we compute $\zeta^{n+\frac{1}{2},*}, U^{n+\frac{1}{2}}$ and $u^{n+\frac{1}{2}}$:

$$\begin{aligned}
\zeta^{n+\frac{1}{2},*} &= \zeta^n - \Delta t \left[\frac{\partial}{\partial x} \left(h^n U^{n+\frac{1}{2}} \right) + \frac{\partial}{\partial y} \left(h^n V^{n+\frac{1}{2},*} \right) \right] \\
U^{n+\frac{1}{2}} &= U^n - \Delta t \left[g \frac{\partial}{\partial x} \left(\alpha \zeta^n + (1-\alpha) \zeta^{n+\frac{1}{2},*} \right) + \bar{G}_u \left(u^n, v^n \right) \right] \\
u^{n+\frac{1}{2}}(k) &= u^n(k) - \Delta t \left[g \frac{\partial}{\partial x} \left(\alpha \zeta^n + (1-\alpha) \zeta^{n+\frac{1}{2},*} \right) + G_u \left(u^n, v^n \right)(k) \right] \\
&\quad + \Delta t \frac{\partial}{\partial z} \left[k_z \frac{\partial}{\partial z} \left(u^{n+\frac{1}{2}}(k) \right) \right]
\end{aligned}$$

Followed by a depth-integrated calibration of $u^{n+\frac{1}{2}}$:

$$u^{n+\frac{1}{2}}(k) = u^{n+\frac{1}{2}}(k) - \overline{u^{n+\frac{1}{2}}(k)} + U^{n+\frac{1}{2}}$$

Then, we compute $\zeta^{n+\frac{1}{2}}, V^{n+\frac{1}{2}}$ and $v^{n+\frac{1}{2}}$:

$$\begin{aligned}
\zeta^{n+\frac{1}{2}} &= \zeta^n - \Delta t \left\{ \frac{\partial}{\partial x} \left[\left(\alpha h^n + (1-\alpha) h^{n+\frac{1}{2},*} \right) U^{n+\frac{1}{2}} \right] \right. \\
&\quad \left. + \frac{\partial}{\partial y} \left[\left(\alpha h^n + (1+\alpha) h^{n+\frac{1}{2},*} \right) V^{n+\frac{1}{2}} \right] \right\} \\
V^{n+\frac{1}{2}} &= V^n - \Delta t \left[g \frac{\partial}{\partial y} \left(\alpha \zeta^n + (1-\alpha) \zeta^{n+\frac{1}{2}} \right) + \bar{G}_v \left(u^{n+\frac{1}{2}}, v^n \right) \right] \\
v^{n+\frac{1}{2}}(k) &= v^n(k) - \Delta t \left[g \frac{\partial}{\partial y} \left(\alpha \zeta^n + (1-\alpha) \zeta^{n+\frac{1}{2}} \right) + G_v \left(u^{n+\frac{1}{2}}, v^n \right)(k) \right] \\
&\quad + \Delta t \frac{\partial}{\partial z} \left[k_z \frac{\partial}{\partial z} \left(v^{n+\frac{1}{2}}(k) \right) \right]
\end{aligned}$$

2D-3D coupling :

$$v^{n+\frac{1}{2}}(k) = v^{n+\frac{1}{2}}(k) - \overline{v^{n+\frac{1}{2}}(k)} + \bar{v}^{n+\frac{1}{2}}$$

For a constituent T :

$$\begin{aligned}
h^{n+\frac{1}{2}} T^{n+\frac{1}{2}} &= h^n T^n - \Delta t \left\{ \frac{\partial}{\partial x} \left[\left(\alpha h^n + (1-\alpha) h^{n+\frac{1}{2},*} \right) u^{n+\frac{1}{2}} T^n \right] \right. \\
&\quad + \frac{\partial}{\partial y} \left[\left(\alpha h^n + (1-\alpha) h^{n+\frac{1}{2},*} \right) v^{n+\frac{1}{2}} T^n \right] \\
&\quad \left. + \frac{\partial}{\partial z} \left[h^{n+\frac{1}{2}} w^{n+\frac{1}{2}} T^n \right] \right\}
\end{aligned}$$

From $n+1/2$ to $n+1$:

The first explicit formulation of $U^{n+1,*}$ is:

$$U^{n+1,*} = U^{n+\frac{1}{2}} - \Delta t \left[\bar{G}_u \left(u^n, v^n \right) + g \frac{\partial \zeta^{n+\frac{1}{2}}}{\partial x} \right]$$

then, we compute $\zeta^{n+1,*}, V^{n+1}$ and v^{n+1} :

$$\begin{aligned}
\zeta^{n+1,*} &= \zeta^{n+\frac{1}{2}} - \Delta t \left[\frac{\partial}{\partial x} \left(h^{n+\frac{1}{2}} U^{n+1,*} \right) + \frac{\partial}{\partial y} \left(h^{n+\frac{1}{2}} V^{n+1} \right) \right] \\
V^{n+1} &= V^{n+\frac{1}{2}} - \Delta t \left[g \frac{\partial}{\partial y} \left(\alpha \zeta^{n+\frac{1}{2}} + (1-\alpha) \zeta^{n+1,*} \right) + \bar{G}_v \left(u^{n+\frac{1}{2}}, v^{n+\frac{1}{2}} \right) \right] \\
v^{n+1}(k) &= v^{n+\frac{1}{2}}(k) - \Delta t \left[g \frac{\partial}{\partial y} \left(\alpha \zeta^{n+\frac{1}{2}} + (1-\alpha) \zeta^{n+1,*} \right) + G_v \left(u^{n+\frac{1}{2}}, v^{n+\frac{1}{2}} \right)(k) \right] \\
&\quad + \Delta t \frac{\partial}{\partial z} \left[k_z \frac{\partial}{\partial z} \left(v^{n+1}(k) \right) \right]
\end{aligned}$$

Followed by a depth-integrated calibration of v^{n+1} :

$$v^{n+1}(k) = v^{n+1}(k) - \overline{v^{n+1}(k)} + V^{n+1}$$

Then, we compute ζ^{n+1}, U^{n+1} and $u^{n+\frac{1}{2}}$:

$$\begin{aligned}
\zeta^{n+1} &= \zeta^{n+\frac{1}{2}} - \Delta t \left\{ \frac{\partial}{\partial x} \left[\left(\alpha h^{n+\frac{1}{2}} + (1-\alpha) h^{n+1,*} \right) \bar{u}^{n+1} \right] \right. \\
&\quad \left. + \frac{\partial}{\partial y} \left[\left(\alpha h^{n+\frac{1}{2}} + (1-\alpha) h^{n+1,*} \right) \bar{v}^{n+1} \right] \right\} \\
\bar{u}^{n+1} &= \bar{u}^{n+\frac{1}{2}} - \Delta t \left[g \frac{\partial}{\partial x} \left(\alpha \zeta^{n+\frac{1}{2}} + (1-\alpha) \zeta^{n+1} \right) + \bar{G}_u \left(u^{n+\frac{1}{2}}, v^{n+1} \right) \right] \\
u^{n+1}(k) &= u^{n+\frac{1}{2}}(k) - \Delta t \left[g \frac{\partial}{\partial x} \left(\alpha \zeta^{n+\frac{1}{2}} + (1-\alpha) \zeta^{n+1} \right) + G_u \left(u^{n+\frac{1}{2}}, v^{n+1} \right)(k) \right] \\
&\quad + \Delta t \frac{\partial}{\partial z} \left[k_z \frac{\partial}{\partial z} \left(u^{n+1}(k) \right) \right]
\end{aligned}$$

2D-3D coupling :

$$u^{n+1}(k) = u^{n+1}(k) - \overline{u^{n+1}(k)} + \bar{u}^{n+1}$$

For a constituent T :

$$\begin{aligned}
h^{n+1} T^{n+1} &= h^{n+\frac{1}{2}} T^{n+\frac{1}{2}} - \Delta t \left\{ \frac{\partial}{\partial x} \left[\left(\alpha h^{n+\frac{1}{2}} + (1-\alpha) h^{n+1,*} \right) u^{n+1} T^{n+\frac{1}{2}} \right] \right. \\
&\quad + \frac{\partial}{\partial y} \left[\left(\alpha h^{n+\frac{1}{2}} + (1-\alpha) h^{n+1,*} \right) v^{n+1} T^{n+\frac{1}{2}} \right] \\
&\quad \left. + \frac{\partial}{\partial z} \left[h^{n+1} w^{n+1} T^{n+\frac{1}{2}} \right] \right\}
\end{aligned}$$

where :

$$
\begin{aligned}
G_v(u^n, v^n)(k) \;=\; & -f\left(u^n(k) - \overline{u^n(k)}\right) \\
& -f u^{n+1/2,(*)} \\
& +\pi_y(k) \\
& +\frac{1}{\rho}\frac{\partial Pa}{\partial y} \\
& +\delta_{kmax,k}\frac{\tau_s}{\rho h^{n,(*)}} \\
& -\delta_{1,k}\frac{Cd}{h^{n,(*)}}v^n(1) \\
& +\left(u^n(k)\frac{\partial v^n(k)}{\partial x} + v^n(k)\frac{\partial v^n(k)}{\partial y} + w^n(k)\frac{\partial v^n(k)}{\partial z}\right) \\
& +\frac{\partial}{\partial x}\left(\nu\frac{\partial v^n(k)}{\partial x}\right) + \frac{\partial}{\partial y}\left(\nu\frac{\partial v^n(k)}{\partial y}\right)
\end{aligned}
$$

4.3 Transport formulations

4.4 Boundary formulations

The pen boundary conditions (OBC) described in section 2.4 are applied to the boundaries of the 2Dh model.

First, we must consider the following implicit finite difference representations of barotropic equations (3.7) and (3.8):

$$\frac{\zeta^{n+1}-\zeta^{n}}{\Delta t/2}+\left(\frac{\partial\left(h^{i+1/2}U^{n+1}\right)}{\partial x}\right)=-\left(\frac{\partial\left(h^{j+1/2}V^{n+1/2}\right)}{\partial y}\right)$$

$$\frac{U^{n+1}-U^{n}}{\Delta t}+\alpha_{\zeta}g\left(\frac{\partial\zeta^{n+1}}{\partial x}\right)=EXPL\left(\zeta^{n},uz_{k}^{n},vz_{k}^{n+1/2},b_{k}^{n+1/2}\right)^{n,l}$$

All the others terms are explicitly differenced and grouped together in the expression : $EXPL\left(\zeta^{n},uz_{k}^{n},vz_{k}^{n+1/2},b_{k}^{n+1/2}\right)$.

However, for every grid line j, it is necessary to consider all the nodes i. The corresponding variables U_i and ζ_i are grouped together in a global vector $(U_1,\zeta_2,U_2,...\zeta_{i_{max}-1},U_{i_{max}-1})^T$. Then, a tridiagonal matrix can be compiled for the unknow values :

$$\begin{pmatrix} a & b & & & & \\ c & a & b & & & \\ & \ddots & \ddots & \ddots & & \\ & & \ddots & \ddots & \ddots & \\ & & & c & a & b \\ & & & & c & a \end{pmatrix}\begin{pmatrix} u_1 \\ \eta_2 \\ \vdots \\ \vdots \\ \eta_{i_{max}-1} \\ u_{i_{max}-1} \end{pmatrix}=\begin{pmatrix} y_1^1 \\ y_2^2 \\ \vdots \\ \vdots \\ y_{i_{max}-1}^2 \\ y_{i_{max}-1}^1 \end{pmatrix}$$

In the case of an eastern boundary, $\zeta_{i_{max}}$ must be provided.

Then, the last term $y_{i_{max}-1}^1$ in the right-hand side column matrix must be modified in order to introduce the corresponding OBC : $\zeta_{i_{max}}=\frac{1}{2}\sqrt{\frac{h_0}{g}}\left(w_{1i_{max}}-w_{3i_{max}}\right)$ (w_3 is specified on the boundary, w_1 extrapolated).

It should be noted that the extrapolation of w_1 required to modify the last line of the tridiagonal matrix. A first order extrapolation algorithm is used in order to keep the generic tridiagonal formulation.

Once the tridiagonal system is solved, the eastern boundary values *i.e.* : $u_{i_{max}}$ and $\zeta_{i_{max}}$ must be calculated.

In the case of a western boundary, the first term y_1^1 in the right-hand side column matrix must be modified in order to introduce the corresponding OBC and after that, the first line of the tridiagonal matrix. Once the tridiagonal system is solved, the western boundary values can be computed.

4.5 WAD algorithm

By introducing a monochromatic solution (C-3) (*cf.* appendix C) in the 2D time scheme (*cf.* sect. 3.2.1) the global scheme can be written as:

$$\left\{\begin{array}{rcl} u^{n+1/2,\star} &=& u^n - i\frac{\Delta t}{2}\left[u_0k_x + v_0k_y\right]u^n - igk_x\frac{\Delta t}{2}\eta^n \\ v^{n+1/2,\star} &=& v^n - i\frac{\Delta t}{2}\left[u_0k_x + v_0k_y\right]v^n - igk_y\frac{\Delta t}{2}\eta^n \end{array}\right.$$

$$\left\{\begin{array}{rcl} \eta^{n+1/2,\star} &=& \eta^n - ih_0k_x\frac{\Delta t}{2}\left[\alpha\, u^n + (1-\alpha)\, u^{n+1/2}\right] - ih_0\frac{\Delta t}{2}k_y\left[\alpha v^n + (1-\alpha)v^{n+1/2,\star}\right] \\ && \quad -i\frac{\Delta t}{2}\left[u_0k_x + v_0k_y\right]\eta^n \\ u^{n+1/2} &=& u^n - igk_x\frac{\Delta t}{2}\left[\alpha\,\eta^n + (1-\alpha)\,\eta^{n+1/2,\star}\right] - i\frac{\Delta t}{2}\left[u_0k_x + v_0k_y\right]u^{n+1/2,\star} \end{array}\right.$$

$$\left\{\begin{array}{rcl} \eta^{n+1/2} &=& \eta^n - ih_0k_x\frac{\Delta t}{2}\left[\alpha\, u^n + (1-\alpha)\, u^{n+1/2}\right] - ih_0\frac{\Delta t}{2}k_y\left[\alpha v^n + (1-\alpha)v^{n+1/2}\right] \\ && \quad -i\frac{\Delta t}{2}\left[u_0k_x + v_0k_y\right]\left[\alpha\eta^n + (1-\alpha)\eta^{n+1/2,\star}\right] \\ v^{n+1/2} &=& v^n - igk_y\frac{\Delta t}{2}\left[\alpha\,\eta^n + (1-\alpha)\,\eta^{n+1/2}\right] - i\frac{\Delta t}{2}\left[u_0k_x + v_0k_y\right]v^{n+1/2,\star} \end{array}\right.$$

$$\left\{\begin{array}{rcl} u^{n+1,\star} &=& u^{n+1/2} - i\frac{\Delta t}{2}\left[u_0k_x + v_0k_y\right]u^{n+1/2} - igk_x\frac{\Delta t}{2}\eta^{n+1/2} \\ v^{n+1,\star} &=& v^{n+1/2} - i\frac{\Delta t}{2}\left[u_0k_x + v_0k_y\right]v^{n+1/2} - igk_y\frac{\Delta t}{2}\eta^{n+1/2} \end{array}\right.$$

$$\left\{\begin{array}{rcl} \eta^{n+1,\star} &=& \eta^{n+1/2} - ih_0k_x\frac{\Delta t}{2}\left[\alpha u^{n+1/2} + (1-\alpha)u^{n+1,\star}\right] - ih_0\frac{\Delta t}{2}k_y\left[\alpha v^{n+1/2} + (1-\alpha)v^{n+1}\right] \\ && \quad -i\frac{\Delta t}{2}\left[u_0k_x + v_0k_y\right]\eta^{n+1/2} \\ v^{n+1} &=& v^{n+1/2} - igk_y\frac{\Delta t}{2}\left[\alpha\,\eta^{n+1/2} + (1-\alpha)\,\eta^{n+1,\star}\right] - i\frac{\Delta t}{2}\left[u_0k_x + v_0k_y\right]v^{n+1,\star} \end{array}\right.$$

$$\left\{\begin{array}{rcl} \eta^{n+1} &=& \eta^{n+1/2} - ih_0k_x\frac{\Delta t}{2}\left[\alpha\, u^{n+1/2} + (1-\alpha)\, u^{n+1}\right] - ih_0\frac{\Delta t}{2}k_y\left[\alpha v^{n+1/2} + (1-\alpha)v^{n+1}\right] \\ && \quad -i\frac{\Delta t}{2}\left[u_0k_x + v_0k_y\right]\left[\alpha\eta^{n+1/2} + (1-\alpha)\eta^{n+1,\star}\right] \\ u^{n+1} &=& u^{n+1/2} - igk_x\frac{\Delta t}{2}\left[\alpha\,\eta^{n+1/2} + (1-\alpha)\,\eta^{n+1}\right] - i\frac{\Delta t}{2}\left[u_0k_x + v_0k_y\right]u^{n+1,\star} \end{array}\right.$$

Applying a positive constraint on the intermediate estimates $\eta^{n+1/2,\star}, \eta^{n+1,\star}$ is not useful. The time step algorithm is therefore written as:

$$\eta^{n+1/2} = \eta^n - \frac{\Delta t}{2}\frac{\partial}{\partial x}\left[\mathrm{hex}_{i,j}\left(\alpha\, u^n + (1-\alpha)\, u^{n+1/2}\right)\right] - \frac{\Delta t}{2}\frac{\partial}{\partial y}\left[\mathrm{hey}_{i,j}\left(\alpha\, v^n + (1-\alpha)\, v^{n+1/2}\right)\right]$$

The high-order fluxes are obtained by solving the original implicit scheme (*cf.* sect. 3.2.2).

The monotone fluxes are computed using a first-order *upwind* scheme:

$$\begin{aligned} F_{i-1/2,j} &= (\mathrm{h0}_{i-1,j} + \eta^n_{i-1,j}) u^n_{i,j}, \quad \text{si } u^n_{i,j} > 0 \\ &= (\mathrm{h0}_{i,j} + \eta^n_{i,j}) u^n_{i,j}, \quad \text{si } u^n_{i,j} < 0 \end{aligned} \tag{4.1}$$

where h0 is the central depth previously introduced in section 2.5.

This scheme is based on the following assumption: In the WAD areas the velocity is weak, and the stability condition $u\Delta t/\Delta x \leq 1$ relative to the explicit scheme is unaffected. Thus, the fluxes given by (4.1) may support a positive depth.

Bibliography

[1] Blayo E. , Debreu L. (2004) : Revisiting open boundary conditions from the point of view of characteristic variables. *Ocean Modelling*, **9**, 231-252

[2] Blayo E. (2006) : Méthode des caractéristiques pour les équations primitives : séparation en modes verticaux. ???

[3] Blumberg A.F., Mellor G.L. (1987) : A description of a three-dimensional coastal ocean circulation model. In *Three-dimensional coastal ocean models*. **Coastal and Estuarine Sciences - 4**, A.G.U.

[4] Boris J.P., BookD.L. (1973) : Flux-corrected transport I:SHASTA - A fluis transport algorithm that works. *J. Comput. Phys.*, **11**, 38-69

[5] Burchard H., Petersen O. (1999) : Models of turbulence in the marine environment. *Journal of Marine Systems*, **21**, 29-53.

[6] Burchard H., Bolding K. (2001) : Comparative analysis of four second-moment turbulence closure models for oceanic mixed layers. *J. Phys. Oceanogr.*, **31**, 1943-1968.

[7] Burchard H., Deleersnijder K. (2001) : Stability of algebraic non-equilibrum second-order closure models. *Ocean Modeling*, **3**, 33-50.

[8] Canuto V.M., Howard A., Cheng Y., Dubovikov M.S. (2001) : Ocean turbulence i: one point closure model. Momentum and heat vertical diffusivities. *J. of Phys. Oceanogr.*, **31**, 1413-1426.

[9] Cushman-Roisin B. (1994) : *Introduction to Geophysical Fluid Dynamics*. **Prentice-Hall**.

[10] Duhaut T., Honnorat M., Debreu L. (2008) : Développements numériques pour le modèle MARS. *Rapport PREVIMER contrat N°06/2 210 290*

[11] Galperin B., Kantha L.H., Haasid S., Rosati A. (1988) : A quasi-equilibrum turbulent energy model for geophysical flows. *Journal of Atmospheric Science*, **45**, 55-62.

[12] Gaspar P., Grégoris Y., Lefèvre J.M. (1990) : A simple eddy kinetic energy model for simulations of the oceanic vertical mixing : tests at station Papa and long-term upper ocean study site. *J. Geophys. Res.*, **95**, No C9, 16179-16193

[13] Guyon E., Hulin J.P., Petit L. (1991) : *Hydrodynamique Physique*. **Savoirs Actuels**. Editions du CNRS.

[14] Hedström K. (2000) : Technical manual for a coupled sea-ice/ocean circulation model. OCMS study MMS 97-0017

[15] Kantha L.H., Clayson C.A. (1994) : An improved mixed layer model for geophysical applications. *J. of Geophys. Res.*, **99**, 25235-25266.

[16] Kidder S.Q., Vonder Haar T.H. (1995) : *Satellite Meteorology: An Introduction.* **Academic Press**, San Diego, 466 pp.

[17] Kolmogorov A.N. (1941) The local structure of turbulence in incompressible viscous fluid at very large Reynolds numbers. *C. R. Acad. Sci. URSSS*, **30**, 301-305

[18] Kundu K.P. (1990) : *Fluid Mechanics.* **Academic Press**.

[19] Leonard A. (1979) : A stable an accurate convective modelling procedure based on quadratic upstream interpolation. *Comput. methods. Appl. Mech. Eng.*, **19**, 59-98.

[20] Leonard A. (1991) : The ultimate conservative difference scheme applied to unsteady one-dimensional advection. *Comput. methods. Appl. Mech. Eng.*, **88**, 17-74.

[21] Lazure P., Dumas F. (2005) : An external-internal mode coupling for a 3D hydrodynamical model for application at regional scale. *Advances in Water Ressources*, **9**, 233-250

[22] Marin J., Vandermeirsch F. (2007) : Développement de conditions aux frontières ouvertes par la méthode des caractéristiques. *Rapport IFREMER/DYNECO/PHYSED N°06-58*

[23] Mellor G., Yamada T. (1974) : A hierarchy of a turbulence closure model for planetary boundary layers. *J. Atmos. Science*, **31**, 1791-1806

[24] Mellor G., Yamada T. (1982) : Development of a turbulence closure model for geophysical fluid problems. *Reviews of geophysics and space physics*, **20**, 851-875

[25] Mellor G.L., Blumberg A.F. (1985): Modelling vertical and horozontal diffusivities with the sigma coordinate system. *Mon. Weather Rev.*, **113**, 1379-83.

[26] Mellor G.L. (1991): An equation of state for numerical models of ocean and estuaries. *Journal of Atmospheric and Oceanic Technology*, **8**, 609-611.

[27] Okubo A. (1974). Some speculations on oceanic diffusion diagrams. Rapp. P.-v. Réun. Cons. int. Explor. Mer 167: 77-85.

[28] Pacanowski R.C., Philander S.G.H. (1981) : Parameterization of vertical mixing in numerical models of tropical oceans. *J. Phys. Oceanogr.*, **11**, 1443-1451

[29] Palma E.D., Matano R.P. (1998) : On the implementation of passive open boundary conditions for a general circulation model : the barotropic mode. *J. Geos. Res.*, **103**, 1319-1341

[30] Pérenne N. (2006) : MARS - A Model for Applications at Regional Scale - Documentation Utilisateur. *Rapport IFREMER*

[31] Pérenne N. (2006) : MARS - A Model for Applications at Regional Scale - Documentation Scientifique. *Rapport IFREMER*

[32] Rodi W., (1993) : *Turbulence models and their applications in hydraulics.* A state-of-the art review. **A.A. Balkema Publishers**.

[33] Smagorinsky J. (1963) : General circulation experiments with the primitive equations - I. The basic experiment. *Monthly Weather Review*, **8**, 99-165.

[34] Umlauf L., Burchard H. (2003) : A generic length-scale equation for geophysic turbulence models. *Journal of Marine Research*, **61**, 235-265.

[35] Vandermeirsch F. (2004) : Couplage d'un modèle côtier shallow-water à partir de la méthode des caractéristiques. *Rapport IFREMER*

[36] Warner J.C., Sherwood C. R., Arango H. G., Signell R. P. (2003) : Performance of four turbulence closure models implemented using a generic length scale method. *Ocean Modelling*, **8**, 81-113.

[37] Wilcox D.C. (1998) *Turbulence Modelling for CFD*. DCW Industries, Inc., Canada.

[38] Zalesak S.T. (1979) : Fully multidimensional flux-corrected transport algorithms for fluids. *J. Comput. Phys.*, **31**, 335-362

Air-sea interactions

[39] Ayina H-L., Bentamy A. (2007) : Une Approche pour Améliorer les Flux Turbulents Estimés à l'aide des capteurs Satellitaires. *Journal International de Télédétection*, **7**, 1-2-3-4, 91-110.

[40] Berliand M.E., Berliand T.G. (1952) : Determining the net long-wave of the earth with consideration of the effect of cloudiness. *Isv. Akad. Nauk. SSSR Ser. Geofis*, **1**

[41] Bignami F., Marullo S., Santoleri R. et Schiano M.E. (1995) : Long-wave radiation budget in the Mediterranean Sea. *Journal of Geophysical Research* **100**, C2, 2501-2514.

[42] Budyko M.I. (1974) : *Climate and Life*. **Academic Press**. 508 pp.

[43] Businger, J.A., Wyngaard J.C., Izumi Y. and Bradley E. F. (1971): Flux-profile relation-ships in the Atmospheric surface layer, *Journal of Atmospheric Science*, **28**, 181-189.

[44] Charnock, H., 1955: Wind stress on a water surface. *Quart. J. Roy. Meteor. Soc.*, **81**, 639-640.

[45] Clark N. E., Eber L., Laurs R.M., Renner J.A. and Saur J.F.T. (1974) : Heat exchange between ocean and atmosphere in the eastern North Pacific for 1961-71. NOAA Tech. Rep. NMFS SSRF-682, U.S Department of Commerce, Washington, DC.

[46] Da Silva A.M., Young C.C., Levitus S., 1994 : Atlas of surface marine data 1994. Algorithms and procedures, 74 pp., NOAA Atlas NESDIS 6, U. S. Department of Commerce, NOAA NESDIS, USA, vol.1.

[47] Dupuis H., P. K. Taylor, A. Weill, and K. B. Katsaros (1997) : Inertial dissipation method applied to derive turbulent fluxes over the ocean during the SOFIA/ASTEX and SEMAPHORE experiments with low to moderate wind speeds. *Journal of Geophysical Research*, 21115-21129.

[48] Dyer A. J. (1974) : A review of flux-profile relationships. *Boundary Layer Meteorology* **7**, 363-372.

[49] Fairall , C.W., Bradley, D. P. Rogers, J. B. Edson, and G. S. Young, 1996 : Bulk parameterization of air-sea fluxes for Tropical Ocean-Global Atmosphere Coupled-Ocean Atmosphere Response Experiment. *J. Geophys. Res.*, **101**, 3747-3764.

[50] Fairall, C.W., E.F. Bradley, J.E. Hare, A.A. Grachev, and J.B. Edson, 2003: Bulk parameterization of air-sea fluxes: Updates and verification for the COARE algorithm. *Journal of Climate*, **16**, 571-591.

[51] Geernaert G. (1990): Bulk parameterizations for wind stress and heat fluxes in the surface waves and fluxes, 1, G. L. Geernaert, and W. J. Plant, Kluwer Academic Publishers, 91-172.

[52] Gill A. (1992) : *Atmosphere-Ocean Dynamics*. International Geophysics Series, volume 30. ed. W. Donn, **Academic Press**.

[53] Goody R. M., Young Y.L. (1989) : *Atmospheric Radiation (Theoretical basis)*. 2nd ed., **Oxford Univ. Press**, 519pp

[54] Grachev, A. A., C. W. Fairall, and E. F. Bradley (2000) : Convective profile constants revisited. *Boundary Layer Meteorology*, **94**, 495-515.

[55] Hare J.E., Persson P.O.G., Fairall C.W.,and J.B. Edson (1999) : Behavior of Charnock's relationship for high wind conditions. Preprints, 13th Symp. On Boundary Layers and Turbulence, Dallas, TX, *Amer. Meteor. Soc.*, 252-255

[56] Hastenrath, S. and P. J. Lamb (1978) : Heat Budget Atlas of the Tropical Atlantic and Eastern Pacific Oceans, PP.90, University of Wisconsin Press.

[57] Jabouille, P., J. Redelsperger, and J. Lafore, 1996 : Modification of surface fluxes by atmospheric convection in the TOGA COARE region. *Mon. Wea. Rev.*, **124**, 816-837, doi:10.1175/1520-0493.

[58] Josey S., Kent E. et Taylor P. (1999) : New insights into the ocean heat budget closure problem from analysis of the SOC air-sea flux climatology. *Journal of Climate* **12**, 9, 2856-2880.

[59] Kraus, E. B., 1972: Atmosphere-ocean interactions. London Oxford University press. Large, W. G. and S. Pond, 1981 : Open ocean momentum flux measurements in moderate to strong winds. *J. Phys. Oceanogr.*, **11**, 324-336.

[60] Large W. G.,Pond S. (1981): Open ocean momentum flux measurements in moderate to strong winds. *J. Phys. Oceanograph.*, **11**, 324-336.

[61] Large W. G., Yeager S. G. (2004) : Diurnal to Decadal Global Forcing for Ocean and Sea-ice Models : The data sets and flux climatologies, NCAR Technical Note, PP 1-105.

[62] Luyten P., De Mulder T. (1992) : A module representing surface fluxes of momentum and heat. MUMM's contribution of MAST-OO5O-C. Tech. Report., **9** 1-30.

[63] Monin A. S., Obukhov A. M. (1954) : Dimensionless characteristics of turbulence in the surface layer. *Akad. Nauk. SSSR, Geofiz. Inst., Tr.*, **24**, 163-187.

[64] Oost, W., G. Komen, C. Jacobs, and C. van Oort, 2002: New evidence for a relation between wind stress and wave age from measurements during ASGAMAGE. *Boundary-Layer Meteorology*, **103**, 409-438.

[65] Rosati A., Miyakoda K. (1998) : A General Circulation Model for Upper Ocean Simulation. *Journal of Physical Oceanography* **18**, 1601-1626.

[66] Smith, S.D., Banke E.G. (1975) : Variation of the seasurface drag coefficient with wind speed. *Quart. J. Roy. Meteorol. Soc.*, **101**, 665-663.

[67] Smith, S.D. (1988) : Coefficients for sea surface wind stress, heat flux and wind profiles as a function of wind speed and temperature. *Journal of Geophysical Research*, **93**, 15467-15472.

[68] Taylor, P. K. and M. J. Yelland, 2001: The dependence of sea surface roughness on the height and steepness of the waves. *J. Phys. Oceanogr.*, 31, 572-590.

[69] Webb, E. K., G. I. Pearman, and R. Leuning, 1980 : Correction of flux measurements for density effects due to heat and water vapour transfer. *Quart. J. Roy. Meteor. Soc.*, 106, 85-100.

Appendix A

Second order equations

A.1 Turbulent fluctuation equations

Subtracting instantaneous equations from first-order equations leads to the following fluctuation equations :

A.1.1 Continuity equation

$$\frac{\partial u_i'}{\partial x_i} = 0 \tag{A-1}$$

A.1.2 Momentum equations

$$\begin{aligned}\rho_0 \left[\frac{\partial u_i'}{\partial t} + u_j' \frac{\partial \overline{u_i}}{\partial x_j} + \overline{u_j} \frac{\partial u_i'}{\partial x_j} + \frac{\partial}{\partial x_j} \left(u_i' u_j' - \overline{u_i' u_j'} \right) \right] = \\ -\rho' g \delta_{i3} - \frac{\partial p'}{\partial x_i} - 2\epsilon_{ijk}\rho_0 \Omega_j u_k' + \mu \frac{\partial}{\partial x_j} \left(\frac{\partial u_i'}{\partial x_j} + \frac{\partial u_j'}{\partial x_i} \right)\end{aligned} \tag{A-2}$$

A.1.3 Salt equation

$$\frac{\partial S'}{\partial t} + u_j' \frac{\partial \overline{S}}{\partial x_j} + \overline{u_j} \frac{\partial S'}{\partial x_j} + \frac{\partial}{\partial x_j} \left(S' u_j' - \overline{S' u_j'} \right) = \mathcal{D} \frac{\partial^2 S'}{\partial x_j^2} \tag{A-3}$$

A.1.4 Thermal conservation

$$\rho_0 C_p \left[\frac{\partial T'}{\partial t} + u_j' \frac{\partial \overline{T}}{\partial x_j} + \overline{u_j} \frac{\partial T'}{\partial x_j} + \frac{\partial}{\partial x_j} \left(T' u_j' - \overline{T' u_j'} \right) \right] = \mathcal{K} \frac{\partial^2 T'}{\partial x_j^2} - \frac{\partial R_j'}{\partial x_j} \tag{A-4}$$

A.2 Second order equations

Second-order equations are obtained by following these two steps :

1 - First, each fluctuation equation (A-2), (A-3), and (A-4) is mutiplied by one fluctuation among the others variables T', S' ou u_i'.
2 - Next, the time operator defined in (1.13) is applied to these equations.

A.2.1 Reynolds tensor

Regarding the momentum variables, we get :

$$\frac{D\overline{u_i'u_j'}}{Dt} + \frac{\partial}{x_k}\left(\overline{u_i'u_j'u_k'}\right) + \overline{u_i'u_k'}\frac{\partial\overline{u_j}}{\partial x_k} + \overline{u_j'u_k'}\frac{\partial\overline{u_i}}{\partial x_k} = \nu\left(\frac{\partial^2\overline{u_i'u_j'}}{\partial x_k^2} - 2\overline{\frac{\partial u_i'\partial u_j'}{\partial x_k^2}}\right)$$
$$-\frac{1}{\rho_0}\left(\overline{u_i'\frac{\partial p'}{\partial x_j}} + \overline{u_j'\frac{\partial p'}{\partial x_i}}\right) - \frac{g}{\rho_0}\left(\overline{\rho' u_i'}\delta_{j3} + \overline{\rho' u_j'}\delta_{i3}\right) - 2\Omega_k\left(\epsilon_{jkl}\overline{u_i'u_l'} + \epsilon_{ikl}\overline{u_j'u_l'}\right) \qquad \text{(A-5)}$$

where : $\nu = \mu/\rho_0$.

A.2.2 Turbulent kinetic energy

The turburlent kinetic energy e^2 related to the fluctuations u_i' is written as:

$$e = \frac{1}{2}\left(\overline{u_i'u_i'}\right) \qquad \text{(A-6)}$$

The TKE equation is obtained after summing the three equations of the Reynolds tensor $D\left(\overline{u_i'u_i'}\right)/Dt$. Thus we get:

$$\underbrace{\frac{De}{Dt}}_{I} = \underbrace{-\frac{1}{2}\frac{\partial}{\partial x_k}\left(\overline{u_i'u_j'u_k'}\right)}_{II}\underbrace{-\frac{1}{\rho_0}\overline{u_i'\frac{\partial p'}{\partial x_i}}}_{III} + \underbrace{\nu\left[\frac{1}{2}\frac{\partial^2 e}{\partial x_k^2} - \left(\frac{\partial u_i'}{\partial x_k}\right)^2\right]}_{IV}\underbrace{-\overline{u_i'u_k'}\frac{\partial\overline{u_i}}{\partial x_k}}_{V}\underbrace{-\frac{g}{\rho_0}\overline{\rho' u_i'}\delta_{i3}}_{VI} \qquad \text{(A-7)}$$

where :

I : TKE trend ;
II : spatial transport (advection) ;
III : pressure fluctuation ;
IV : heat dissipation ;
V : shear production ;
VI : buoyancy (loss) production .

In practice, the underlined terms II and III are grouped together.

Appendix B

Spherical coordinate

B.1 Momentum equations

B.2 Continuity equation

B.3 Advection-diffusion equation

Appendix C

2Dh linearized scheme

C.1 Equations

2Dh equations (3.7) to (3.9) can be simplified as follows :

$$\begin{aligned} \frac{\partial U}{\partial t} + U\frac{\partial U}{\partial x} + V\frac{\partial U}{\partial y} - fV + g\frac{\partial \zeta}{\partial x} &= 0 \\ \frac{\partial V}{\partial t} + U\frac{\partial U}{\partial y} + V\frac{\partial V}{\partial y} + fU + g\frac{\partial \zeta}{\partial y} &= 0 \\ \frac{\partial (hU)}{\partial x} + \frac{\partial (hV)}{\partial y} + \frac{\partial \zeta}{\partial t} &= 0 \end{aligned} \tag{C-1}$$

Thereafter, bottom and surface friction, baroclinic pressure gradient, horizontal diffusion and atmosphic pressure are omitted.

Moreover we assume the *linearization* of the nonlinear system (C-1) around a "steady state" (h_0, u_0, v_0). Thus, the linearized equations may be written as:

$$\begin{aligned} \frac{\partial U}{\partial t} + u_0\frac{\partial U}{\partial x} + v_0\frac{\partial U}{\partial y} - fV + g\frac{\partial \zeta}{\partial x} &= 0 \\ \frac{\partial V}{\partial t} + u_0\frac{\partial U}{\partial y} + v_0\frac{\partial V}{\partial y} + fU + g\frac{\partial \zeta}{\partial y} &= 0 \\ h_0\frac{\partial U}{\partial x} + u_0\frac{\partial \zeta}{\partial x} + h_0\frac{\partial V}{\partial x} + v_0\frac{\partial \zeta}{\partial x} + \frac{\partial \zeta}{\partial t} &= 0 \end{aligned} \tag{C-2}$$

The numerical formulations of this 2Dh linearized scheme (C-2) are outlined in the next section.

The time scheme is based on a two-step agorithm :

1 - At a half-time step $n + \frac{1}{2}$, the variables (ζ, U) and (ζ, V) are updated.
2 - Then, at time step $n + 1$, variables (ζ, V) and (ζ, U).

C.2 Von Neumann analysis

Von Neumann analysis is a procedure used to check the *stability* of a finite difference scheme. The stability of numerical schemes is closely associated with numerical error. A finite difference scheme is stable if the errors made at a time step of the calculation does not cause the errors to increase

(remain bounded) as the computations are continued. A neutrally stable scheme is one in which errors remain constant as the computations are carried forward.

The Von Neuman analysis method is based on the Fourier decomposition of numerical error.

Consider the time evolution of a single Fourier mode of wave-number $\mathbf{k} = (k_x, k_y)$:

$$X(\mathbf{x}, t) = \widehat{X}\ e^{i(\mathbf{k}\cdot\mathbf{x}-\omega t)} \tag{C-3}$$

where :

$\mathbf{x} = (x, y)$: location vector ;
$\widehat{X} = \left(\hat{\zeta}, \hat{u}, \hat{v}\right)$ vector's magnitude ;
ω : frequency.

At time $t^n = n\Delta t$, we can write $X^n = \hat{X}\ e^{i(\mathbf{k}\cdot\mathbf{x}-\omega n\Delta t)}$. Then we have:

$$X^{n+1} = e^{-i\omega\Delta t} X^n$$

$\lambda_e = e^{-i\omega\Delta t}$ is the eigenvalue.

C.3 Numerical formulations

$$\left\{\begin{array}{rcl} U^{n+\frac{1}{2},*} &=& U^n - \frac{1}{2}i\Delta t(u_0k_x + v_0k_y)U^n - \frac{1}{2}igk_x\Delta t\,\zeta^n \\ V^{n+\frac{1}{2},*} &=& V^n - \frac{1}{2}i\Delta t(u_0k_x + v_0k_y)V^n - \frac{1}{2}igk_y\Delta t\,\zeta^n \end{array}\right. \tag{C-4}$$

$$\left\{\begin{array}{rcl} \zeta^{n+\frac{1}{2},*} &=& \zeta^n - \frac{1}{2}ih_0k_x\Delta t\left(\alpha\,U^n + (1-\alpha)\,U^{n+\frac{1}{2}}\right) \\ && \quad - \frac{1}{2}ih_0k_y\Delta t\left(\alpha\,V^n + (1-\alpha)\,V^{n+\frac{1}{2},*}\right) \\ && \quad - \frac{1}{2}i\Delta t(u_0k_x + v_0k_y)\,\zeta^n \\ U^{n+\frac{1}{2}} &=& U^n - \frac{1}{2}igk_x\Delta t\Big(\alpha\,\zeta^n + (1-\alpha)\,\zeta^{n+\frac{1}{2},*}\Big) \\ && \quad - \frac{1}{2}i\Delta t(u_0k_x + v_0k_y)\left(\alpha\,U^n + (1-\alpha)\,U^{n+\frac{1}{2},*}\right) \end{array}\right. \tag{C-5}$$

$$\left\{\begin{array}{rcl} \zeta^{n+\frac{1}{2}} &=& \zeta^n - \frac{1}{2}ih_0k_x\Delta t\left(\alpha\,U^n + (1-\alpha)\,U^{n+\frac{1}{2}}\right) \\ && \quad - \frac{1}{2}ih_0k_y\Delta t\left(\alpha\,V^n + (1-\alpha)\,V^{n+\frac{1}{2}}\right) \\ && \quad - \frac{1}{2}i\Delta t(u_0k_x + v_0k_y)\,\left(\alpha\,\zeta^n + (1-\alpha)\,\zeta^{n+\frac{1}{2},*}\right) \\ V^{n+\frac{1}{2}} &=& V^n - \frac{1}{2}igk_y\Delta t\Big(\alpha\,\zeta^n + (1-\alpha)\,\zeta^{n+\frac{1}{2}}\Big) \\ && \quad - \frac{1}{2}i\Delta t(u_0k_x + v_0k_y)\left(\alpha\,V^n + (1-\alpha)\,V^{n+\frac{1}{2},*}\right) \end{array}\right. \tag{C-6}$$

$$\left\{\begin{array}{rcl} U^{n+1,*} &=& U^{n+\frac{1}{2}} - \frac{1}{2}i\Delta t(u_0k_x + v_0k_y)\,U^{n+\frac{1}{2}} - \frac{1}{2}igk_x\Delta t\,\zeta^{n+\frac{1}{2}} \\ V^{n+1,*} &=& V^{n+\frac{1}{2}} - \frac{1}{2}i\Delta t(u_0k_x + v_0k_y)\,V^{n+\frac{1}{2}} - \frac{1}{2}igk_y\Delta t\,\zeta^{n+\frac{1}{2}} \end{array}\right. \tag{C-7}$$

$$\left\{\begin{array}{rcl}\zeta^{n+1,*} &=& \zeta^{n+\frac{1}{2}} - \frac{1}{2}ih_0k_x\Delta t\left(\alpha\, U^{n+\frac{1}{2}} + (1-\alpha)\, U^{n+1,*}\right)\\ &&\quad - \frac{1}{2}ih_0k_y\Delta t\left(\alpha\, V^{n+\frac{1}{2}} + (1-\alpha)\, V^{n+1}\right)\\ &&\quad - \frac{1}{2}i\Delta t(u_0k_x + v_0k_y)\,\zeta^{n+\frac{1}{2}}\\ V^{n+1} &=& V^{n+\frac{1}{2}} - \frac{1}{2}igk_y\Delta t\Big(\alpha\,\zeta^{n+\frac{1}{2}} + (1-\alpha)\,\zeta^{n+1,*}\Big)\\ &&\quad - \frac{1}{2}i\Delta t(u_0k_x + v_0k_y)\,\left(\alpha\, V^{n+\frac{1}{2}} + (1-\alpha)\, V^{n+1,*}\right)\end{array}\right. \tag{C-8}$$

$$\left\{\begin{array}{rcl}\zeta^{n+1} &=& \zeta^{n+\frac{1}{2}} - \frac{1}{2}ih_0k_x\Delta t\left(\alpha\, U^{n+\frac{1}{2}} + (1-\alpha)\, U^{n+1}\right)\\ &&\quad - \frac{1}{2}ih_0k_y\Delta t\left(\alpha\, V^{n+\frac{1}{2}} + (1-\alpha)\, V^{n+1}\right)\\ &&\quad - \frac{1}{2}i\Delta t(u_0k_x + v_0k_y)\,\left(\alpha\,\zeta^{n+\frac{1}{2}} + (1-\alpha)\,\zeta^{n+1,*}\right)\\ U^{n+1} &=& U^{n+\frac{1}{2}} - \frac{1}{2}igk_x\Delta t\Big(\alpha\,\zeta^{n+\frac{1}{2}} + (1-\alpha)\,\zeta^{n+1}\Big)\\ &&\quad - \frac{1}{2}i\Delta t(u_0k_x + v_0k_y)\,\left(\alpha\, U^{n+\frac{1}{2}} + (1-\alpha)\, U^{n+1,*}\right)\end{array}\right. \tag{C-9}$$

Among these forms, steps (C-4) and (C-7) are explicit updates of the barotropic velocity components U and V. This first step was included to reduce the artificial diffusivity induced by the finite difference representation of the nonlinear terms.

The others forms (C-5) and (C-6) then (C-8) and (C-9) are semi-implicit updates.

To sum up, this algorithm requires two explicit estimates and four tridiagonal matrices to be solved at each time step (*cf.* Appendix D).

C.4 Numerical analysis

A valuable method for obtaining the characteristic equation of time integration schemes, which are discrete approximations of a set of differential equations, is to formulate the eigenvalue problem in terms of the amplification matrix.

The finite difference scheme of system (C-2) is conditionnally stable. This may be readily established by using the amplification matrix method yielding the three roots (*cf.* [10])

$$\lambda_e^{\pm} = \exp -i\left(\mathbf{Fr}\cdot\vec{\gamma} \pm \sqrt{\gamma_x^2+\gamma_y^2}\right) \quad \lambda_e^3 = \exp -i\mathbf{Fr}v\cdot\vec{\gamma}$$

where

$$\mathbf{Fr} = \left(\frac{u_0}{c}, \frac{v_0}{c}\right)^T$$

is the Froude vector and $\vec{\gamma} = c\mathbf{k}\Delta t = (\gamma_x, \gamma_y)^T$ is the variable vector.

It is convenient to define the angular wave number $\mathbf{k} = (k_x, k_y)^T$ and the velocity vector $\mathbf{u}_0 = (u_0, v_0)^T$ in polar coordinates :

$$k_x \;=\; k\,\cos\theta\;, \qquad k_y \;=\; k\,\sin\theta \tag{C-10}$$

$$u_0 \;=\; w\,\cos\theta\;, \qquad v_0 \;=\; w\,\sin\theta \tag{C-11}$$

Then, parameter γ (radian) and the Froude number are given by the forms :

$$\gamma \ = ck\Delta t \qquad Fr \ = \ \frac{w}{c} \tag{C-12}$$

Order : Formulations as described above for $\alpha = \frac{1}{2}$ compose a second-order scheme; a first-order scheme otherwise.

Stability : $\alpha < \frac{1}{2}$ gives the stability requirement for this scheme. At $\alpha \geq \frac{1}{2}$, if $Fr > 0$, the amplification matrix is greater than one in magnitude and so the scheme is unstable.

C.4.1 Case $Fr = 0$:

Figure C.1 shows the case of a barotropic zonal flow ($\theta = 0$) assuming a linearization around a state at rest ($Fr = 0$).

Left graphs give the eigenvalues $\lambda^{\pm}$ modulus versus variable γ . Right graphs give the ratio :

$$R^{\pm} = \frac{\arg(\lambda_G^{\pm})}{\arg(\lambda_e^{\pm})}$$

between numerical and theoretical velocity versus variable γ.
The former 2Dh scheme embeded in MARS was analyzed by (*cf.* [10]).

The graphs shown above indicate that the new scheme is slightly damping the short scale motions. On the other hand, in case α close to $\frac{1}{2}$, the new scheme gives higher accurate phase velocity for large scale motions.

C.4.2 Case $Fr \neq 0$:

In case of a Froude number $Fr = \frac{1}{20}$, figure C.2 shows the eigenvalues modulus versus parameter γ (left graphs). Right graphs give the ratio R. Three discrete values of the parameter α are examined : 0, 0.45 and 0.5. The direction of analysis is $\theta = 0$ (a zonal flow).
In figure C.3, the direction of analysis is $\theta = \frac{\pi}{4}$.

The new scheme produces a compromise solution to solve short and large scale motions with the same time step.

Furthermore, this scheme is based on an alternating direction implicit algorithm. Thus, using this method will ensure omnidirectional accuracy.

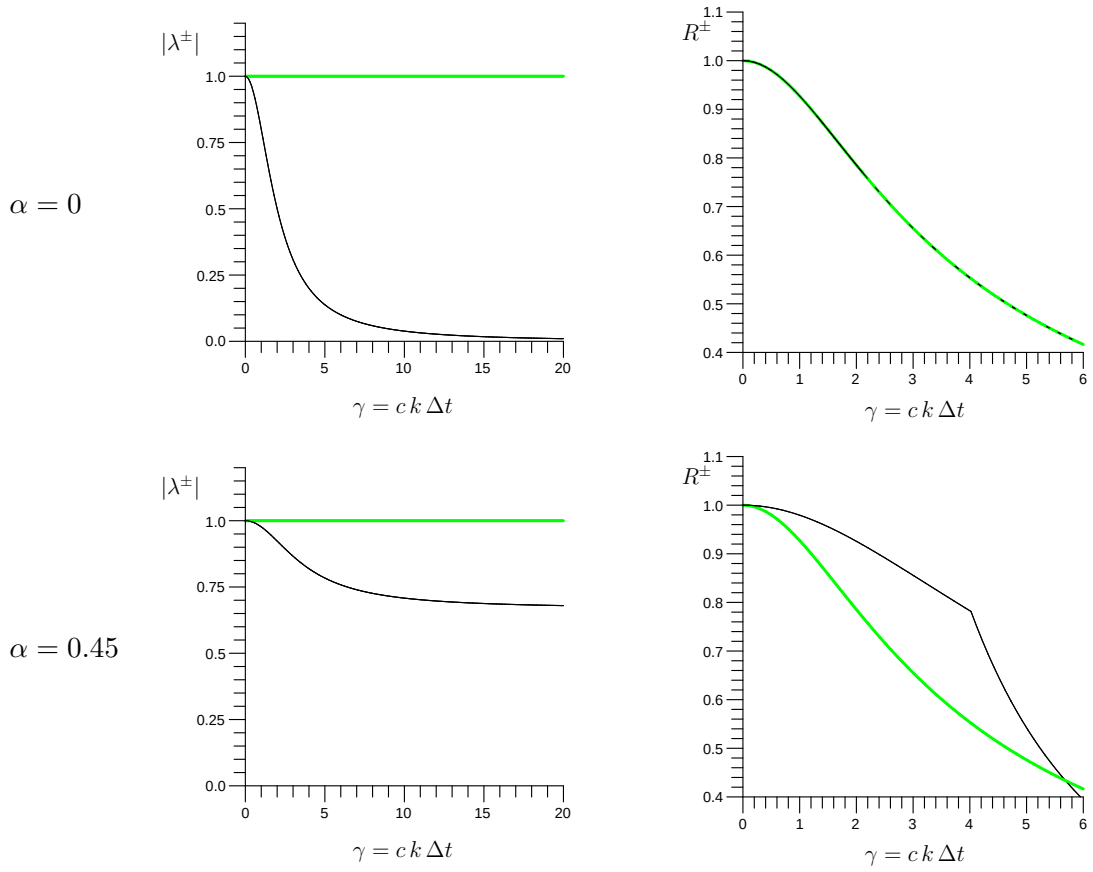

(a) Modulus (b) Argument

Figure C.1: : Eigenvalues modulus and argument versus variable $\gamma = c\,k\Delta t$ for $Fr = 0$, $\alpha = 0$ (top) and $\alpha = 0.45$ (bottom). Green line : Actual scheme ; black line : Old scheme.

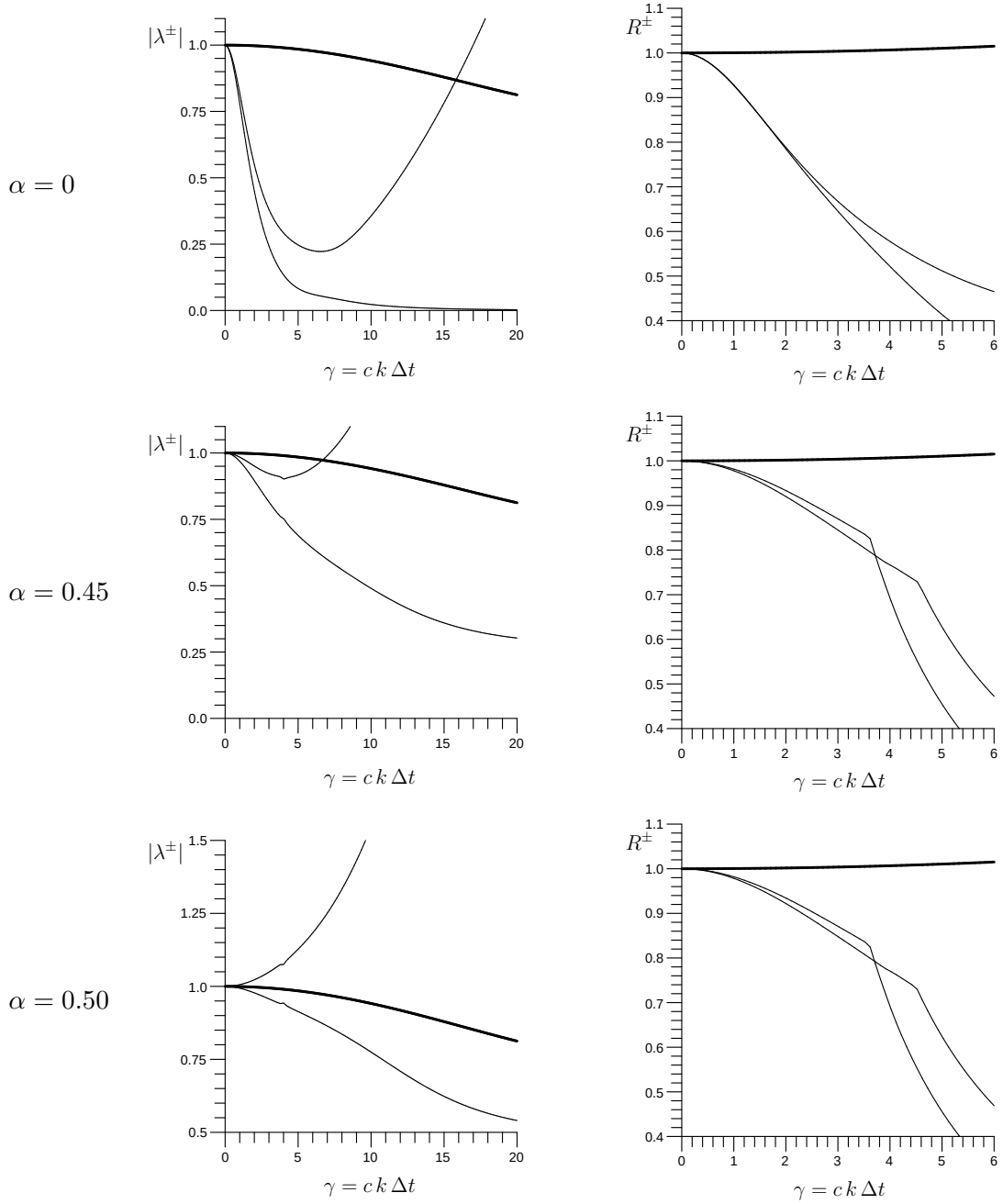

(a) Modulus (b) Argument

Figure C.2: Eigenvalues modulus and argument versus variable $\gamma = c\,k\Delta t$ for $Fr = 0.05$ and $\theta = 0$. Small line : $\lambda_G^{\pm}$; bold line : λ_G^3.

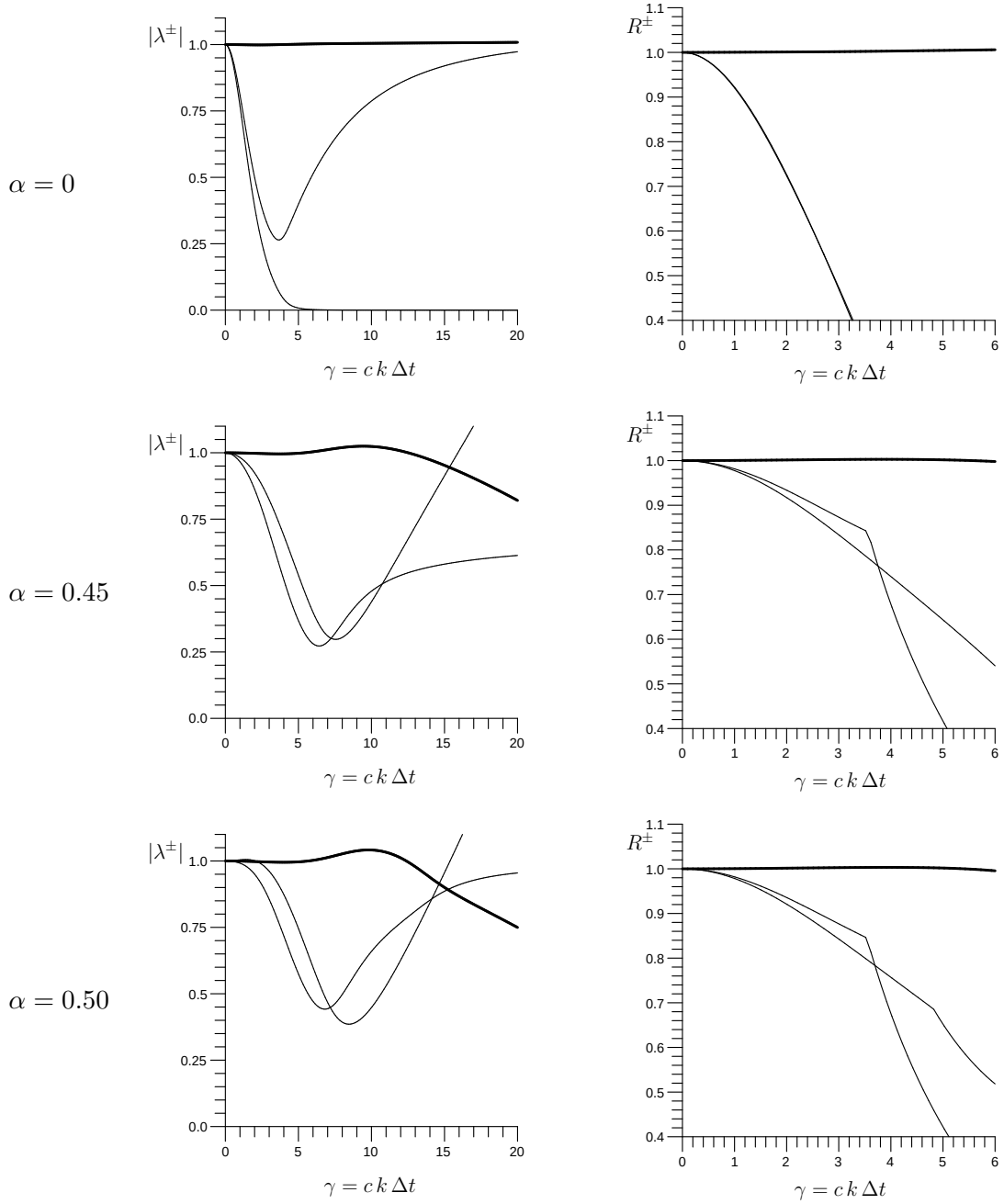

(a) Modulus (b) Argument

Figure C.3: Eigenvalues modulus and argument versus variable $\gamma = c\,k\Delta t$ for $Fr = 0.05$ and $\theta = \frac{\pi}{4}$. Small line : $\lambda_G^{\pm}$; bold line : λ_G^3.

Appendix D

Tridiagonal matrix

Hereforth we describe the algorithm used to get the solutions (ζ_{n+1}, U_{n+1}) at the $(n+1)th$ time level in terms of the known solutions at the $(n+1/2)th$ and earlier time levels.

For every line j, by considering all spatial nodes i produces a tridiagonal system which can be written in a general form :

$$\mathbf{M} \cdot \mathbf{x} = \mathbf{y} \tag{D-1}$$

where :

$$\mathbf{M} = \begin{pmatrix} bu_{1,j} & cu_{1,j} & 0 & & & & & & \\ axe_{2,j} & bxe_{2,j} & cxe_{2,j} & 0 & & & & & \\ 0 & au_{2,j} & bu_{2,j} & cu_{2,j} & 0 & & & & \\ & \ddots & \ddots & \ddots & \ddots & \ddots & & & \\ & & 0 & axe_{i,j} & bxe_{i,j} & cxe_{i,j} & 0 & & \\ & & & 0 & au_{i,j} & bu_{i,j} & cu_{i,j} & 0 & \\ & & & & \ddots & \ddots & \ddots & \ddots & \ddots \end{pmatrix}$$

and

$$\mathbf{x} = \begin{pmatrix} U_{1,j,n+1} \\ \zeta_{2,j,n+1} \\ U_{2,j,n+1} \\ \vdots \\ \zeta_{i,j,n+1} \\ U_{i,j,n+1} \\ \vdots \end{pmatrix} \qquad \mathbf{y} = \begin{pmatrix} y2du_{1,j} \\ y2dxe_{2,j} \\ y2du_{2,j} \\ \vdots \\ y2dxe_{i,j} \\ y2du_{i,j} \\ \vdots \end{pmatrix}$$

The various coefficients $au_{i,j}$, $bu_{i,j}$, $cu_{i,j}$, $y2du_{i,j}$ and $axe_{i,j}$, $bxe_{i,j}$, $cxe_{i,j}$, $y2dxe_{i,j}$ are given in section 4.1.

Inner domain : In the inner domain, the **M** matrix elements are :

$$\begin{array}{ll} au_{i,j} = -g\frac{\Delta t}{2\Delta x} & axe_{i,j} = -(H^u_{i-1,j} + \zeta_{i-1,j,n+\frac{1}{2},*})\frac{\Delta t}{2\Delta x} \\ bu_{i,j} = 1 & bxe_{i,j} = 1 \\ cu_{i,j} = g\frac{\Delta t}{2\Delta x} & cxe_{i,j} = (H^u_{i,j} + \zeta_{i,j,n+\frac{1}{2},*})\frac{\Delta t}{2\Delta x} \end{array}$$

those for $\mathbf{y}$:

$$y2du = U_{i,j,n+\frac{1}{2}} - \frac{\Delta t}{2}\left(\bar{G}_u(u_{i,j,n+\frac{1}{2}}, v_{i,j,n+1})\right)$$
$$y2dxe = \zeta_{i,j,n+\frac{1}{2}} - \frac{\Delta t}{2\Delta y}\left(h^v_{i,j,n+1} v_{i,j,n+1} - h^v_{i,j-1,n+1} v_{i,j-1,n+1}\right)$$

Along the open-sea boundaries, the sea surface elevation ζ must be provided. Then, in case of a western boundary the first term $y2du_{1,j}$ of the right-hand side column matrix $\mathbf{y}$ must be modified as follows :

$$y2du_{1,j}|_{West} = y2du_{1,j} + g\frac{\Delta t}{2\Delta x}\zeta_{1,j,n+1}$$

Table of symbols

b	:	buoyancy
c	:	dissolved matter concentration
C_p	:	specific heat capacity
C_d	:	drag coefficient
e	:	turbulent kinetic energy
Fr	:	Froude number
f	:	Coriolis parameter
F	:	Force
g	:	gravity
g'	:	reduced gravity
h	:	instantaneous depth
H	:	bottom depth
k	:	wave number
l	:	mixing length
$\mathcal{M}$	:	mass
N	:	Brunt-Väisälä frequency
p	:	pressure
p_a	:	atmospheric pression
Q	:	air-sea flux
R_i	:	Richardson number
S	:	salinity
t	:	time
T	:	temperature
u, v, w	:	velocity components
u', v', w'	:	velocity fluctuations
U, V	:	barotropic velocity components
u^*	:	friction velocity
$\tilde{w}$	:	vertical velocity in the σ coordonnates
z_0	:	roughness

α_T	:	thermal expansion coefficient
β_S	:	coefficient of saline contraction
ϵ	:	TKE dissipation
κ	:	Von Karman constant
λ	:	wave length
ν_V	:	vertical coefficient of eddy diffusivity
ν_H	:	horizontal coefficient of eddy diffusivity
ρ	:	density of sea water
ρ'	:	density fluctuation
ρ_0	:	reference density
τ	:	Reynolds stress
ζ	:	sea surface elevation
σ	:	vertical stretched coordinate
$\Pi_{x,y}$	:	pressure gradient components